

CHARACTERIZATION OF LIPOSOMAL CELECOXIB FORMULATION
AS A DRUG DELIVERY SYSTEM
IN COLORECTAL CANCER CELL LINES

A THESIS SUBMITTED TO
THE GRADUATE SCHOOL OF NATURAL AND APPLIED SCIENCES
OF
MIDDLE EAST TECHNICAL UNIVERSITY

BY

ASLI ERDOĞ

IN PARTIAL FULFILLMENT OF THE REQUIREMENTS
FOR
THE DEGREE OF DOCTOR OF PHILOSOPHY
IN
BIOTECHNOLOGY

FEBRUARY 2012

Approval of the thesis:

**CHARACTERIZATION OF LIPOSOMAL CELECOXIB FORMULATION
AS A DRUG DELIVERY SYSTEM
IN COLORECTAL CANCER CELL LINES**

submitted by **ASLI ERDOĞ** in partial fulfillment of the requirements for the degree
of **Doctor of Philosophy in Biotechnology Department, Middle East Technical
University** by,

Prof. Dr. Canan Özgen _____
Dean, Graduate School of **Natural and Applied Sciences**

Prof. Dr. Nesrin Hasırcı _____
Head of Department, **Biotechnology**

Assist. Prof. Dr. Sreeparna Banerjee _____
Supervisor, **Biological Sciences Dept., METU**

Assoc. Prof. Dr. Ayşen Tezcaner _____
Co-Supervisor, **Engineering Sciences Dept., METU**

Examining Committee Members:

Prof. Dr. Türkan Eldem _____
Pharmaceutical Biotechnology Dept., Hacettepe Univ.

Assist. Prof. Dr. Sreeparna Banerjee _____
Biological Sciences Dept., METU

Assoc. Prof. Dr. Dilek Keskin _____
Engineering Sciences Dept., METU

Assist. Prof. Dr. A.Elif Erson Bengan _____
Biological Sciences Dept., METU

Assoc. Prof. Dr. Mayda Gürsel _____
Biological Sciences Dept., METU

Date: _____

I hereby declare that all information in this document has been obtained and presented in accordance with academic rules and ethical conduct. I also declare that, as required by these rules and conduct, I have fully cited and referenced all material and results that are not original to this work.

Name, Last name: Aslı Erdoğ

Signature :

ABSTRACT

CHARACTERIZATION OF LIPOSOMAL CELECOXIB FORMULATION AS A DRUG DELIVERY SYSTEM IN COLORECTAL CANCER CELL LINES

Erdoğ, Aslı

Ph.D., Department of Biotechnology

Supervisor: Assist. Prof. Dr. Sreeparna Banerjee

Co-Supervisor: Assoc. Prof. Dr. Ayşen Tezcaner

February 2012, 154 pages

Colorectal carcinoma (CRC) is one of the most common cancers and is the leading cause of cancer deaths in much of the developed world. Owing to the high incidence of drug resistance and potential toxic effects of chemotherapy drugs, much research is currently underway to design better strategies for smart drug delivery systems. Cyclooxygenase-2 (COX-2) pathway is associated with poor prognosis in colon carcinomas. The selective COX-2 inhibitor drug Celecoxib (CLX) has been shown to possess COX-2 independent anti-carcinogenic effects in addition to inhibition of prostaglandins synthesis. The aim of the presented thesis was to develop a liposomal delivery system for CLX and to evaluate functional effects in CRC cell lines. Starting with multilamellar vesicles capable of CLX encapsulation and retention, nano sized liposomes were prepared and characterized *in vitro*. The optimum composition was determined as 10:1 DSPC: Cholesterol

molar ratio and Polyethylene glycol (PEG) grafting at 2% of phospholipids. The extent of cellular association of PEGylated liposome formulation was analyzed quantitatively and cellular localization was analyzed qualitatively. We detected that CLX loaded PEGylated liposomes inhibited proliferation and cellular motility of cancer cells in a 2D model system. Our results showed that, Epidermal Growth Factor Receptor (EGFR) targeted CLX loaded immunoliposomes were extremely cytotoxic in cancer cells with high EGFR expression but not in cells devoid of EGFR expression. This delivery system may pioneer studies that may potentially circumvent the harmful systemic side effects of cancer preventive and chemotherapy drugs as well as allow the use of targeted combinatorial therapies.

Key words: Liposome, cancer, Celecoxib

ÖZ

İLAÇ TAŞIYICI SİSTEM OLARAK LİPOZOMAL CELECOXİB FORMÜLASYONUNUN KOLOREKTAL KANSER HÜCRELERİNDE KARAKTERİZASYONU

Erdoğ, Aslı

Doktora, Biyoteknoloji Bölümü

Tez Yöneticisi: Yrd.Doç.Dr. Sreeparna Banerjee

Ortak Tez Yöneticisi: Doç.Dr. Ayşen Tezcaner

Şubat 2012, 154 sayfa

Kolorektal kanser (CRC) çok yaygın görülen kanser tiplerinden biridir ve gelişmiş ülkelerde kansere bağlı ölümlerin başta gelen sebeplerindendir. Hastalarda sıkça rastlanan ilaç direnci gelişmesi durumu ve kemoterapi ilaçlarının muhtemel toksik etkileri düşünüldüğünde, araştırmalar şu anda akıllı ilaç taşıma sistemleri ve stratejileri geliştirmeye yoğunlaşmıştır. Siklooksijenaz-2 (COX-2) yolağı, kolon kanserinde kötü prognoz ile ilişkilidir. Seçici COX-2 inhibitörü ilaç Celecoxib (CLX); prostaglandin sentezini inhibe etmenin yanısıra COX-2'den bağımsız anti-karsinojenik etkilere de sahiptir. Sunulmakta olan tez çalışmasının amacı, CLX için lipozomal ilaç taşıma sistemi geliştirilmesi ve CRC hücre hatlarında fonksiyonel etkisinin değerlendirilmesidir. CLX enkapsülasyonu ve tutulumu sağlayan çok katmanlı veziküller ile başlanan çalışmada; nano boyutta lipozomlar hazırlanmış ve

in vitro kořullarda karakterize edilmiřtir. Optimum kompozisyon 10:1 DSPC:Chol mol oranı ve fosfolipidlerin %2'si oranında Polietilen glikol (PEG) kaplaması olarak belirlenmiřtir. PEGile edilmiř lipozom formülasyonunun hücreler ile etkileřim derecesi kantitatif olarak ve lipozomların hücrenel konumu kalitatif olarak analiz edilmiřtir. CLX yüklenmiř PEGile edilmiř lipozomların, kanser hücrelerinde proliferasyonunu ve 2-boyutlu hücre költürü modelinde hücrenel hareketlilięi inhibe ettięi gösterilmiřtir. Epidermal Büyüme Faktörü Reseptörü'ne (EGFR) hedefli CLX yüklü immünolipozomlar ile yürütölen bařlangıç seviyesindeki çalıřmalarda, EGFR'yi yüksek seviyede ifade eden kanser hücrelerinde son derece sitotoksik etki gösterdięi, ancak EGFR'yi ifade etmeyen hücrelerde etkili olmadığı görölmüřtür. Tasarlanan bu ilaç tařıma sistemi, kanser önleyici ve kemoterapi ilaç tedavilerindeki zararlı sistemik yan etkileri önleme potansiyeli ile birlikte hedefli kombinasyon terapilerine imkan saęlayabilecektir.

Anahtar kelimeler: Lipozom, kanser, Celecoxib

This thesis is dedicated to
all my sisters and brothers around the world
who appreciate science, seek the True meaning of life
and respect freedom of thought...

ACKNOWLEDGEMENTS

I would like to express my deepest gratitude to my supervisor Assist.Prof Sreeparna Banerjee for her guidance, encouragement and support throughout my study. I would also like to thank my co-supervisors Assoc.Prof. Ayşen Tezcaner and Assoc.Prof. Dilek Keskin together with my PhD Thesis Committee members Prof. Dr. Türkan Eldem and Assist.Prof A. Elif Erson Bensan for their invaluable input throughout the entire process of this thesis study.

My special thanks go to:

Prof. Dr. Haluk Hamamcı, Dr. Şeyda Açar, Dr. Ali Oğuz Büyükkileci, Dr. Ceylan Büyükkileci, Dr. Ebru Özer Uyar, Didem Dedeoğlu, Eda Alagöz, Benek Abat, Lütfiye Kurt and Gül Sarıbay from Food Engineering Industrial Biotechnology group,

Dr. Can Özen, Dr. Deniz Yücel, Fatma Gül, Dr. Tamay Şeker, Dr. İbrahim Çam from METU Central lab,

Dr. Erhan Astarıcı, Aslı Sade, Seda Tunçay, Shabnam Enayat, İsmail Çimen, Mümine Küçükdemir, Richardas Rachkauskas, Şeyma Ceyhan, Neva Çalışkan, Yanuar Limasale, Roman Furman, Nilüfer Sayar and Derya Dönertaş from Lab.B-59,

Assoc.Prof. Mayda Gürsel, Dr. Pembegül Uyar, Nihal Şimşek Özek and Ferhunde Aysin from METU Biological Sciences Department,

Dr. Gökşen Çapar, Dr. Özlem Aydın, Ayşegül Kavas, Özge Erdemli, Mert Baki, Yiğit Öcal, Ömer Aktürk and Seylan Aygün from METU Engineering Sciences Department,

Assoc.Prof. İhsan Gürsel and Tamer Kahraman from Bilkent University Molecular Biology and Genetics Department.

I am grateful to these very special people for being a second family for me:

Prof. Dr. Yılmaz Dündar, Mehmet Dođramacı, Hayrettin Zor, Ahmet Kayı, İlknur and Hakan Çakmak, Servet Işık, Zehra Mirzaođlu, Elif and Aytunç Göy, İter Önder, Yıldız and Taylan Korkmaz, Güliz and Mutlu Balık, Eda Özsoy, Lütfiye Özdirek, Kurtuluş Yıldırım, Didem Coral, Alper Yiđit, Dr. Begüm Güney, Semra Ünlü, Hande Çıralı, Mr. Aykut Deniz and his family.

I would like to express my sincere gratitude to my family Gülay and İlhami Erdođ, Asude and Cevdet Yorulmaz, Hava Er, Sevilay Er, Gökçe Erdođ and Batuhan Erdođ for their endless support and patience.

This thesis project was financially supported by METU BAP-2007-R-08-11-02, and TÜBİTAK 108T297 projects. Also this work would not be possible without the generous support from TÜBİTAK BİDEB 2211 Domestic PhD scholarship between 2006 and 2011.

TABLE OF CONTENTS

ABSTRACT	iv
ÖZ.....	vi
ACKNOWLEDGEMENTS	ix
TABLE OF CONTENTS	xi
LIST OF TABLES	xv
LIST OF FIGURES.....	xvi
LIST OF ABBREVIATIONS	xix
CHAPTERS	1
1 INTRODUCTION.....	1
1.1 Cancer.....	1
1.1.1 Colorectal cancer.....	3
1.1.2 Drug delivery systems for cancer therapy.....	6
1.2 COXs and cancer.....	10
1.2.1 COX-2 inhibitors.....	13
1.2.2 Crosstalk between COX-2 and EGFR pathways.....	16
1.3 Liposomal drug delivery systems.....	21
1.3.1 Conventional liposomes	24
1.3.2 Long circulating liposomes	28
1.3.3 Targeted liposomes	29
1.4 Aim of the study	33
2 MATERIALS AND METHODS.....	35

2.1	Materials.....	35
2.2	Methods.....	37
2.2.1	Preparation of liposomes.....	37
2.2.1.1	Preparation of MLVs.....	37
2.2.1.2	Preparation of LUVs	38
2.2.1.3	Preparation of PEGylated LUVs	39
2.2.1.4	Preparation of ILs.....	40
2.2.2	Quantification of Celecoxib	41
2.2.2.1	Spectrophotometric method	41
2.2.2.2	HPLC method.....	42
2.2.3	Quantification of phospholipids (DSPC)	42
2.2.4	Characterization of liposomes.....	43
2.2.4.1	Particle size analysis.....	43
2.2.4.2	Morphological characterization by Transmission Electron Microscopy (TEM).....	44
2.2.4.3	Drug encapsulation efficiency and percent drug loading.....	44
2.2.4.4	<i>In vitro</i> release profiles.....	45
2.2.4.5	IgG conjugation efficiency.....	46
2.2.5	Cell culture conditions	46
2.2.6	Evaluation of cellular association of liposomes.....	47
2.2.6.1	Laser scanning confocal microscopy (LSCM) analysis.....	47
2.2.6.2	Fluorescence activated cell sorting (FACS) analysis.....	49
2.2.7	Cellular viability and toxicity assay	50
2.2.8	<i>In vitro</i> scratch wound healing assay	50
2.2.9	Statistical analyses	51
3	RESULTS	52
3.1	Characterization of CLX loaded MLVs.....	52

3.1.1	Particle size distribution and morphology of MLVs.....	52
3.1.2	Drug encapsulation efficiency and percent drug loading.....	58
3.1.3	<i>In vitro</i> release profiles.....	59
3.2	Characterization of CLX loaded LUVs and PEGylated LUVs.....	61
3.2.1	Particle size distribution and morphology.....	61
3.2.2	Drug encapsulation efficiency and percent drug loading.....	64
3.2.3	<i>In vitro</i> release profiles.....	66
3.2.4	Cellular association of PEGylated liposomes	69
3.2.4.1	Laser scanning confocal microscopy analysis	69
3.2.4.2	Fluorescence activated cell sorting analysis (FACS).....	77
3.2.5	Cellular toxicity of pure CLX and CLX loaded liposomes.....	82
3.2.6	Inhibition of cellular motility by CLX loaded PEGylated liposomes..	88
3.3	Characterization of CLX loaded ILs	92
3.3.1	ILs prepared by mouse IgG conjugation	92
3.3.1.1	Particle size distribution analysis	92
3.3.1.2	Drug encapsulation efficiency.....	94
3.3.1.1	IgG conjugation efficiency.....	95
3.3.2	Anti-EGFR IgG conjugated ILs	98
3.3.3	Cellular toxicity of EGFR targeted ILs	100
4	DISCUSSION	104
4.1	Characteristics of CLX loaded MLVs.....	104
4.2	Characteristics of CLX loaded LUVs and PEGylated LUVs	109
4.3	Characteristics of CLX loaded ILs.....	119
5	CONCLUSION	125
	REFERENCES.....	128
	APPENDICES.....	142

APPENDIX A CALIBRATION CURVES AND CHROMATOGRAMS.....	142
APPENDIX B FLUORESCENCE EXCITATION AND EMISSION SPECTRA OF FLUROPHORES	144
APPENDIX C CLX CONCENTRATIONS USED IN IN VITRO EXPERIMENTS	146
APPENDIX D CHARACTERISTICS OF HUMAN COLORECTAL ADENOCARCINOMA CELL LINES	148
APPENDIX E STATISTICAL ANALYSES OF RELEASE AND ENCAPSULATION CHARACTERISTICS OF LIPOSOMES	151
CURRICULUM VITAE	153

LIST OF TABLES

TABLES

Table 2. 1 Composition of lipid films	38
Table 3. 1 Particle size of CLX loaded MLVs.....	53
Table 3. 2 Characteristics of CLX loaded MLVs.....	59
Table 3. 3 Particle size of liposomes with variable cholesterol and PEG contents..	63
Table 3. 4 CLX encapsulation efficiency and percent CLX loading	66
Table 3. 5 Percentage of viable HCT-116 cells after liposome treatments.....	103
Table A. 1 Celecoxib concentrations used in <i>in vitro</i> experiments to achieve anticarcinogenic effects.....	146
Table A.2 Characteristics of human colorectal adenocarcinoma cell lines HCT-116, HT-29 and SW620	148
Table A. 3 Statistical analyses of released amount of CLX from MLVs.....	151
Table A. 4 Statistical analyses of CLX EE and percentage loading	152

LIST OF FIGURES

FIGURES

Figure 1- 1 Diagram for steps of molecular pathogenesis of sporadic colon cancer and colitis-associated colon cancer	5
Figure 1- 2 Selective COX-2 inhibitors	15
Figure 1- 3 EGFR pathway and downstream pathways	17
Figure 1- 4 Crosstalk between the EGFR and COX-2 pathways	20
Figure 1- 5 Evolution of liposomes	23
Figure 1- 6 Liposome-cell interactions	27
Figure 2- 1 Chemical structures of DSPC and DSPE-PEG	36
Figure 2- 2 Mini-extruder system.....	39
Figure 2- 3 Conjugation reaction between maleimide functional group and reactive sulfhydryl group	41
Figure 3- 1 Representative particle size distribution analysis results for MLVs	54
Figure 3-2 TEM images of MLVs.....	56
Figure 3- 3 <i>In vitro</i> CLX release from MLVs in PBS at 37°C.	61
Figure 3- 4 TEM images of CLX loaded and Empty PEGylated liposomes.	64
Figure 3- 5 <i>In vitro</i> CLX release from non-PEGylated LUVs in PBS at 37°C	67
Figure 3- 6 <i>In vitro</i> CLX release from PEGylated LUVs in PBS at 37°C.....	68
Figure 3- 7 LSCM analysis of cell associated Rhodamine labeled PEGylated liposomes.....	70
Figure 3- 8 LSCM analysis of localization of cell associated Rhodamine labeled liposomes and Transferrin-AlexaFluor680 conjugate.....	72
Figure 3-9 Cellular localization of Rhodamine labeled liposomes after 30 minutes of treatment	74

Figure 3-10 Cellular localization of Rhodamine labeled liposomes after 2 hours of treatment.....	75
Figure 3-11 Cellular localization of Rhodamine labeled liposomes after 6 hours of treatment.....	76
Figure 3-12 <i>In vitro</i> cellular association of fluorescently labeled liposomes by FACS.....	78
Figure 3-13 Dot plots for HCT-116 cell populations associated with fluorescently labeled liposomes	79
Figure 3-14 Dot plots for SW620 cell populations associated with fluorescently labeled liposomes	80
Figure 3-15 Single parameter histograms for cell populations associated with fluorescently labeled liposomes	81
Figure 3-16 Percentage of liposome associated cells detected by FACS analysis ..	82
Figure 3- 17 Cellular toxicity of pure CLX on HT-29 and SW620 cells by MTT assay	83
Figure 3-18 Cellular toxicity of CLX loaded PEGylated liposomes on HT-29 cells by MTT assay.....	86
Figure 3- 19 Cellular toxicity of CLX loaded PEGylated liposomes on SW620 cells by MTT assay.....	87
Figure 3-20 <i>In vitro</i> scratch wound healing assay with SW620 cells up to 120 h..	89
Figure 3- 21 Percent area closure in wound healing assay after 120 hours	90
Figure 3- 22 <i>In vitro</i> scratch wound healing assay with SW620 cells up to 60 h...	91
Figure 3- 23 Representative images for particle size distribution analysis of ILs ...	93
Figure 3- 24 CLX encapsulation efficiency in IL preparations	94
Figure 3- 25 SDS-PAGE analysis of reduced IgG molecules.....	96
Figure 3- 26 IgG conjugation efficiency for CLX loaded and Empty ILs.....	97
Figure 3- 27 Representative images of size distribution analysis of ILs	99

Figure 3-28 Cellular toxicity of CLX loaded EGFR targeted liposomes..... 101

LIST OF ABBREVIATIONS

- % EE: Percentage encapsulation efficiency
- 2-MEA: 2-mercaptoethylamine or cysteamine
- AP-1: Activator protein 1
- APC: Adenomatous polyposis coli
- BSA: Bovine serum albumin
- CA: Carbonic anhydrase
- cAMP: Cyclic adenosine monophosphate
- CD19: Cluster of differentiation 19
- CD20: Cluster of differentiation 20
- Chol: Cholesterol
- CIN: Chromosomal instability
- CLX: Celecoxib
- CLX-IL: CLX loaded immunoliposome
- CLX-LUV-PEG: CLX loaded PEGylated LUV
- COX : Cyclooxygenase
- CRC : Colorectal carcinoma
- DDS: Drug delivery system
- DIC: Differential interference contrast
- DiI: 1,1'-dioctadecyl-3,3,3',3'-tetramethylindodicarbocyanine
- DiO: 3,3'-dioctadecyloxacarbocyanine perchlorate
- DMBA: Dimethylbenzanthracene
- DMSO: Dimethyl sulfoxide
- DSC: Differential scanning calorimetry

DSPC: 18:0 PC; 1,2-Distearoyl-sn-glycero-3-phosphocholine
DSPE-PEG(2000)Maleimide: 1,2-distearoyl-sn-glycero-3-phosphoethanolamine-N-maleimide(polyethylene glycol)-2000
DTT: 2-Dithiothreitol
DXR: Doxorubicin
EDC: 1-ethyl-3-(3-dimethylaminopropyl) carbodiimide hydrochloride
EDTA: Ethylenediaminetetraacetic acid
EGFR : Epidermal growth factor receptor
Egr-1: eErly growth response protein 1
EPR: Enhanced permeability and retention effect
FACS: Fluorescence activated cell sorting
FAK: Focal adhesion kinase
FAP: Familial adenomatous polyposis
FCS: Forward Scatter
FDA: Food and Drug Association
HBS: HEPES buffered saline
HDL: High density lipoproteins
HEPES: 4-(2-hydroxyethyl)-1-piperazineethanesulfonic acid
HER2: Human epidermal receptor 2
HMVEC: Human dermal microvascular endothelial cell
HNPCC: Hereditary non-polyposis colorectal cancer
HUVEC : Human umbilical vein endothelial cell
i.m.: intramuscular
i.v.: intravenous
Ig: Immunoglobulins
IL: Immunoliposome
IkB kinase β : Inhibitor of kappa B kinase β

LDL: Low density lipoproteins
LOX : Lipoxygenase
LSCM: Laser scanning confocal microscopy
LUV: Large unilamellar vesicles
MAbs: monoclonal antibodies
MAPK: Mitogen-activated protein kinase
Mean RFI or Mean FL-1: Mean Relative Fluorescence Intensity
MIN: Multiple intestinal neoplasia
MLV: Multilamellar vesicles
MMP : Matrix metalloprotease
mPEG(2000)-DSPE: 1,2-distearoyl-sn-glycero-3-phosphoethanolamine-N-methoxy(polyethylene glycol)-2000
MPS: Mononuclear phagocyte system
MSI: Microsatellite instability
MTT: 3-(4,5-Dimethylthiazol-2-yl)-2,5-diphenyltetrazolium bromide
MWCO: Molecular weight cut-off
NCI: National Cancer Institute
NF- κ B: Nuclear factor kappa B
NHS: N-hydroxysuccinimide
NSAIDs: Non-steroidal anti-inflammatory drugs
NSCLC: Non-small cell lung cancer
ODC: Ornithine decarboxylase
p.o.: oral
PAGE: Polyacrylamide Gel Electrophoresis
PBS: Phosphate buffered saline
PC: Polycarbonate

PdI: Polydispersity index
PDK-1: Phosphoinositide-dependent kinase 1
PEG: Polyethylene glycol
PES: Polyethersulfone
PG: Prostaglandin
PI3K: Phosphatidylinositol 3-kinase
PKB: Protein kinase B
PLGA: Poly (lactic-co-glycolic acid)
PP: Polypropylene
PPAR: Peroxisome proliferator-activated receptor
Rhodamine DHPE or Rh-PE : Lissamine™ rhodamine B 1,2-dihexadecanoyl-sn-glycero-3-phosphoethanolamine, triethylammonium salt
S.E.M: Standard error of the mean
s.q.: subcutaneous
SATA: N-succinimidyl S- acetylthioacetate
SCCHN: Squamous cell carcinoma of the head and neck
SM: Sphingomyelin
SMPB: N-succinimidyl-4-p-maleimidophenyl-butyrate
SP-DiOC₁₈(3): 3,3'-dioctadecyl-5,5'-di(4-sulfophenyl)oxacarbocyanine, sodium salt
SPDP: N-succinimidyl 3-(2-pyridyldithio) propionate
SSC: Side scatter
SUV: Small unilamellar vesicles
TEM: Transmission Electron Microscopy
TGF α : Transforming growth factor α
TKI: Tyrosine Kinase Inhibitor
Tr-AF680: Human Transferrin-AlexaFluor680 conjugate
VCAM-1: Vascular cell adhesion molecule-1

VEGF : Vascular endothelial growth factor

WHO: World Health Organization

Z avg: Average hydrodynamic diameter

β -ME: β -mercaptoethanol

CHAPTER 1

INTRODUCTION

1.1 Cancer

“Cancer accounts for 7.1 million deaths annually (12.6% of the total cancer cases)” and “the number of new cases is expected to rise from 10 million to 15 million by 2020” as stated in the latest report of World Health Organization (WHO). Lung, stomach, colorectal, liver and breast cancer are the leading causes of cancer deaths each year.

Transformation of a normal cell into a cancerous cell can be due to genetic factors and three categories of environmental carcinogenic effects: physical (e.g. UV, ionizing radiation), chemical (e.g. tobacco smoke, aflatoxin) and biological (e.g. certain types of viruses and bacteria). During the formation of a tumor; a single cancerous cell undergoes cell division at a rate higher than healthy cells, and cancer cells consume higher amount of nutrients and oxygen supply from the blood stream. Tumor cells therefore continue dividing regardless of the limited nutrient supply and also many tumor cells escape from apoptosis although the amount of nutrients is not sufficient. The vasculature that is originally designed to supply the healthy tissue with glucose and oxygen can not fulfill the requirements of the tumor mass.

The tumor cells at the outer borders of a tumor mass have comparably better access to nutrient supply while an area of necrosis forms at the center of tumors due to death cells. Tumors rely on diffusion for delivery of nutrients and elimination of toxic metabolic products. In time, the tumor reaches a steady state size, where the proliferation rate becomes equal to the rate of cell death. This maximum size of most tumors is around 2 mm³ mainly due to limitations of diffusion of materials (Jones and Harris, 1998). To expand beyond this size, new connections with the circulatory system are formed as the tumor requires the formation of new blood vessels called “angiogenesis”.

Currently used treatment modalities for cancer include surgery, radiation therapy, chemotherapy and immunotherapy. Surgery can aid in both diagnosis and treatment of cancer and it is still the most widely used treatment with high chance of cure especially if the tumor has not spread to the organs other than the origin of the tumor. Radiation therapy is another local therapy that targets actively dividing cells. High-energy photons (x-rays and gamma rays) with radioactive sources such as cobalt, cesium or Particle beams (electrons, protons, neutrons, alpha and beta particles) are directed towards target tissue and causes damage to DNA and other cellular macromolecules. Conventional chemotherapy is a systemic treatment involving administration of drugs to prevent uncontrolled cell division, mostly interfering with division cycle of the rapidly dividing cells. Besides the cancerous cells, the cell types that are affected most by the chemotherapy are bone marrow/blood cells, cells of hair follicles, cells lining the digestive tract and the reproductive tract. Enzyme inhibitors, apoptosis inducing drugs and angiogenesis inhibitors are called the targeted therapy that can spare the normal cells from the cytotoxic effects of chemotherapy drugs. The delivery route of chemotherapy drugs can be oral (p.o.), intravenous (i.v.), intramuscular (i.m.) or subcutaneous (s.q.); i.v.

route is the most commonly used one. Immunotherapy either actively stimulates the body's own immune system to fight the disease or exerts the therapeutic effects passively by administered immune system components. Naked monoclonal antibodies (MAbs), radiolabeled antibodies or MAbs conjugated to bacterial toxins are some examples. Immunotherapy has been more successful in the early stages of the disease. These therapeutic agents can be administered as a monotherapy or more commonly as a combination therapy. Combination therapy approaches can be combination of multiple drugs (combination chemotherapy) or combination of multiple approaches of surgery, radiotherapy, chemotherapy and immunotherapy.

1.1.1 Colorectal cancer

Colorectal cancer (CRC) occurs in the tissues of the colon and rectum. Colorectal cancer is one of the leading causes of cancer related deaths throughout the world (McCormick et al., 2002). According to the estimated values from National Cancer Institute (NCI), by the end of year 2012, 51,690 deaths are expected due to CRC despite the increased screening and prevention efforts.

Histopathologically, the disease starts with hyperproliferation of the colon mucosa and the formation of benign adenomas with varying size, shape and dysplasia (Hamilton, 1992). Those adenomas turn into adenocarcinoma and finally invasive colorectal carcinoma through various stages due to oncogene activations, loss of tumor suppressors or epigenetic changes (Figure 1- 1). In sporadic CRC, inactivating mutations of both alleles of the tumor suppressor gene adenomatous polyposis coli (APC) and dysregulation of K-RAS proto-oncogene and induction of COX-2 expression are among the earliest events. An additional pathway responsible for CRC is microsatellite instability (MSI) which is observed in almost all

adenocarcinomas from patients with human non polyposis colorectal cancer (HNPCC) and 10-15% of sporadic colorectal cancers (Aaltonen et al., 1994; Gryfe et al., 1997; Konishi et al., 1996; Leslie et al., 2002). Chronic inflammation is another recognized risk factor for epithelial carcinogenesis. Patients suffering from inflammatory bowel diseases, such as ulcerative colitis and Crohn's disease are at increased risk of developing CRC, suggesting a link between chronic inflammation and cancer. The major carcinogenic events that cause sporadic CRC, such as chromosomal instability (CIN), MSI and hypermethylation, also occur in colitis-associated CRC. Oxidative stress is anticipated to have a role in this process. Inflammatory cells can produce reactive oxygen and nitrogen species that can cause damage in the genes involved in pathways such as tumor suppressor p53 and DNA repair genes. Other factors such as NF- κ B and COXs can possibly have contribution (Itzkowitz and Yio, 2004).

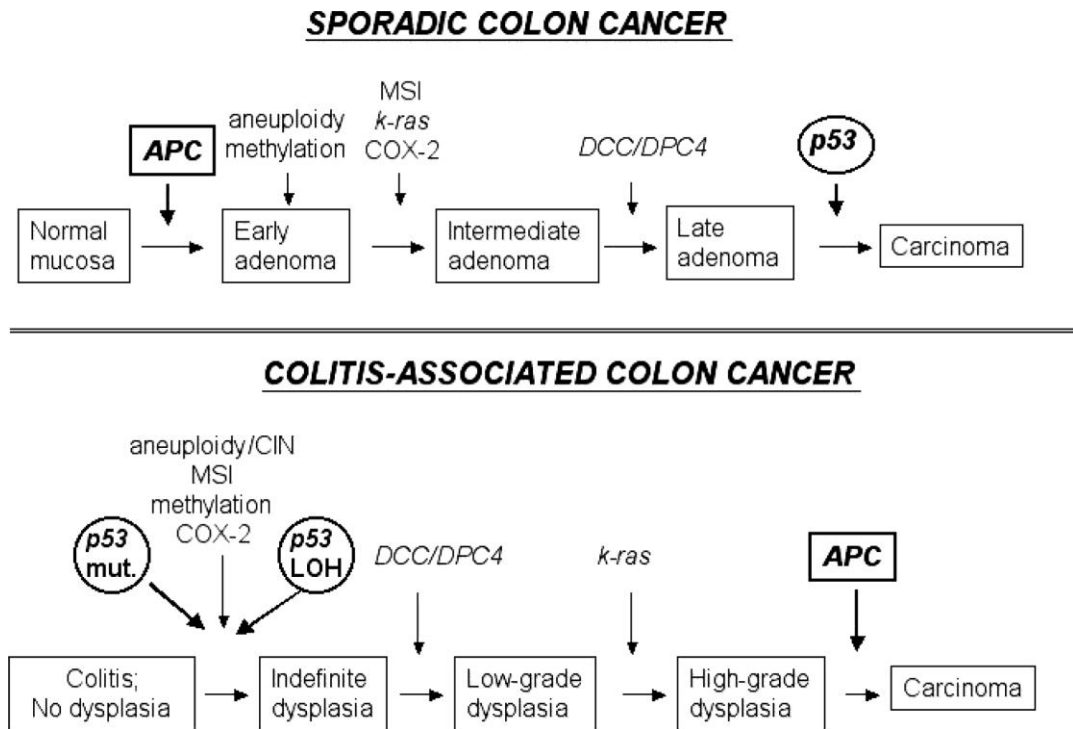


Figure 1- 1 Diagram for steps of molecular pathogenesis of sporadic colon cancer and colitis-associated colon cancer
(Itzkowitz and Yio, 2004)

Tumor cells or cells recruited to the tumor microenvironment produce inflammatory cytokines and chemokines that promote growth of tumor cells, disturb their differentiation processes and support the survival of cancer cells. Clinical observations in large populations and epidemiological studies have shown that regular use of aspirin and other non-steroidal anti-inflammatory drugs (NSAIDs)

over a time period of 10 to 15 years can provide 40 to 50% reduction in the relative risk of developing colon cancer (Thun et al., 1991). More convincing evidence was obtained in the clinical studies where treatment with NSAID sulindac resulted in regression of adenomas in familial adenomatous polyposis (FAP) patients, who inherit a mutation in the APC gene (Giardiello et al., 1993). Therefore CRC represents a valuable platform to investigate the relationship between chronic inflammation and progression of cancer and test the effectiveness of new anti-inflammatory therapeutic agents.

1.1.2 Drug delivery systems for cancer therapy

A transformed (or malignant) cell and a normal cell have certain structural, functional and metabolic differences which can be exploited to design targeted therapy strategies in cancer. Some of the critical features are uncontrolled cellular proliferation, angiogenesis, tissue invasion and metastasis, evasion of apoptosis and insensitivity to growth inhibitory or death signals. The targeted approaches can be developed through the use of more specific anticancer agents or through methods of delivery. In the conventional cancer treatment strategies; the dose (or the extent of tissue removal in case of surgery) is limited by the damage caused in the surrounding or overall healthy tissue in the body. However; customized targeted systems can aid in achieving improved therapeutic index by increasing the local dose of the therapeutics and at the same time reducing the local or systemic side effects (Peer et al., 2007).

The main concerns of any targeted drug delivery system (DDS) are the capability of effective loading and delivery of a desired therapeutic cargo (either small molecule drugs or macromolecules such as DNA, RNA or peptides) to its target. Drug

loading can show great variation depending on carrier materials and methods of fabrication. Aside from drug loading, the rate of release determines the final in vivo distribution of the loaded drug and, hence, the overall effectiveness of the targeted therapy.

DDSs can be administered to the body via different routes such as pulmonary, oral, subcutaneous or by peripheral i.v. injection, the latter being the most reproducible way. The primary physiological determinants affecting the in vivo performance of i.v. administered nanoparticle DDS are the interactions with blood components, filtration by kidney and removal by the liver and spleen that are the major part of the mononuclear phagocyte system (MPS) (Bertrand and Leroux, 2011). Opsonization is a process of plasma protein deposition on particles that results in increased clearance rate by the MPS. Proteins of the complement system are the crucial players in the opsonization related clearance of DDS and surface properties such as charge, hydrophobicity and irregular surface morphology have important roles (Storm et al., 1995). Particles aimed for longer circulation times should be ideally 100 nm or less in diameter and have hydrophilic surface properties in order to reduce the clearance by macrophages (Storm et al., 1995). Hydrophobic particles are more susceptible to being taken up by the liver, or by the spleen and lungs (Brigger et al., 2002). Grafting the particle surfaces with hydrophilic polymers can generate a masking effect at the particle surface which can repel plasma proteins thereby prevent opsonization. Polyethylene glycol (PEG) is a well known biocompatible and relatively non-toxic polymer that has been used in pharmaceutical formulations to improve plasma circulation time. The molecular weight of the drug or DDS is another concern due to the glomerular filtration process in the kidneys. Particles with hydrodynamic diameters less than 5 nm and molecular weight below 60 kDa are cleared from the systemic circulation by the

kidneys (Bertrand and Leroux, 2011). The Kupffer cells of the liver are responsible for phagocytic activity and they account for 80–90% of the total body macrophage population. Contacts between DDSs and macrophages occur via the recognition of opsonins on the particle surface or through interactions with scavenger receptors on Kupffer cells. The size and radius of curvature of the particles are also relevant parameters regarding DDS-cell contacts and internalization. DDSs with diameters larger than 400 nm are captured rapidly by the cells of the MPS (Harashima et al., 1994; Torchilin, 2007). It is worth to mention that, the accumulation of particulate DDS in spleen is inversely proportional to hepatic uptake due to differences in blood flow; therefore PEGylated DDSs that can avoid uptake in the liver are delivered to the spleen in higher amounts compared to non-PEGylated ones (Allen et al., 1995). In general, long circulation times of DDSs can be correlated with positive clinical outcomes like enhanced tumor accumulation and sustained pharmacological effects (Perrault et al., 2009). However, prolonged residence of the DDS in the bloodstream can also cause undesired side effects. For example, patients treated with doxorubicin (DXR) loaded PEGylated liposomes with extended plasma circulation time elicited dose-limiting cutaneous toxicities (Lorusso et al., 2007).

A high level of selectivity towards cancerous tissue can be obtained by designing targeted particulate or colloidal drug delivery systems for chemotherapy drugs or combination therapies. In the tumor tissue, secreted factors such as vascular endothelial growth factor (VEGF) which is also known as vascular permeability factor (VPF) enhance the permeability of the vasculature (Senger et al., 1983). Moreover, the rapid vascularization process that takes place in order to fulfill the requirements of fast growing cancer cells results in disordered vascular permeability. This increased vascular permeability at the tumor sites causes a selective increase in the extent of transfer of macromolecules from circulation to

tumor tissues. Furthermore, at the tumor sites the lymphatic system can not operate as effective as in the normal tissue to drain the accumulated interstitial fluid (Swartz, 2001). Therefore, retention of DDSs in the tumor interstitium is increased, enabling cellular interactions or high local concentrations of the delivered contents. This phenomena is called the “enhanced permeability and retention effect” (EPR effect) (Maeda and Matsumura, 1989). In other words, the defective vascular architecture coupled with dysfunctional lymphatic drainage allows the “passive targeting” of DDSs. Studies performed with liposomal DDSs with variable sizes demonstrated that the threshold for extravasation is approximately 400 nm, while particles with diameters below 200 nm were found to be more effective in terms of accumulation at the tumor site (Hobbs et al., 1998; Yuan et al., 1995).

In case of “active targeting”; particular surface antigens that are overexpressed in cancer cells are of major interest. Carbohydrates such as lectins (Yamazaki et al., 2000) or polypeptides such as cell surface receptors can be ideal targets for drug delivery provided that they are not expressed at all or expressed at lower levels in other tissues.

Targeting ligands are required not only to enable binding to surface proteins with high affinity, but also to induce internalization of the drug delivery systems. The crucial aspect of internalization was reported elaborately in xenograft models where Doxorubicin-loaded HER2 targeted immunoliposomes produced marked improvements in therapeutic results in HER2-overexpressing tumors when compared to the other treatment conditions tested, including free doxorubicin, nontargeted liposomal doxorubicin, recombinant anti-HER2 MAb trastuzumab, and combinations of these other agents (Park et al., 2002). Although the accumulation of non-targeted liposomes in solid tumor site due to EPR effect did not show anti-

tumor efficacy, HER2 targeted IL were effective in binding and internalization by HER2 overexpressing cells (Kirpotin et al., 2006). Another example was immunoliposomes containing anti-CD19 ligand that can be internalized exhibiting a more significant therapeutic outcome, while immunoliposomes prepared with non-internalizing anti-CD20 ligand did not lead to comparable efficacy (Sapra and Allen, 2002). In contrast to these examples, delivery by DDSs that are not internalized might be argued to offer other advantages such as exposure of more number of cells in the solid tumor area after the contents are released and in addition death of neighboring cells even if they lack the target surface proteins (Allen, 1994).

1.2 COXs and cancer

Cyclooxygenases (COX) are lipid oxidizing enzymes producing prostaglandins (PG), prostacyclins and thromboxanes. There are two major isoforms of COX enzymes; COX-1 and COX-2. Although COX-1 is constitutively expressed in many tissues and has some housekeeping functions, COX-2 expression is induced by inflammatory stimuli like cytokines, growth factors, tumor promoters, and viral infection, resulting in increased synthesis of prostaglandins (PGs) in inflamed or neoplastic tissues (Subbaramaiah et al., 1996). Moreover, COX-2 is found to be overexpressed in several human cancers (Prescott and Fitzpatrick, 2000). PGH_2 , the precursor prostaglandin generated by COX enzymes, can be converted to PGD_2 , PGJ_2 , PGE_2 and PGI_2 by different prostaglandin synthases which in turn function in different signaling pathways via specific G-protein coupled receptors (Funk, 2001).

In order to examine the role of COX in CRC, the expression levels of COX-1 and COX-2 were determined in human adenomas and adenocarcinomas (Eberhart et al., 1994; Sano et al., 1995). The results pointed out that there was a little difference in COX-1 expression between the neoplastic and adjacent normal tissue, on the other hand COX-2 expressions were found to be increasing in adenoma and adenocarcinoma tissues with respect to normal colonic mucosa. This variation in the expression profiles suggests that tumor growth can be suppressed through inhibition of NSAIDs. However, the argument that “elevated levels of COX-2 are a consequence of the carcinogenic process and that the enzyme has no direct role in promoting CRC growth” is still valid (Gupta and DuBois, 2000b). Oshima et al. employed a genetic approach to investigate the role of COX-2 in colorectal tumorigenesis. By assessing the development of intestinal polyposis in *Apc*^{Δ716} mice (a murine model for human FAP) in a wild-type and homozygous null COX-2 genetic background, it was discovered that the number and size of polyps was reduced dramatically in the COX-2 null mice compared to COX-2 wild-type mice (Oshima et al., 1996). In addition, when *Apc*^{Δ716} COX-2 wild-type mice were treated with a novel selective COX-2 inhibitor, MF tricyclic, number of polyps was reduced more significantly than in treatment with non-selective COX inhibitor drug sulindac. This experiment was one of the first to offer solid evidence to support the hypothesis that NSAIDs can inhibit tumor growth via inhibition of COX-2. More recent studies have confirmed a pro-oncogenic role for COX-2. For example, Liu et al. developed transgenic mice in which the murine mammary tumor virus promoter/enhancer regulates human COX-2 expression. Their gain-of-function study have shown that overexpression of COX-2 alone was sufficient to induce cellular transformation in transgenic mice. Similar study by Neufang et al. suggested that in basal keratinocytes transgenic expression of COX-2 resulted in dysplasia and epidermal hyperplasia offering an association between the COX-2

expression and pre-neoplastic lesion development in the skin (Neufang et al., 2001). In addition, in urinary bladder basal epithelial cells, COX-2 overexpression triggered translational cell hyperplasia, transitional cell carcinomas and dysplasia (Klein et al., 2005).

This association of COX-2 overexpression and cancer becomes more meaningful with the known fact that regular use of COX inhibitors, Non-steroidal anti-inflammatory drugs (NSAIDs), such as aspirin has a protective effect in variety of cancers. NSAIDs are effective for inflammatory pain relief and significantly, more recently, for the prevention of colorectal cancer (Dubois et al., 1998; Smalley and DuBois, 1997). The use of aspirin (Baron et al., 2003) and non-aspirin non-steroidal anti-inflammatory drugs (NSAIDs) is found to halve the risk of colon cancer and is an important factor for chemoprevention (Smalley et al., 1999). Part of the antitumor activity of NSAIDs stems from COX inhibition, particularly the COX-2 isoform. COX-2 dependent effects involve the inhibition of apoptosis as well as promotion of cell migration and invasion while the stromal effects involves angiogenesis and metastasis promotion (Gupta and Dubois, 2001).

Regardless from their inhibition of COX-1 and COX-2, high doses of NSAIDs have been documented to be modifying the biology of the cultured cells. For instance in all wild type, COX-1^{-/-}, COX-2^{-/-} or COX-1^{-/-}/COX-2^{-/-} mice, fibroblast cells were found to be sensitive to NSAID-induced cell death (Zhang et al., 1999). Since, depending on the dose and the type used, any xenobiotic agent may have more than one target, these results might not be surprising. I κ B kinase β (Yin et al., 1998), peroxisome proliferator-activated receptor (PPAR) family of nuclear hormone receptors (Lehmann et al., 1997; Yamamoto et al., 1999) and the pro-apoptotic gene *BAX* (Zhang et al., 2000) are some of these COX independent targets. In all of these

targets, effects independent from COX were observed at 50-1,000 μM drug concentrations which corresponds to 1- to 200-fold higher than serum concentration of celecoxib (2-5 μM approximately) sufficient reduce the growth of tumors in CRC animal models (Williams et al., 2000). Although it is highly probable that the best biochemical targets of NSAIDs at these concentrations are COX enzymes, there could be other high affinity targets which are affected as well.

1.2.1 COX-2 inhibitors

Conventional NSAIDs are non-specific COX inhibitors which can bind to active site of both COX-1 and COX-2. Inhibition of COX-1 activity results in serious side effects such as gastrointestinal bleeding (Wolfe et al., 1999). However, recently developed specific COX-2 inhibitors (coxibs) are shown to have reduced risk of gastrointestinal side effects (Figure 1-3). Nevertheless specific COX-2 inhibitors may not be completely safe. Rofecoxib (brand name Vioxx®) was withdrawn from the market due to increased risk of myocardial infarction and stroke. Celecoxib (brand name Celebrex®) (CLX) is currently available on the market for the treatment of arthritis. Similar to other NSAIDs such as ibuprofen, naproxen, and meloxicam; Celecoxib has the safety warning on the product label, especially for the patients with previous history of cardiovascular events.

The effects of coxibs in terms of chemoprevention were reported in several clinical studies. Administration of rofecoxib at 25 mg a day for 9 months, demonstrated a significant reduction of rectal polyposis in a placebo-controlled study (Higuchi et al., 2003). The chemopreventive effects of CLX was investigated in a relatively large randomized study in FAP patients where 6 months of treatment with 800 mg CLX per day resulted in a dose-dependent reduction of duodenal and rectal

adenomas (Steinbach et al., 2000). On the other hand, no significant decrease in the number and size of polyps was observed compared to placebo in patients receiving 200 mg CLX a day (Phillips et al., 2002).

Although safety issues persist, some pleiotropic effects of CLX were discovered that are either COX-2 dependent or COX-2 independent. COX-2 dependent effects can be classified as induction of apoptosis, inhibition of angiogenesis, inhibition of invasiveness, modulation of inflammation and immune-suppression and conversion of carcinogens (FitzGerald, 2003). COX-2 independent effects include but are not limited to inhibition of cell cycle progression, induction of apoptosis and inhibition of angiogenesis (Grosch et al., 2006) (listed in Table A.1) and reduction of membrane fluidity and metastatic potential in cell culture models (Sade et al., 2012). Additionally, the COX-2 independent anti-tumor effect of CLX was shown in a rat model which was not a direct effect of cytotoxicity but rather related to its effects on tumor microenvironment (de Heer et al., 2008). The antiproliferative effect of CLX is unique in this family of compounds, that is one of the reasons why Celecoxib is the only coxib that is approved adjuvant treatment of patients with familial adenomatous polyposis (FAP) (Schiffmann et al., 2008).

Considering the possible systemic side effects of oral formulations, there is a growing interest on new drug delivery systems for coxibs (**Figure 1- 2**). Taking into account that most COX-2 inhibitors are water insoluble drugs and oral formulations have low bioavailability (between 22% and 40%) (FitzGerald and Patrono, 2001), drug delivery systems with a wide range of sizes, physicochemical properties and routes of delivery were designed; PLGA microparticles, chitosan microspheres, beta cyclodextrin-drug complex in multilamellar liposomes are a few examples developed for CLX (Jain et al., 2007; Thakkar et al., 2004). Recently, a liposomal

CLX formulation was also tested and proven effective in DMBA induced rat model of colon cancer; even though this formulation did not contain any cholesterol or PEG (Perumal et al., 2011).

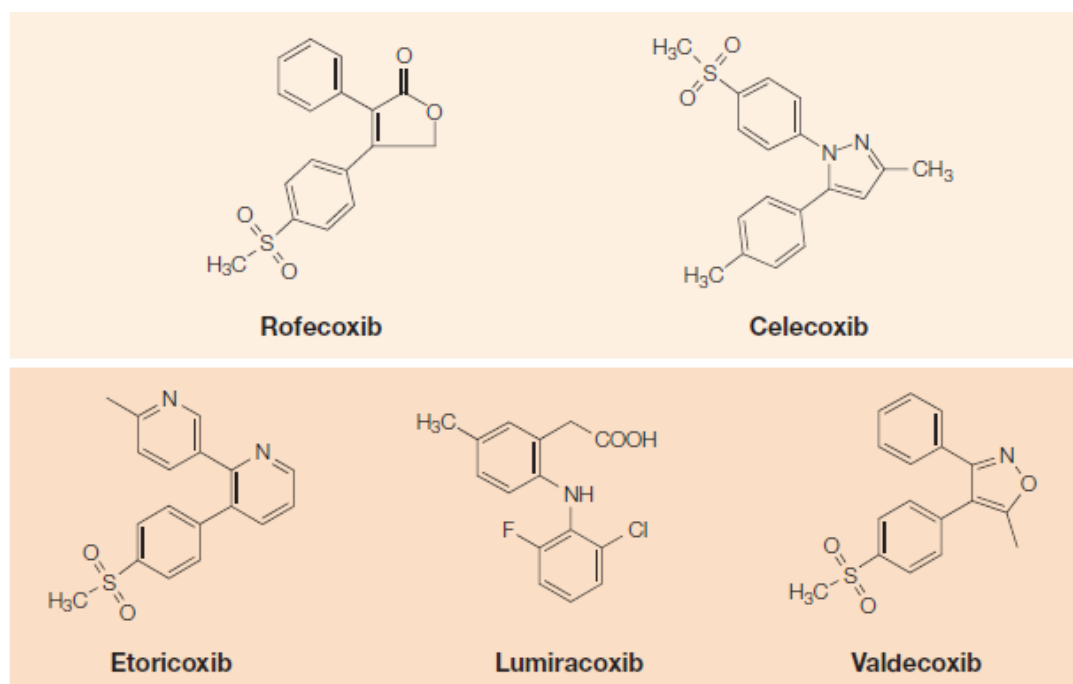


Figure 1- 2 Selective COX-2 inhibitors

Rofecoxib and Celecoxib are first generation; Etoricoxib, Lumiracoxib and Valdecoxib are second generation inhibitors (FitzGerald, 2003)

1.2.2 Crosstalk between COX-2 and EGFR pathways

The EGFR is a member of a family of four closely related receptors: EGFR, ERBB2 (commonly known as HER-2/neu), ERBB-3 and ERBB-4. The ligands of EGFR comprise a large family of growth factors including EGF, TGF α , amphiregulin (AREG), heparin binding-EGF-like growth factor (HBEGF), and betacellulin (BTC). Among these growth factors, TGF α has key modulatory functions in the proliferation processes of both normal and malignant epithelial cells. TGF α binds to EGFR causing subsequent activation of the EGFR tyrosine kinase enzymatic activity that triggers multiple intracellular signaling cascades (Aaronson, 1991). After ligand binding, the inactive monomers of the receptors undergo homodimerization or heterodimerization between EGFR and another member of the family. Following dimerization, the intracellular tyrosine kinase domain of the receptor is activated, via autophosphorylation, which initiates further activation of downstream intracellular events (Wells, 1999). The signaling pathway involves activation of RAS and MAPK, which activates several nuclear proteins, including cyclin D1, a protein required for progression of cell cycle from G1 to S phase. EGFR signaling is critical for cell proliferation and other crucial processes that are linked to cancer progression, including inhibition of apoptosis, induction of angiogenesis and metastasis (Figure 1- 3) (Noonberg and Benz, 2000; Perry et al., 1998; Wells, 1999; Woodburn, 1999). In cancer cells several mechanisms can be responsible from activation of the EGFR autocrine growth pathway, such as overexpression of the EGFR, increased concentration of ligand(s), decreased phosphatase activity, decreased receptor turnover, and the presence of aberrant receptors, including EGFR gene alterations (Ciardiello and Tortora, 2001). In connection with activation of EGFR pathway, the most common EGFR mutant found in human cancer is EGFRvIII (Moscatello et al., 1998). The frequently

amplified EGFRvIII is a truncated protein that has deletions in domains I and II of the extracellular domain of EGFR. This causes EGFRvIII to be activated independently of ligand interaction leading to constitutively activated tyrosine kinase domain which stimulates cell proliferation (Voldborg et al., 1997). TGF α and/or EGFR are overexpressed in many different solid human cancers, including breast, colorectal carcinomas, gastric, prostate, bladder, head and neck, ovarian and glioblastomas, in which it is associated with advanced disease state and poor prognosis (Salomon et al., 1995; Woodburn, 1999). Overexpression of EGFR has also been associated with resistance to other treatments including chemotherapy and radiotherapy and hormonal therapy (Akimoto et al., 1999; Chen et al., 2000; Salomon et al., 1995).

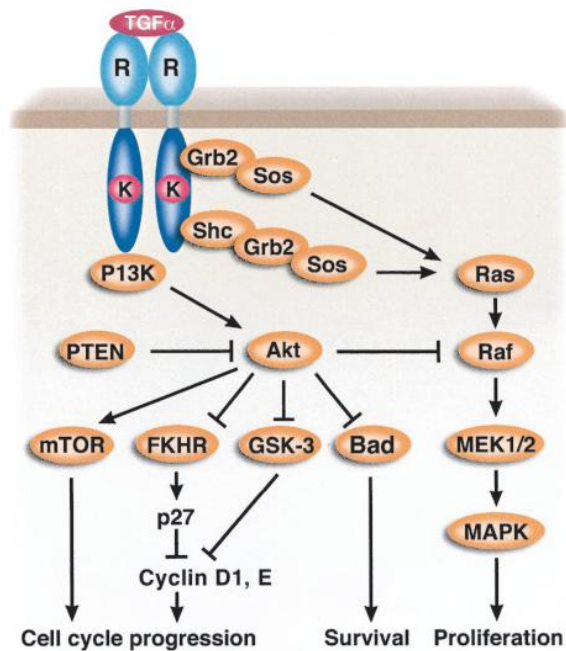


Figure 1- 3 EGFR pathway and downstream pathways

(Mendelsohn and Baselga, 2003)

In cancer therapy, the strategies to block EGFR signaling include anti-EGFR monoclonal antibodies (MAb) or fragments as therapeutic agents themselves to prevent receptor activation or conjugated to toxins or pro-drugs; low molecular weight tyrosine kinase inhibitors (TKIs) that interfere with receptor signaling and antisense oligonucleotides or ribozymes that block receptor translation (Ciardiello et al., 2001; Jannot et al., 1996; Yamazaki et al., 1998). Small molecule TKIs can prevent the autophosphorylation of the intracellular tyrosine kinase domain of the receptors; on the other hand, MAbs or fragments can compete with natural ligands EGF and transforming growth factor alpha (TGF α) in binding to EGFR to prevent downstream signaling and as a result show growth inhibitory effect (Fan et al., 1994). There are murine antibodies (postfix-omab, e.g., edrecolomab) which are highly immunogenic, chimeric antibodies (postfix- ximab, e.g., cetuximab) which have human sequences for constant regions and are less immunogenic, humanized antibodies with 95% human sequences (postfix-zumab, e.g., trastuzumab) in which only the complementarity determining regions (CDR) at the antigen binding site are from murine origin and finally there are human antibodies developed by the use of transgenic mice such as the Xenomouse® (postfix- mumab, e.g., panitumumab) which were made possible by the humanization of the murine humoral immune system by replacing the mouse antibody generating loci with the human heavy and light chains.

The effectiveness of EGFR targeted therapies depends not only on EGFR expression status, but also KRAS, BRAF and PI3K mutations and their expression levels can be decisive in identifying the patient populations that are most likely to benefit from the therapy (Banerjee and Flores-Rozas, 2010).

Cetuximab (Erbix, IMC-225) is an EGFR IgG1 manufactured as a human/mouse chimeric monoclonal antibody (MAb). The MAb C225 interacts with the ligand binding domain of the EGFR to block ligand binding and initiates receptor endocytosis and intracellular trafficking. In February 2004, Cetuximab was approved for use in patients with metastatic CRC by the U.S. Food and Drug Association (FDA). In March 2006, Cetuximab received another approval for the treatment of head and neck cancer by FDA. Currently more than 40 countries approved to use Cetuximab and thousands of patients have been treated with this drug.

There is convincing evidence that a crosstalk exists between EGFR and COX-2 pathways. Activation of EGFR signaling by ligand binding, dimerization and autophosphorylation leads to increase in MAPK activity that results in AP-1 mediated induction of COX-2 transcription. When COX-2 transcription increases, more PGs are produced including PGE₂. Several recent studies have reported that PGE₂ can activate EGFR signaling and thereby stimulate cell proliferation. The mechanism(s) by which this occurs might be; through matrix metalloproteinase dependent transactivation of EGFR, through activation of the cAMP/protein kinase A pathway by PGE₂ leading to increased expression of EGFR ligand amphiregulin, and also transactivation of EGFR by an intracellular Src-mediated event independent of the release of an extracellular ligand of EGFR (Dannenberget al., 2005). In all these possible mechanisms, a positive feedback loop is initiated by exposure to COX-2-derived PGE₂ and by this means, activation of EGFR results in enhanced expression of COX-2 and increased synthesis of PGs. This leads, in turn, to a further enhancement of EGFR activity (Figure 1-4) (Choe et al., 2005).

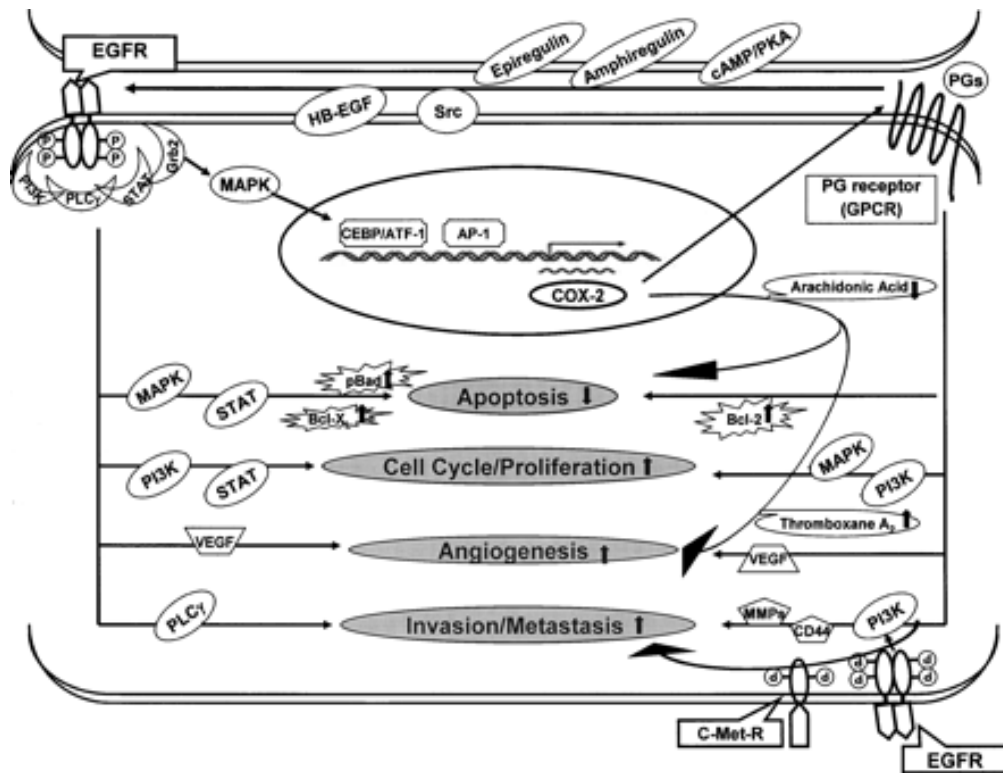


Figure 1- 4 Crosstalk between the EGFR and COX-2 pathways

(Choe et al., 2005)

There is considerable attention on cancer chemoprevention and treatment therapies targeting both EGFR and COX-2 (Buchanan et al., 2007; Choe et al., 2005; Gupta and DuBois, 2000a). Simultaneously blocking the proliferative signaling pathway initiated by EGFR and inhibiting synthesis of prostaglandins by COX-2 has shown synergistic effect in xenograft models for squamous cell carcinoma of the head and neck (SCCHN) and for intestinal cancer (Buchanan et al., 2007; Zhang et al., 2005). These studies are not limited to pre-clinical settings, but there are several clinical

trials employing combinations of EGFR inhibitors (both tyrosine kinase inhibitor small molecule drugs and anti-EGFR MAb) and COX-2 inhibitors including celecoxib, apricoxib, and sulindac (US Library of Medicine, 2012) .

1.3 Liposomal drug delivery systems

The concept of liposomes and the method of preparation were first described by Bangham et al in 1965 (Bangham et al., 1965). Liposomes are self-assembling phospholipid bilayer structures that can be prepared from natural or synthetic phospholipid sources. These vesicles can encapsulate water soluble molecules in the aqueous volume while water insoluble molecules can be embedded in the hydrophobic region within the lipid bilayer. In general, vesicles can be prepared by three methods: physical dispersion, two-phase dispersion and detergent solubilization (Szoka and Papahadjopoulos, 1980). The simplest and the most widely used protocol for preparing liposomes is the thin lipid film hydration method introduced by Bangham et al (Bangham et al., 1965). The biocompatible and biodegradable components of liposomes make them attractive candidates for drug delivery. Natural phospholipids such as egg phosphatidylcholine are biologically inert, have low toxicity and weakly immunogenic. Furthermore, drugs with different hydrophobicities can be encapsulated into liposomes: highly hydrophobic drugs are entrapped in the lipid bilayer, strongly hydrophilic drugs are encapsulated in the aqueous volume, and drugs with intermediate octanol to water partition coefficient (logP) can partition in the interface between the bilayer and in the aqueous core. Liposomes can be classified according to their lamellarity such as unilamellar, oligolamellar and multilamellar vesicles; according to their size such as small, intermediate, or large; and according to the preparation method such as

reverse phase evaporation vesicles, or dehydrated-rehydrated vesicles (Torchilin and Weissig, 2003). Multilamellar vesicles (MLVs) usually have diameters of 1-5 μm and they are comprised of several concentric lipid bilayers similar to an onion structure. The high lipid content of MLVs serves to passively entrap lipid-soluble drugs. Unilamellar vesicles consist of one lipid bilayer and generally have diameters of 50-250 nm (Torchilin and Weissig, 2003).

Liposomes can be considered as alternative solubilizing agents water insoluble molecules. 50,000 fold increased solubility was reported for a hydrophobic drug when encapsulated by liposomes (Liu et al., 2006). Incorporation of PEG derivatized lipids in the lipid bilayer offers long circulation time in blood stream by inhibiting rapid uptake by reticuloendothelial system. In addition to enhanced permeability and retention effect (EPR), meaning passive targeting of liposomes to tumor site, active targeting is employed by attaching tumor specific ligands or antibodies to the lipid or PEG chains (Gabizon et al., 2006). The evolution of different types of liposomes are reviewed (Torchilin, 2005) as given in **Figure 1- 5**.

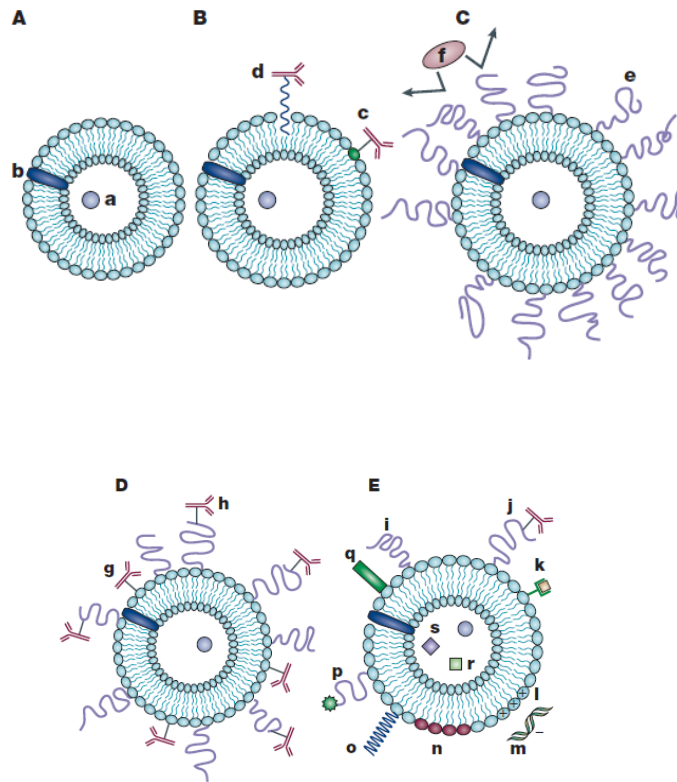


Figure 1- 5 Evolution of liposomes

(a) ‘plain’ liposomes with water soluble drug in the aqueous liposome interior, (b) hydrophobic drug incorporated into the liposomal membrane, (c) Antibody-targeted immunoliposome with antibody covalently coupled to the reactive phospholipids in the membrane, (d) or anchored into the liposomal membrane. (e) Long-circulating liposome coated with a polymer such as PEG, which shields the liposome surface from the interaction with opsonins (f) Long-circulating immunoliposome bearing both protective polymer and antibody, which can be attached to the liposome surface (g) or, preferably, to the distal end of the grafted polymeric chain

Figure 1-5 continued

(h). New-generation liposome, the surface modified (separately or simultaneously) by the attachment/incorporation of the diagnostic label (k); positively charged lipids (l) forming complex with DNA (m); stimuli-sensitive lipids (n); stimuli-sensitive polymer (o); cell-penetrating peptide (p); viral components (q); magnetic particles (r) for magnetic targeting and/or colloidal gold or silver particles (s) for electron microscopy (Torchilin, 2005).

1.3.1 Conventional liposomes

In general, drug therapies suffer from two major problems, namely biodistribution throughout the body and undesired toxic effects in healthy tissues with discontinuous endothelium, such as the liver, spleen, and bone marrow. Liposomal DDSs can overcome these limitations by protecting the encapsulated molecules from degradation and can passively target tissues or organs targeting via specific ligands. On i.v. administration, conventional liposomes are rapidly removed from the blood circulation after being captured by the mononuclear phagocyte system (MPS) (Storm et al., 1995). Therefore, by default liposomal DDSs support efficient delivery of antiparasitic and antimicrobial agents to treat infections localized in the mononuclear phagocytic system (MPS). On the contrary, when the desired site of delivery is beyond the MPS, efficient liposome uptake by the macrophages and removal from circulation become disadvantageous. The MPS does not recognize the liposomes directly but instead recognizes opsonin which are bound to the surface of the liposomes. Complement components which originally function in immediate host defense against invading pathogens comprise another important system to recognize liposomes (Harashima et al., 1994). Complement system acts through initiation of membrane lysis and results in enhanced uptake by the MPS cells

(neutrophils, monocytes, macrophages). The complement dependent release of liposomal contents appears to be one of the dominant factors in determining the biological fate of liposomes *in vivo* (Chonn et al., 1992). A balance between blood opsonic proteins and suppressive proteins has been found to regulate the rate of liposome clearance (Ishida et al 2002). Liposomes can be destabilized in plasma due to their interaction with high (HDL) and low density (LDL) lipoproteins and this interaction results in the rapid release of the encapsulated drug into the plasma (Immordino et al., 2006).

The stability of lipid bilayers and the types of proteins that bind to their surface are affected in great by physicochemical properties of liposomes, such as size, surface charge, hydrophobicity, membrane fluidity and packing density of the lipid bilayers (Chonn et al 1992; Oja et al 1996). Bilayer fluidity can be modified by manipulating the composition of the lipid membranes. Incorporation of cholesterol (Chol) in the bilayer decreases the interaction of phospholipids and HDL by increasing the packing of phospholipids in the lipid bilayer (Damen et al., 1981). The type of phospholipid source is also a matter of concern regarding the stability of liposomes. Senior et al (1982) reported that liposomes prepared from phosphatidylcholine (PC) with unsaturated fatty acyl chains tend to be less stable in the blood circulation than liposomes prepared from PC with saturated fatty acyl chains (with a high phase transition temperature) or from sphingomyelin (SM). Uptake of liposomes by MPS can be also reduced by modulating the size and charge of the liposomes. In general, larger liposomes are eliminated from the blood circulation more rapidly than smaller ones (Senior and Gregoriadis, 1982). Phagocytes can distinguish between the sizes of foreign particles as observed in longer half-life of small unilamellar vesicles (SUVs) than that of multilamellar vesicles (MLVs). Based on the available information in the literature, it can be

concluded that the binding of opsonins to liposomes and similarly the enhanced uptake of liposomes by the MPS are size-dependent events (Harashima et al 1994).

Possible types of liposome-cell interactions are reviewed and given in **Figure 1- 6** (Torchilin, 2005).

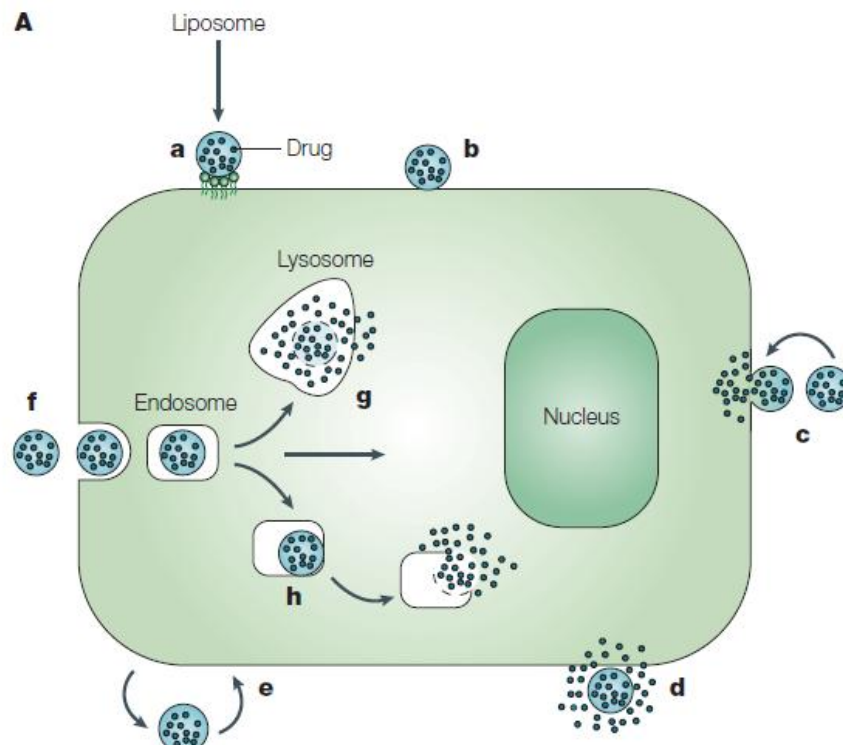


Figure 1- 6 Liposome-cell interactions

(a) specific or (b) nonspecific adsorption onto the cell surface, (c) fusion with the cell membrane, (d) destabilization by cell membrane components and micropinocytosis, (e) direct or transfer-protein-mediated exchange of lipid components with the cell membrane, (f) specific or nonspecific endocytosis (g), delivery by the endosome into the lysosome, (h) endosome destabilization (Torchilin, 2005).

1.3.2 Long circulating liposomes

Surface modification by hydrophilic polymers is a commonly used method in liposomal delivery systems. The main goals of surface modification are to prevent particle aggregation and to reduce the capture of the DDS by cells of the MPS. Due to their low degree of immunogenicity and antigenicity; (Abuchowski et al., 1977) Polyethylene ethylene glycol (PEG) molecules of various chain lengths can be used to provide a protective shield over the phospholipid bilayer. PEG is a linear polyether diol that has a chemically inert backbone and hydroxyl groups available for derivatization. There are commercially available PEG derivatives that are covalently bound to phospholipids, functional groups, proteins, and even fluorescent probes.

For intravenous delivery route, the size of colloidal DDS should be preferably below 200 nm in order to prevent opsonization and thereby activation of the complement system. (Harashima et al., 1994; Vonarbourg et al., 2006). On the contrary, any agent with molecular weight below 30 kDa would be subject to rapid renal clearance (Greish et al., 2003). Unlike low molecular weight small molecule drugs that tend to be cleared rapidly from blood circulation, drug carrier systems including liposomes have the crucial advantage of long circulation times enabling higher intratumor concentrations, known as EPR effect as introduced in Section 1.1.2. Passive targeting of liposomal delivery systems provides better therapeutic efficacy with fewer systemic adverse effects in solid tumors as well as in infectious and inflammatory conditions.

Liposomes benefit from “steric stabilization” achieved by conjugation of PEG to the liposome surface and sterically stabilized liposomes have lower

reticuloendothelial uptake, prolonged circulation time in the blood, and higher accumulation in tumors (Immordino et al., 2006). However, it was previously shown that surface grafted PEG (Mw 2000) at more than 1.3 mol% of total lipid (2% of total phospholipid) substantially reduced the uptake and cytotoxicity of doxorubicin-loaded anti-HER2 immunoliposomes in the cultures of target cells (Park et al., 1995).

1.3.3 Targeted liposomes

Besides long circulation feature brought by PEGylation and passive targeting effects, an ideal DDS should be able to carry the desired therapeutic agent to specific locations in the body. This can be achieved by active targeting via attachment of certain peptides, proteins or oligosaccharides onto the DDS surface. In cases where cell surface receptors are employed as targets; the ligand-receptor binding offers improved delivery and retention of the carrier within the disease site where the target cell population is located. Accumulation of liposomal delivery systems at the target site does not necessarily result in superior therapeutic efficacy unless cellular uptake of the liposomes occurs (Kirpotin et al., 2006).

Targeting ligands including antibodies can be either adsorbed on liposome surface or covalently bound to lipids or PEG chains on the surface (**Figure 1- 6**). There is a possibility that adsorbed molecules can be released and create a competitive effect on binding to target cells, for that reason covalent bonds are preferred for binding of ligands to surfaces. When antibodies are bound directly to the liposome surface, binding affinity for the target proteins on cell surface reduces due to the steric hindrance caused by the high density of PEG coating. Therefore, linking antibodies (or antibody fragments) to the distal end of PEG chains is a better approach

(Drummond et al., 1999). PEG molecules can be incorporated into the bilayer membrane via lipid anchors such as DSPE.

Monoclonal antibodies are among the most widely used targeting moieties that possess well established protocols for both production and characterization. Antibodies are naturally produced by B cells in response to antigens including pathogens. Immunoglobulins (Ig) are large glycoproteins consisting of two pairs of light and heavy chains that are held together by intra-chain disulfide bonds. In mammals, there are five classes namely IgG, IgM, IgA, IgE, or IgD. Targeted liposomes are formed using mostly IgG and occasionally IgM molecules. IgG exists as a monomer whereas the soluble form of IgM generally exists as a pentamer. Antibodies can be subjected to enzymatic degradation or reducing agents to generate smaller fragments while preserving the antigen binding function. For example, treatment of IgG with papain or pepsin can be used to generate Fab' and F(ab')₂ fragments, respectively. The size differences of IgGs or IgG fragments are of importance when conjugating the molecules to liposomes, particularly affecting parameters such as conjugation efficiency and liposome aggregation (Ansell et al., 2000).

In order to construct antibody-liposome conjugates (immunoliposomes), primarily four types of methods are used: amine modification, carbohydrate modification, disulfide modification, and noncovalent conjugation (Ansell et al., 2000). Amine modification protocols can involve cross-linking agents such as 1-ethyl-3-(3-dimethylaminopropyl) carbodiimide hydrochloride (EDC) or N-hydroxysuccinimide (NHS), also heterobifunctional cross-linkers such as N-succinimidyl 3-(2-pyridyldithio)propionate (SPDP), N-succinimidyl S-acetylthioacetate (SATA) and N-succinimidyl-4-p-maleimidophenyl-butyrate

(SMPB) which offer better control on the conjugation reaction. Carbohydrate modifications can be applied on the glycosylated antibodies where the carbohydrate groups are typically attached to the C_H² domain within the Fc region. Directed conjugation through antibody carbohydrate avoids the antigen binding regions while allowing for use of intact antibody molecules. Mild oxidation of the polysaccharide sugar residues with sodium periodate generates aldehyde groups (Beduneau et al., 2007). A crosslinking or modification reagent containing a hydrazide functional group then can be bound to these aldehydes for coupling to another molecule.

For covalent conjugation of IgG fragments to liposomes, one of the most widely used approaches is the reaction of sulfhydryl groups with maleimide functional groups. Small molecule reducing agents such as β -mercaptoethanol (β -ME), 2-mercaptoethylamine (cysteamine or 2-MEA) or 2-Dithiothreitol (DTT) can be used to cleave intra-chain disulfide bonds and produce reactive sulfhydryl groups. β -ME or DTT reagents reduce all the disulfide bonds resulting in dissociating heavy and light chains, whereas milder reagent 2-MEA cleaves preferably the hinge region of the IgGs thereby producing monovalent IgG without dissociating heavy and light chains. This enables the preservation of the antigen recognition sites at the distal ends (Ansell et al., 2000). Under neutral pH, the thiol is added to the double bond of the maleimide to form a thioether bond. The reaction of maleimides with amines is possible at higher pH values than reaction of maleimides with thiols, hence maleimide and thiol reaction is said to be specific at neutral pH. After the conjugation reaction, unreacted antibodies of antibody fragments need to be removed from the mixture, in other words immunoliposomes should be purified. Any residual fragments can cause a competition effect for the target receptors when administered to body, therefore would mislead the pharmacokinetic and distribution

studies. Immunoliposomes can be purified by ultra centrifugation, ultra filtration, dialysis and size exclusion chromatography (Torchilin and Weissig, 2003).

There are a few reports of Phase I clinical trials with immunoliposomal drug formulations. PEGylated liposomes loaded with Doxorubicin were functionalized with F(ab')₂ fragments of the human MAb GAH (the IL named MCC-465) were tested on patients with metastatic or recurrent stomach cancer to determine maximum tolerated dose, dose limiting toxicity and define recommended phase II dose and pharmacokinetics parameters (Matsumura et al., 2004). Similarly, Doxorubicin loaded anti-EGFR ILs were prepared by conjugating Fab' fragments of the MAb C225 (Cetuximab) to assess maximum tolerated dose together with pharmacokinetics and anti tumor response (Rochlitz et al., 2011).

The EGFR family member HER2/*neu* glycoprotein is another surface antigen that is frequently used for active targeting purposes. Although normal healthy tissue is positive for HER2 expression, overexpression is unique to tumors; especially breast cancers (25%–30% of cases), gastric, colon, ovarian, and non-small-cell lung carcinoma (Baselga and Mendelsohn, 1994). Therefore HER2 is suitable for targeting liposomes selectively to malignant HER2 overexpressing cells.

1.4 Aim of the study

The serious picture about current situation of CRC has been summarized as “Colorectal cancer (CRC) leads to approximately 550,000 annual deaths worldwide and is thus a major public health concern. Once an individual presents with CRC, the disease is often advanced and current treatment regimens are often not effective” (Mann and DuBois, 2004).

Recently, COX-2 inhibitor therapy has emerged as a promising novel therapy for CRC chemoprevention and/or treatment. CLX can offer COX-2 dependent and COX-2 independent anti-carcinogenic effects including inhibition of cell cycle progression, induction of apoptosis and inhibition of angiogenesis. Given that there might be a positive feedback loop between EGFR and COX-2 pathways, simultaneous blockade of the EGFR and COX-2 pathways has proven effective in preclinical models and is currently being tested in clinical trials.

However, most conventional chemotherapeutics used in the clinic have limitations such as the inability to deliver therapeutics at high concentrations to the target tissues or causing severe toxic effects on normal organs and tissues. Many anticancer drugs, following oral or i.v. administration, have large volumes of distribution resulting from their rapid uptake into all the tissues of the body. In order to overcome these problems by providing “selective” delivery to the affected area; the ideal solution would be to target the drug only to those organs, tissues, or cells affected by the disease. Using drug carriers like liposomes can alter the pharmacokinetics and biodistribution of anticancer drugs. In addition to passive targeting of long circulating liposomes to tumor sites due to EPR effect, active

targeting strategies utilizing MAbs directed against cancer specific cell surface proteins have proven valuable.

The aim of the study can be summarized as:

- i. Design and characterization of liposomes capable of CLX encapsulation and retention
- ii. *In vitro* delivery of the CLX loaded PEGylated liposomes to cancer cell lines and functional evaluation of liposomal CLX treatment
- iii. Preliminary studies reflecting the possibility of designing a targeted delivery system for CLX using a monoclonal antibody against EGFR on the surface of the liposomes.

CHAPTER 2

MATERIALS AND METHODS

2.1 Materials

18:0 PC (1,2-Distearoyl-*sn*-Glycero-3-Phosphocholine) (DSPC), Cholesterol (ovine wool, >98%), 18:0 mPEG(2000)-DSPE (1,2-distearoyl-*sn*-glycero-3-phosphoethanolamine-N-[methoxy(polyethylene glycol)-2000) and DSPE-PEG(2000)Maleimide (1,2-distearoyl-*sn*-glycero-3-phosphoethanolamine-N-[maleimide(polyethylene glycol)-2000) were purchased from Avanti Polar Lipids (USA) (Figure 2- 1). Celecoxib (CLX) capsules were obtained from Ranbaxy Laboratories Limited (India). Celecoxib USP30 was purchased from Yick-Vic Chemicals & Pharmaceuticals (Hong Kong). SP-DiOC₁₈(3) was kindly provided by Assoc. Prof. Dr. İhsan Gürsel from Bilkent University Department of Molecular Biology and Genetics, Ankara Turkey. Lissamine™ rhodamine B 1,2-dihexadecanoyl-*sn*-glycero-3-phosphoethanolamine, triethylammonium salt (Rhodamine DHPE or Rh-PE) and human Transferrin-AlexaFluor680 conjugate (Tr-AF680) were purchased from Invitrogen (USA). Cysteamine hydrochloride (2-MEA) was purchased from Applichem (Darmstadt, Germany). Human IgG and mouse IgG (free of azide and BSA, lyophilized) were from Sigma-Aldrich (USA). Anti-EGFR monoclonal antibody (free of azide and BSA) was purchased from Thermo Scientific, Pierce Protein Research Products (Rockford, IL USA).

Chloroform and methanol were obtained from Merck (Germany). MTT reagent (3-(4,5-Dimethylthiazol-2-yl)-2,5-Diphenyltetrazolium Bromide) was purchased from Invitrogen (USA). Ultra filtration device (VivaSpin2) with MWCO 300 kDa membrane was purchased from Sartorius (Germany).

Human colon cancer cell line HCT-116 was purchased from German Collection of Microorganisms and Cell Cultures (DSMZ, Germany) and SW620 were purchased from American Type Culture Collection (ATCC, USA). Cell culture media and supplements were from Biochrom (Berlin, Germany). Human colorectal carcinoma cell line HT-29 was purchased from ŞAP Enstitüsü (Ankara, Turkey). Cell culture grade plastic ware was obtained from Greiner Bio-One GmbH (Germany).

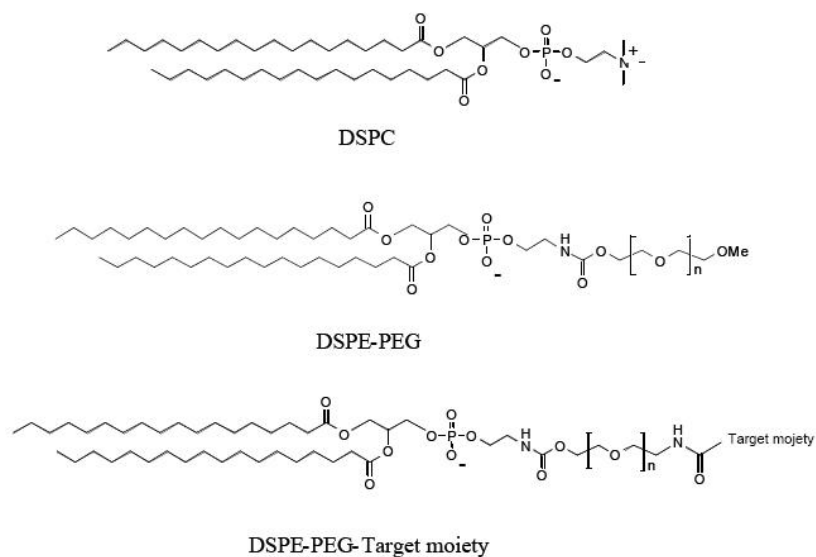


Figure 2- 1 Chemical structures of DSPC and DSPE-PEG

2.2 Methods

2.2.1 Preparation of liposomes

2.2.1.1 Preparation of MLVs

MLVs were prepared according to thin lipid film hydration method (Bangham et al., 1965). DSPC, cholesterol and Celecoxib were dissolved in chloroform to prepare stock solutions and mixed in proportions given in Table 2. 1 in round bottom Polypropylene (PP) tubes. Chloroform was evaporated under a gentle argon stream to form a thin lipid film. Lipid films were kept overnight under vacuum at 100 mbar to remove residual chloroform, then flushed with argon and stored at 4°C. Lipid films were hydrated with 1 ml PBS (0.1 M, pH=7.4) by heating at 70°C and vortex mixing in 2 minute cycles for a total duration of 1 hour. Tubes were sonicated in a bath type sonicator at 70°C for 15 minutes and allowed to reanneal at room temperature for at least 2 hours. MLVs were separated from untrapped drug by two subsequent centrifugations at 12,000 \times g for 15 minutes. Pellet was washed with PBS in between.

Table 2. 1 Composition of lipid films

	DSPC only	DSPC:Chol 10:1	DSPC:Chol 5:1	DSPC:Chol 2:1
DSPC (μmol)	40.00	40.00	40.00	40.00
Celecoxib (μmol)	8.78	9.66	10.54	13.17
Cholesterol (μmol)	0.00	4.00	8.00	20.00

2.2.1.2 Preparation of LUVs

The lipids films were prepared as described in Section 2.2.1.1. MLVs were subjected to 10 freeze-thaw cycles using liquid nitrogen to freeze the samples and a 55°C water bath to thaw the samples. LUVs were obtained by extrusion through track-etched polycarbonate (PC) membranes with defined pore sizes (Whatman Nuclepore). Extrusion was performed at 70-75°C by passing liposome suspensions 5 times through 800 nm, 5 times through 400 nm and 15 times through 100 nm membranes using Mini-extruder set (Avanti Polar Lipids, USA) (Figure 2- 2). Glass syringes filled with liposome suspensions were equilibrated at 70-75°C on the aluminum block provided in the Mini-extruder system for 15 minutes. The temperature was maintained constant during extrusion by placing the aluminum block on a heater. The resulting clear suspensions were subjected to size exclusion chromatography to separate untrapped drug from LUVs. Sephadex-G75 was packed in 10 ml disposable PD-10 columns (GE Healthcare, USA) by gravity. The elution buffer was PBS (0.1 M, pH 7.4). Collected fractions of LUVs were pooled and stored at 4 °C. Aliquots were withdrawn and dried completely for further

quantification of CLX and DSPC. For cell culture studies, LUVs were filter sterilized using 0.45 μm Polyethersulfone (PES) filters (Whatman Paradise).



Figure 2- 2 Mini-extruder system

2.2.1.3 Preparation of PEGylated LUVs

The LUVs were prepared as described and subjected to size exclusion chromatography as described in Section 2.2.1.2. mPEG(2000)-DSPE molecules were incorporated to liposomes via post-insertion method (Ishida et al., 1999) as 0.5% and 2% of DSPC content. Previously dried mPEG(2000)-DSPE lipid films were hydrated in PBS above the Critical Micelle Concentration (>20 mM) at 60°C for 60 minutes. Micelles were incubated with freshly extruded LUVs at 60°C for 1 hour with intermittent mixing.

For the preparation of ILs and corresponding non-targeted liposomes; mPEG(2000)-DSPE was added to lipid mixtures at 2% of total lipid. Rhodamine

labeled lipid Rh-PE was included in the lipid mixtures when necessary at 0.5 mol% and protected from light in the following steps.

2.2.1.4 Preparation of ILs

Isotype specific human or mouse IgG were used for optimization of the preparation and characterization of the immunoliposomes.

Lipid films were hydrated using HBS (HEPES buffered saline: 20 mM HEPES, 140 mM NaCl. pH: 7.0). PEGylated LUVs were prepared as described in Section 2.2.1.3 except mPEG(2000)-DSPE was added to lipid mixtures at 1.5% of total lipid and DSPE-PEG(2000)Maleimide was added at 0.5% of total lipid.

IgG reduction reaction conditions were optimized using mouse or human IgG. The concentration of reducing agent 2-MEA was varied between 40 and 200 mM. The effect of reaction duration was tested by changing the reaction durations to 15 minutes, 30 minutes and 90 minutes. Also, an IgG sample was fully reduced with β -ME and boiling to obtain heavy and light chains. Reaction mixture was prepared in deoxygenated HBS/EDTA (10 mM EDTA) to prevent metal catalyzed oxidation of reduced ends. Reduced IgG molecules were subjected to SDS-PAGE analysis followed by Coomassie blue staining in order to visualize fragments.

Monoclonal anti-EGFR mouse IgG (clone C225) was reduced with 200 mM 2-MEA for 90 minutes at 37°C. In order to remove the reducing agent, Zeba Desalting columns (Thermo Scientific) with MWCO 7 kDa were used after equilibrating the columns with HBS/EDTA. Conjugation reaction was performed at room temperature by incubating reduced IgGs with DSPE-PEG(2000)Maleimide

functionalized PEGylated LUVs overnight under Argon gas (Figure 2- 3). For 40 mM of liposomes, 100 μ g IgG was used. Unconjugated IgG fragments, untrapped drug and other unincorporated liposome constituents were removed by Ultra filtration using centrifugal device with MWCO 300 kDa following the manufacturer's instructions (Sartorius VivaSpin2).

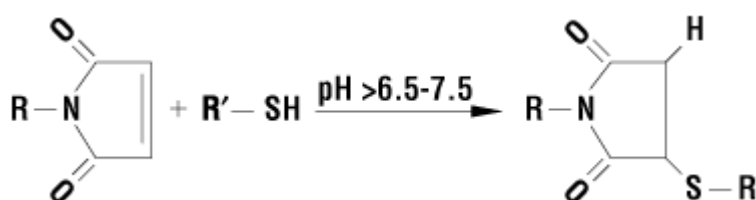


Figure 2- 3 Conjugation reaction between maleimide functional group and reactive sulfhydryl group

2.2.2 Quantification of Celecoxib

The amount of Celecoxib was determined either by direct spectrophotometric measurement at the λ_{max} of the drug or by a modified HPLC method using a C18 column.

2.2.2.1 Spectrophotometric method

Liposome samples were initially dried completely under vacuum, then dissolved in chloroform and analyzed by UV spectrophotometry at 260 nm. CLX concentration

in the solution was calculated from previously constructed CLX calibration curve (range: 10-100 µg/ml) in chloroform where pure solvent was used as blank (Figure A- 1).

2.2.2.2 HPLC method

A modified HPLC method (Dhabu and Akamanchi, 2002) was used to quantitate amount of CLX released to PBS media. Samples were dried completely under vacuum, and then redissolved in pure methanol. A Shimadzu HPLC equipment and Inerstil ODS-3 C18 column (5µm x 250 mm x 4.6 mm) were used under ambient conditions with 85:15 (v/v) methanol:water as mobile phase at a flow rate of 0.8 ml/min. All samples were filtered through 0.45 µm filters before injection. Samples in solution were used within 8 hours of reconstitution. Detection was performed at wavelengths 254 nm and 260 nm. A representative chromatogram is given in Figure A-4. Amount of CLX was calculated from previously constructed calibration curve in methanol (Figure A- 3).

2.2.3 Quantification of phospholipids (DSPC)

DSPC was quantified by UV-visible spectrophotometry using a standard method (Stewart, 1980). Samples were diluted in chloroform at appropriate ratios and mixed with ammonium ferrothiocyanate solution (1:1 v/v) by vortex mixing for 1 minute followed by centrifugation at 5000 *x g* for 5 minutes. The bottom (chloroform) phase was separated and DSPC was quantified at 485 nm using a previously constructed DSPC calibration curve (range: 5-50 µg/ml) where pure solvent was used as blank (Figure A- 2).

2.2.4 Characterization of liposomes

2.2.4.1 Particle size analysis

Average diameters of MLVs were determined by laser diffraction using Malvern Mastersizer 2000 (METU Central Lab). MLV samples were briefly sonicated for 2 minutes before measurement to separate the aggregated spheres. $d(0.5)$ values were reported to represent the volume median diameter where 50% of the distribution is above and 50% is below the median, calculated from the volume distribution data.

LUV and PEGylated LUV samples were diluted 1:10 with PBS. Concentrated ILs containing isotopic mouse IgG were diluted 1:200 in HBS whereas concentrated ILs containing the anti-EGFR monoclonal antibody (clone C225) were diluted 1:750 in HBS. Average hydrodynamic diameters of liposomes were determined by laser diffraction using Zeta sizer after incubation for 1 minute at 25°C (Nano ZS90, Malvern Instruments, METU Central Lab). The hydrodynamic diameters of the particles were reported as Z_{avg} and the PdI value was reported as an indication of the heterogeneity of the distribution. The population of particles with PdI up to 0.05 was considered as “monodisperse”, 0.05 to 0.08 as “nearly monodisperse” and 0.08 to 0.7 as “mid-range polydispersity”.

2.2.4.2 Morphological characterization by Transmission Electron Microscopy (TEM)

For morphological characterization of MLVs, TEM analysis was performed using a LEO 906 E microscope (Ankara University, School of Medicine, Dept. of Histology and Embryology). MLVs (5 μ l) were air-dried on 400 mesh formvar coated copper grids and for negative staining; grids were soaked into 2% uranyl acetate solution for 10 minutes. Grids were gently rinsed with 50 ml of dH₂O to remove excess dye and samples were air-dried. Imaging was performed by operating at 80 kV.

For morphological characterization of CLX loaded and empty PEGylated LUVs; liposomes (40 mM) were diluted 1:50 in PBS followed by negative staining with 2% uranyl acetate on 400 mesh formvar coated copper grids. TEM images of were obtained at 80kV using a JEOL JEM 2100F microscope (METU Central Lab).

2.2.4.3 Drug encapsulation efficiency and percent drug loading

For MLV samples; 50 or 100 μ l aliquots of MLVs were dried completely under vacuum using HETO-spin vac system (HETO, Allerod, Denmark) and redissolved in chloroform by vigorous vortex mixing.

For LUV or PEGylated LUVs; 50 or 100 μ l aliquots of samples were dried completely under vacuum using HETO-spin vac system (HETO, Allerod, Denmark) and redissolved in chloroform by vortex mixing to disrupt the liposomes. CLX amount was determined as described in Section 2.2.2.1.

Drug encapsulation efficiency was calculated as in Equation 1.

$$\% EE = \frac{mg \text{ CLX in liposome}}{mg \text{ CLX initially added}} \times 100 \quad (1)$$

DSPC amount was calculated as described in Section 2.2.3. Cholesterol amount was assumed as 100% of added amounts.

Percent drug loading was calculated as in Equation 2.

$$\% \text{ loading} = \frac{mol \text{ CLX}}{mol \text{ DSPC} + mol \text{ Cholesterol}} \times 100 \quad (2)$$

2.2.4.4 *In vitro* release profiles

For MLVs; one volume of MLVs (125 μ l) was directly mixed with 10 volumes of PBS (1250 μ l) in polypropylene tubes and incubated at 37°C and agitated at 400 RPM. Aliquots (100 μ l) were withdrawn after 6, 12, 24, 48 and 72 hours. Samples were centrifuged at 12,000 x *g* for 15 minutes. Supernatants were removed; pellets were dried completely under vacuum and then redissolved in chloroform to be analyzed by UV spectrophotometry as described in Section 2.2.2.1. The amount of CLX retained in MLVs was calculated together with the amount of DSPC in the same samples. Three independent experiments were performed.

For LUV or PEGylated LUVs; *in vitro* drug release experiments were performed in a custom made experimental set up with cellulose acetate dialysis membranes

(Molecular weight cut off: 12 kDa, Sigma Aldrich, Germany). For 1 ml liposome suspension, 15 ml release medium (PBS; pH 7.4) was applied at 37°C, under mild and constant agitation conditions. Aliquots (1 ml) withdrawn from release medium at different time points were dried completely under vacuum (Labconco FreeZone, Model 77520) and redissolved in 200 µl pure methanol. All samples were filtered through 0.45 µm filters before quantification by HPLC as described in Section 2.2.2.2. Samples in solution were used within 8 hours of reconstitution. Detection was performed at wavelengths 254 nm and 260 nm.

2.2.4.5 IgG conjugation efficiency

IgG conjugation efficiency to liposomes was determined indirectly by quantification of the unbound IgG molecules collected in the filtrate during ultra-filtration procedure. Bradford protein assay was used to detect the proteins using the micro microplate protocol (range 1-25 µg/ml) following the manufacturer's instructions (Thermo Scientific). The sample (150 µl) was mixed with 150 µl of Coomassie Plus reagent, incubated for 10 minutes at room temperature and absorbance was recorded by a Bio-Rad microplate reader at 570 nm.

2.2.5 Cell culture conditions

The human colon cancer cell line SW620 was routinely cultured in Leibovitz L-15 medium supplemented with 10% FBS, 2 mM L-glutamine and 1% Penicillin-Streptomycin, in a humidified atmosphere at 37°C and 100% air (or supplemented with 2 g/L NaHCO₃ and maintained in 5% CO₂). HCT-116 and HT-29 cell were cultured in McCOY's 5A modified medium supplemented with 10% FBS, 2 mM L-

glutamine and 1% Penicillin-Streptomycin (or phenol-red free RPMI 1640 media supplemented with 10% FBS, 2 mM L-glutamine and 1% Penicillin-Streptomycin for experiments involving fluorescently labeled probes or MTT reagent). Characteristics of human colorectal adenocarcinoma cell lines HCT-116, HT-29 and SW620 are listed in Table A.2.

2.2.6 Evaluation of cellular association of liposomes

Liposomal drug formulations were evaluated in terms of cell surface binding and cellular uptake qualitatively via confocal laser scanning microscopy (CLSM) and quantitatively via fluorescence activated cell sorting (FACS) analysis methods.

2.2.6.1 Laser scanning confocal microscopy (LSCM) analysis

For fluorescence LSCM, SW620 cells were cultured on glass coverslips in 6-well plates at 2×10^5 cell density for 3-4 days and treated with Lissamine-Rhodamine labeled liposomes at 500 μ M and 200 μ M lipid concentration in complete medium containing 10% FBS. After treatment for 30 minutes, 2 hours and 6 hours; media containing labeled liposomes were removed; cells were washed 3 times with PBS, followed by mounting on glass slides. Cell culture grade PBS was used as mounting media. Images were obtained using Plan-Neofluar 40x/1.3 Oil DIC objective in Zeiss LSM 510 system (METU Central Lab, Molecular Biology and Biotechnology Research Center). For each set of analysis, untreated control cells were used as negative controls. Excitation wavelength of 543 nm was used with LP560 filter for emission and imaging was completed in 15 minutes after mounting for live cell

imaging. Excitation and emission spectra of Rhodamine labeled lipid is given in Figure A-5.

In an alternative experimental set up, SW620 cells were cultured on glass cover slips in 6-well or 12-well plates at $1-2 \times 10^5$ cell density for 3-4 days and treated with Rhodamine labeled liposomes at 500 μ M lipid concentration in phenol red free complete medium containing 10% FBS. In order to visualize the early endosomal or recycling compartments, cells were treated with the endosomal marker Transferrin-AlexaFluor680 conjugate (10 μ g/ml final concentration) for 1 hour. Medium containing labeled liposomes was removed; cells were washed 3 times with PBS, fixed with 4% formaldehyde solution (freshly prepared from paraformaldehyde in PBS) and imaging was performed using Laser scanning confocal microscope (Zeiss LSM510, METU Central Laboratory). For each set of analysis, untreated control cells were used as negative control in order to adjust the multi-track configuration parameters. For Rhodamine signal, samples were excited with a HeNe laser at 543 nm and emitted signal was filtered with LP560 emission filter. For Tr-AF680 signal, another HeNe laser was used for excitation at 633 nm and LP650 filter was used for emission signal (Excitation and emission spectra of the two fluorophores were given in Appendix B). Channel cross-talk was minimized by using cells labeled with one fluorophore and adjusting detector gain parameters belonging to the other fluorophore. Signal from Rhodamine label was pseudo colored as red while AF680 signal was pseudo colored as green. Excitation and emission spectra of Rhodamine labeled lipid is given in Figure A-6.

2.2.6.2 Fluorescence activated cell sorting (FACS) analysis

Detailed quantitative analyses of cell association of the CLX loaded fluorescently labeled liposomes were performed using FACS analysis. Liposomes (40 μmol lipids) were post-labeled with membrane labeling dye SP-DiOC₁₈(3) at 20 μM final concentration by incubating at 70°C for 1 hour. Excess dye was removed by Ultra filtration using centrifugal device with MWCO 300 kDa (Sartorius VivaSpin2). Labeled liposome samples were filter sterilized by 0.45 μm PES filters (Whatman). HCT-116 and SW620 cells were cultured in 6-well plates until 80% confluency, treated with labeled liposomes (1000 μM lipid) in phenol-red free complete media containing 10% FBS. After treatment for 30 minutes, 2 hours and 6 hours, the medium was removed and the cells were washed 3 times with PBS and collected by trypsinization. Cells were fixed by dropwise addition of 100 μl 4% Formaldehyde solution during vortex mixing to obtain single cell suspensions. Cross-linking was terminated by addition of 2 ml of 1% BSA in PBS. Cells were collected by centrifugation at 5000 x *g* for 10 minutes, then resuspended in 500 μl PBS and stored at 4°C. Fixed cells were analyzed in AccuriC6 Flow cytometer and CFlow software (Bilkent University, Department of Molecular Biology and Genetics). Initially 10,000 events were collected for each sample in FL-1 channel. During the analysis, gating was performed separately on HCT-116 and SW620 cell populations on the corresponding Forward Scatter (FSC) vs. Side Scatter (SSC) dotplot.

2.2.7 Cellular viability and toxicity assay

Cells were cultured as 10^4 cells/well in 96-well plates and allowed to recover for 48 hours. Cells were treated with the indicated concentrations of CLX solution in DMSO, CLX loaded PEGylated liposomes or ILs in complete media containing 10% FBS. After the indicated treatment durations, the MTT labeling reagent was added to complete media (without phenol red), incubated for 4 hours, and cells were lysed with 1% SDS solution. The absorbance was recorded in a Bio-Rad microplate reader at 570 nm 18 hours later. In this assay, the water soluble MTT (3-(4, 5-dimethylthiazol-2-yl)-2, 5-diphenyltetrazolium bromide) is reduced to an insoluble formazan by mitochondrial dehydrogenases in the viable cells.

2.2.8 *In vitro* scratch wound healing assay

Cellular motility was evaluated by an *in vitro* scratch wound healing assay. SW620 cells were cultured in 12-well plates. When the confluency reached 95%, the monolayer of cells was scratched with a sterile pipette tip followed by treatment with CLX (in DMSO), CLX loaded liposomes and empty liposomes as controls. Immediately after wounding, images were captured with an inverted microscope with 4X or 10X objectives and wound closure was monitored with microscopy up to 120 h (Olympus, Hamburg, Germany). The area fractions of the wounds were calculated using the ImageJ 1.42 program and reported as in Equation 3.

$$\% \text{ Closure} = \frac{\text{Initial wound area} - \text{Final wound area}}{\text{Initial wound area}} \times 100 \quad (3)$$

2.2.9 Statistical analyses

All experiments were repeated at least 3 times. Data analysis and graphing was performed using the GraphPad Prism 5 software package. One-way ANOVA was performed with Tukey's multiple comparison test. When comparison was between two groups; parametric Student's t-test or the non- parametric Mann-Whitney U test applied. Statistically significant difference was considered at the level of $p < 0.05$.

CHAPTER 3

RESULTS

3.1 Characterization of CLX loaded MLVs

3.1.1 Particle size distribution and morphology of MLVs

The particle size distribution was analyzed by laser diffraction principle and hydrodynamic diameter of the particles in solution was calculated utilizing Mie theory by the Malvern Mastersizer2000 software. The hydrodynamic diameter corresponds to the diameter of a spherical particle with same translational diffusion coefficient as the particle being analyzed; therefore it is not a direct measurement of the actual particle size. As an indication of the width of the distribution, $d(0.5)$ and $d(0.9)$ values are reported in Table 3. 1 and representative $d(0.1)$ values can be seen on the representative images. $d(0.5)$ value represents the volume median diameter where 50% of the distribution was above and 50% is below, calculated from the volume distribution. Similarly $d(0.9)$ and $d(0.1)$ values represent the diameter where 90% and 10% of distribution was below the indicated value, respectively.

MLV samples were briefly sonicated for 2 minutes before size distribution measurement to separate the aggregated spheres. This brief sonication did not alter the particle size measurements as inferred from the $d(0.5)$ values from a trial run

before and after sonication process (results not shown). Representative images of size distributions of MLV particles in solution are given in Figure 3.1.

The particle size of CLX loaded MLVs are summarized in Table 3.1. The mean vesicle sizes (d (0.5)) varied between 5.45 ± 0.24 and 6.23 ± 0.13 μm . Addition of cholesterol at a low ratio to DSPC (1:10) resulted in larger MLVs, but did not have any effect at highest ratio (1:2). However, the mean sizes were very similar for all groups and the differences were not at significant levels.

Table 3. 1 Particle size of CLX loaded MLVs

Liposome formulation	MLV size (μm)	
	d(0.5)	d(0.9)
DSPC only	5.49 ± 0.13	16.25 ± 0.86
DSPC:Chol 10:1	6.23 ± 0.13	18.79 ± 2.16
DSPC:Chol 5:1	5.59 ± 0.99	15.89 ± 3.09
DSPC:Chol 2:1	5.45 ± 0.24	19.35 ± 6.30

Values denote Mean \pm S.D. for two independent experiments.

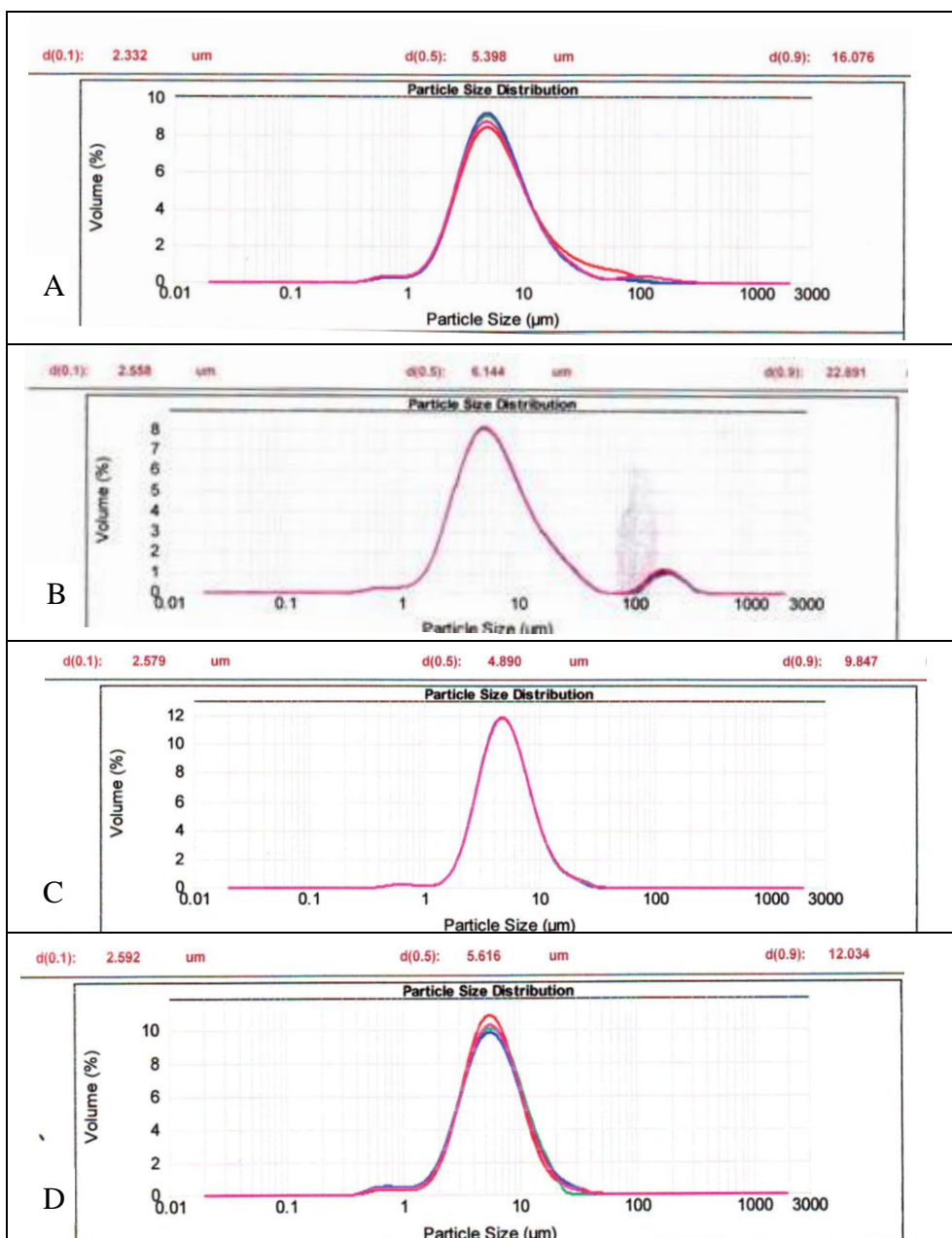


Figure 3- 1 Representative particle size distribution analysis results for MLVs

A) DSPC only, B) DSPC:Chol 10:1, C) DSPC:Chol 5:1, D) DSPC:Chol 2:1

In order to assess the structural stability of MLVs in release media, size distribution analysis was repeated after 72 hours of incubation at 37°C with agitation (results not shown). The regular release medium was PBS (0.1M, pH 7.4). Although there were slight reductions in size of MLVs prepared with cholesterol, it was concluded that MLVs could maintain their structural stabilities during 72 hours of agitation.

The results of TEM imaging clearly demonstrated the multilamellar structure of the MLVs. Since the dye uranyl acetate penetrates through the lipid bilayers, borders of MLVs could be visualized as multiple layers (Figure 3-2). The vesicle sizes observed in TEM images were not considered as indicators of the actual sizes since the number of samples in the imaged area was not sufficient for quantitative analysis.

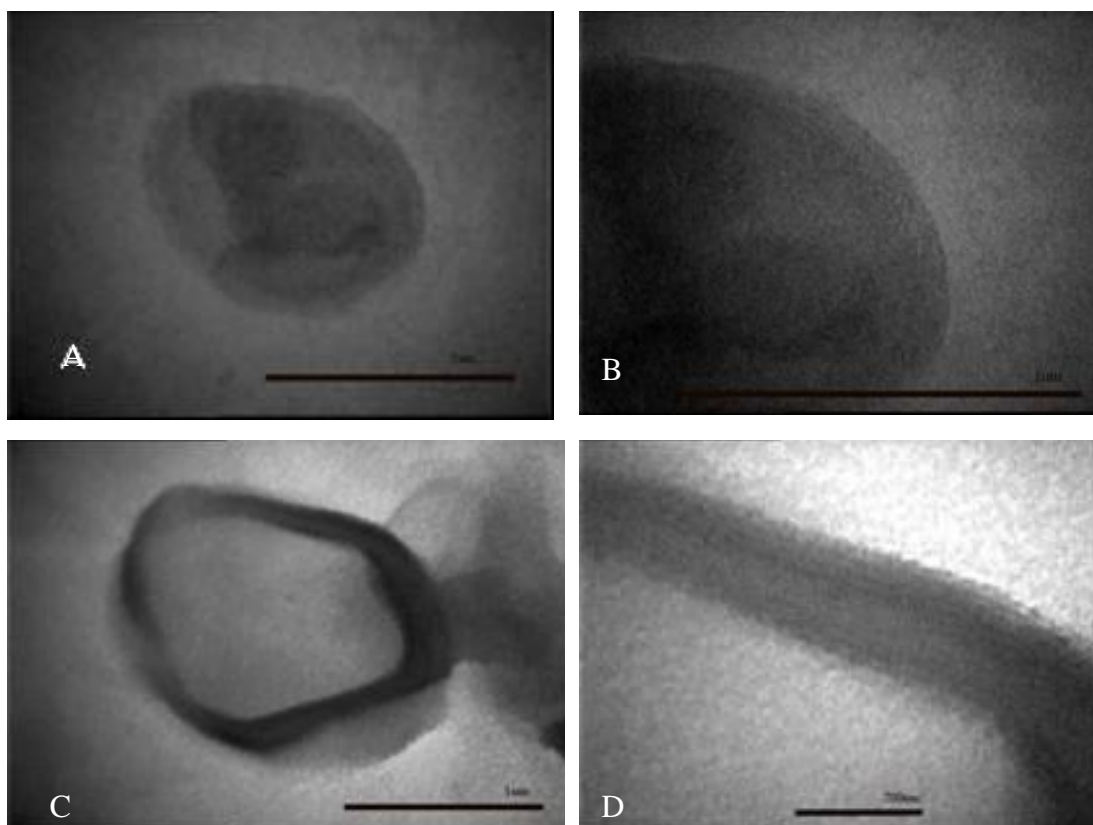


Figure 3-2 TEM images of MLVs

- A. MLV prepared with DSPC only, 77.500X magnification
- B. MLV prepared with DSPC only, 129.300X magnification
- C. MLV prepared with DSPC:Chol 10:1 molar ratio, 60.000X magnification
- D. MLV prepared with DSPC:Chol 10:1 molar ratio, 215.600X magnification

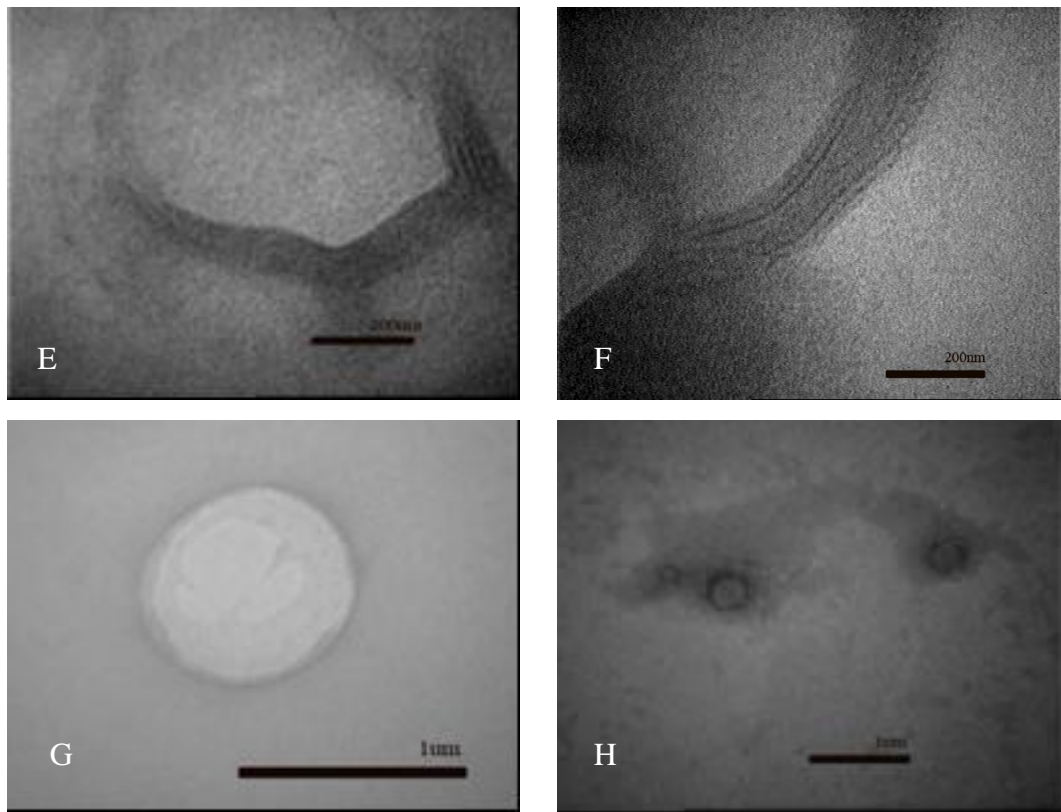


Figure 3-2 continued

- E. MLV prepared with DSPC only, 77.500X magnification
- F. MLV prepared with DSPC only, 129.300X magnification
- G. MLV prepared with DSPC:Chol 10:1 molar ratio, 60.000X magnification
- H. MLV prepared with DSPC:Chol 10:1 molar ratio, 215.600X magnification

3.1.2 Drug encapsulation efficiency and percent drug loading

Percent drug encapsulation efficiency was calculated for CLX loaded MLVs in terms of mg drug encapsulated per mg drug added during lipid film preparation. Results for four different compositions are tabulated in Table 3.2. Increasing the amount of cholesterol in MLVs up to 2:1 mol ratio caused a significant reduction in CLX encapsulation efficiency ($p < 0.01$, one-way ANOVA Dunnett's multiple comparison test with "DSPC only" group as control). The decrease in the encapsulated drug content was proportional to the gradual increase in the cholesterol content. Percentage of drug loading in terms of mol drug per hundred moles of total lipids (DSPC plus cholesterol) was also calculated and is given in Table 3.2. In accordance with EE results, CLX loading to DSPC:Chol liposomes also decreased with increasing cholesterol concentrations. Thus, MLVs prepared with DSPC only had the highest loading of CLX, whereas MLVs having DSPC:Chol molar ratio of 2:1 had the lowest amount of loaded CLX. The difference between the formulations, however, was not statistically significant (ANOVA Dunnett's multiple comparison test with "DSPC only" group as control).

Table 3. 2 Characteristics of CLX loaded MLVs

Liposome formulation	CLX EE (% mg/mg)	CLX loading (% mol/mol lipid)
DSPC only	111.79 ± 5.24	27.56 ± 4.77
DSPC:Chol 10:1	106.13 ± 4.74	26.82 ± 3.07
DSPC:Chol 5:1	100.42 ± 4.34	24.19 ± 2.15
DSPC:Chol 2:1	82.41 ± 3.96**	21.01 ± 0.79

EE: Encapsulation efficiency

Values for EE and loading denote Mean ± S.E.M for three independent experiments. **p<0.01 compared to DSPC only MLVs One-way ANOVA, Tukey's multiple comparison test

3.1.3 *In vitro* release profiles

Among the four formulations used, MLVs without cholesterol released the highest amount of CLX, followed by DSPC:Chol groups of 10:1, 5:1 and 2:1, in a decreasing order (Figure 3-3). The latter two groups showed almost equal rates of release. After 72 hours of release, DSPC MLVs could retain 39% of their initial CLX, whereas DSPC:Chol of 10:1, 5:1 and 2:1 were found to retain 67%, 72% and 77% of their CLX content, respectively. When the percentages of CLX retained in MLVs were normalized to the lipid content of each sample, DSPC only liposomes were seen to retain remarkably lower CLX (11% mol CLX/mol lipid), whereas other MLVs could retain CLX at higher percentages supporting the result that

highest extent of drug release occurred in cholesterol-free formulations. The drug release was not in a sudden burst in any of the four MLVs, especially the cholesterol containing MLVs exhibited a sustained release for even more than 72 hours.

In release profiles, one-way ANOVA using Tukey's multiple comparison test was conducted separately for each time point. The effect of high cholesterol content on the release behavior was apparent even at the 6th hour of release where DSPC only and DSPC:Chol 2:1 MLVs showed significant difference ($p < 0.05$) (Table A. 3). In the following time points, the differences in cumulative amounts of CLX released between DSPC only and the other three cholesterol containing formulations were also significant at different levels, the most noticeable difference ($p < 0.0001$) being at the 72nd hour.

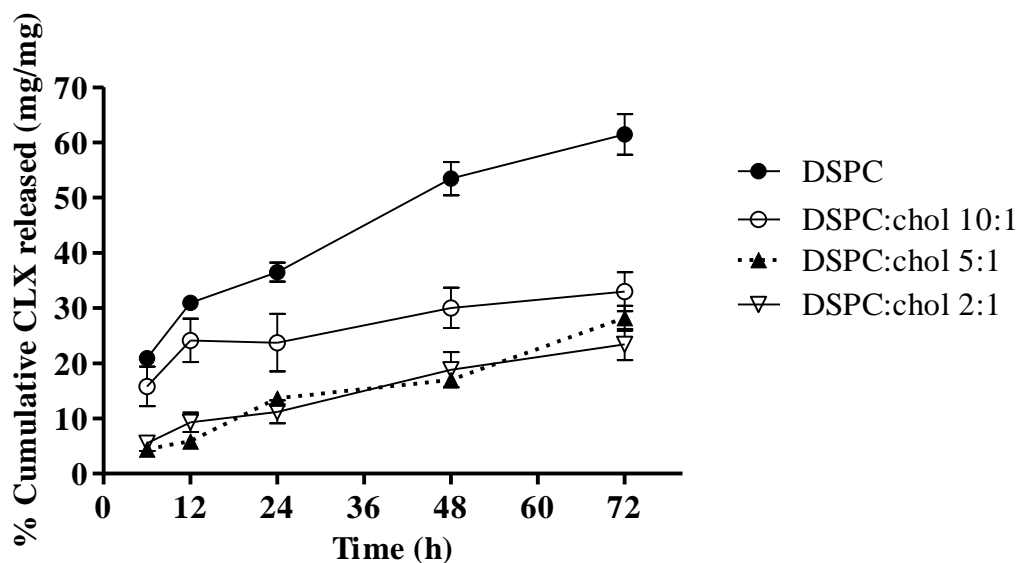


Figure 3- 3 *In vitro* CLX release from MLVs in PBS at 37°C.

Values denote mean \pm S.E.M for three independent experiments.

The amount of CLX released in different time points was analyzed statistically and reported in Table A.3.

3.2 Characterization of CLX loaded LUVs and PEGylated LUVs

3.2.1 Particle size distribution and morphology

The extrusion process resulted in unimodal size distribution of liposomes with a narrow distribution range. Mean hydrodynamic diameters of different formulation groups were in the range 101 ± 3.17 to 146 ± 17.0 . Addition of PEG molecules or cholesterol did not reveal significant differences in particle size distribution of the

vesicles (Table 3.3) except for DSPC:Chol 10:1 formulation with 0.5% PEG. The average value of PDI for 2% PEGylated cholesterol free liposomes was 0.027 ± 0.007 ; this was the lowest among all tested formulations and indicated that particle populations were nearly monodisperse. The non-PEGylated liposomes were in the mid-range polydispersity with PDI values of 0.174 ± 0.019 and 0.178 ± 0.033 for cholesterol free and DSPC:Chol 10:1 formulations, respectively. 0.5% PEGylated liposomes also displayed mid-range polydispersity. DSPC:Chol 5:1 formulation revealed the highest PDI value of 0.384 ± 0.073 which can be considered as contribution of the relatively high Chol content and absence of PEG. Repeating the size distribution analysis two weeks later showed that vesicle sizes were slightly reduced but the reduction was not significant for the formulations containing 2% PEG (results not shown).

TEM results were in accordance with the hydrodynamic diameter measurements and provided additional information revealing spherical morphology and unilamellar structures of CLX loaded vesicles (Figure 3- 4).

Table 3. 3 Particle size of liposomes with variable cholesterol and PEG contents

Liposome formulation	Z_{avg} (nm)	PdI
DSPC only	111.6 ± 2.84	0.174 ± 0.019
DSPC with 0.5% PEG	100.0 ± 2.48	0.223 ± 0.038
DSPC with 2% PEG	101.5 ± 3.47	0.027 ± 0.007
DSPC:Chol 10:1	117.4 ± 3.98	0.178 ± 0.033
DSPC:Chol 10:1 with 0.5% PEG	145.5 ± 17.0	0.137 ± 0.051
DSPC:Chol 10:1 with 2% PEG	101.2 ± 3.17	0.043 ± 0.014
DSPC:Chol 5:1	153.1 ± 12.7	0.384 ± 0.073

Values denote Mean ± S.E.M. , n≥3.

Z_{avg}: Average hydrodynamic diameter of particles. PdI: Polydispersity Index

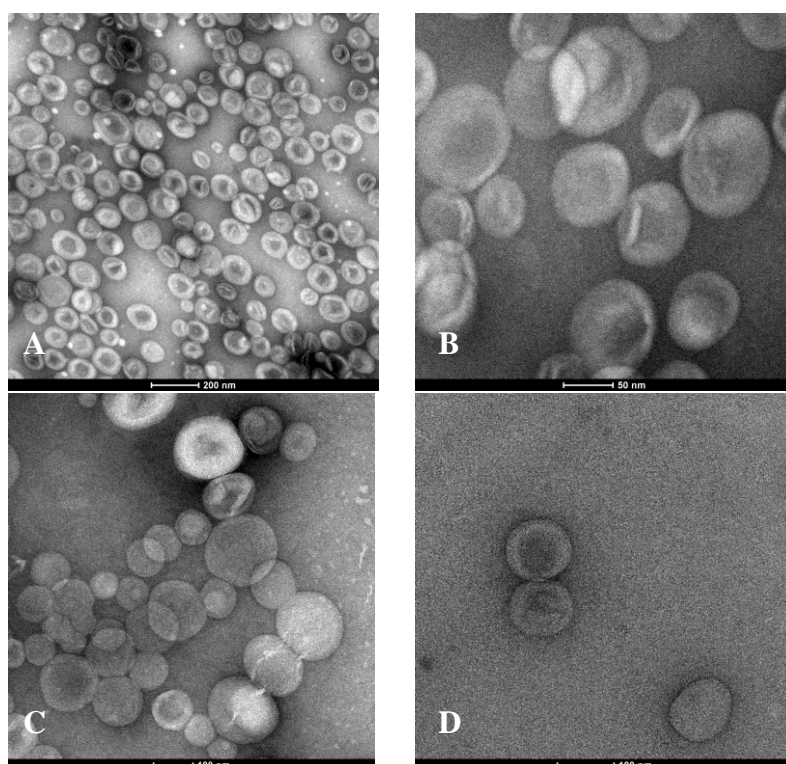


Figure 3- 4 TEM images of CLX loaded and Empty PEGylated liposomes.

A & B : Empty PEGylated LUVs, C & D : CLX loaded PEGylated LUVs

3.2.2 Drug encapsulation efficiency and percent drug loading

The drug encapsulation efficiencies and drug loading percentages were calculated for liposome formulations with varying cholesterol and PEG contents. All formulations were shown to successfully encapsulate more than 70% of the initial amount of the hydrophobic drug CLX that was added during lipid film formation (Table 3. 4). The drug loading percentages, which are a measure of the drug to lipid ratio, were similarly very high and comparable to the theoretical 100% drug loading

values. This also indicated the overall efficiency of the method of preparation regarding the given formulations. In cholesterol-free formulations, interestingly, 2% PEGylated liposomes were found to encapsulate highest percentage of CLX ($p < 0.01$ with respect to non-PEGylated LUVs and $p < 0.001$ with respect to 0.5% PEGylated LUVs). In cholesterol containing formulations, different PEG contents did not result in any significant difference in terms of drug encapsulation efficiency (One-way ANOVA with Tukey's Multiple Comparison Test). Percent CLX loading, being a better indicator of drug content in the final formulations, was statistically comparable in all formulations when analyzed by One-way ANOVA; however when formulations were compared in pairs by t-test, DSPC 2% PEG formulation had significantly different results than several of the other formulations. Although incorporation of cholesterol or PEG-DSPE did not result in a consistent trend, the results revealed the necessity for a detailed investigation of the effect of liposome constituents in drug loading. % EE and loading results were statistically analyzed in pairs by unpaired two-tailed t-test and summarized in Table A.4.

Table 3. 4 CLX encapsulation efficiency and percent CLX loading

Liposome formulation	CLX EE (% mg/mg)	CLX loading (% mol/mol)
DSPC only	92.33 ± 4.31	23.05 ± 1.54
DSPC with 0.5% PEG	78.00 ± 4.47	23.87 ± 2.0
DSPC with 2% PEG	118.80 ± 2.03	24.62 ± 0.36
DSPC:Chol 10:1	104.40 ± 10.36	23.99 ± 0.67
DSPC:Chol 10:1 with 0.5% PEG	73.36 ± 11.15	17.37 ± 0.78
DSPC:Chol 10:1 with 2% PEG	85.69 ± 17.65	17.61 ± 2.56
DSPC:Chol 5:1	103.22 ± 3.63	22.71 ± 0.92

Values denote Mean ± S.E.M. , n≥3.

3.2.3 *In vitro* release profiles

In vitro cumulative percentage CLX release profiles of three different compositions of non-PEGylated LUVs are given in Figure 3- 5. The highest amount of CLX release was observed in the first 12 hours of incubation in PBS. Again, burst release of the drug was not observed from the unilamellar liposomes, as only 15-20% of total CLX was released in the first 12 hours. In the later hours, a lower drug release phase followed and finally a plateau was reached in 96 and 120 hours (results not shown). At the end of the release period, the amount of CLX released from DSPC:Chol 10:1 group was highest, followed by DSPC only and DSPC:Chol 5:1

group. All three groups of liposomes were successful in retaining majority of the loaded CLX during 72 hour release period in PBS.

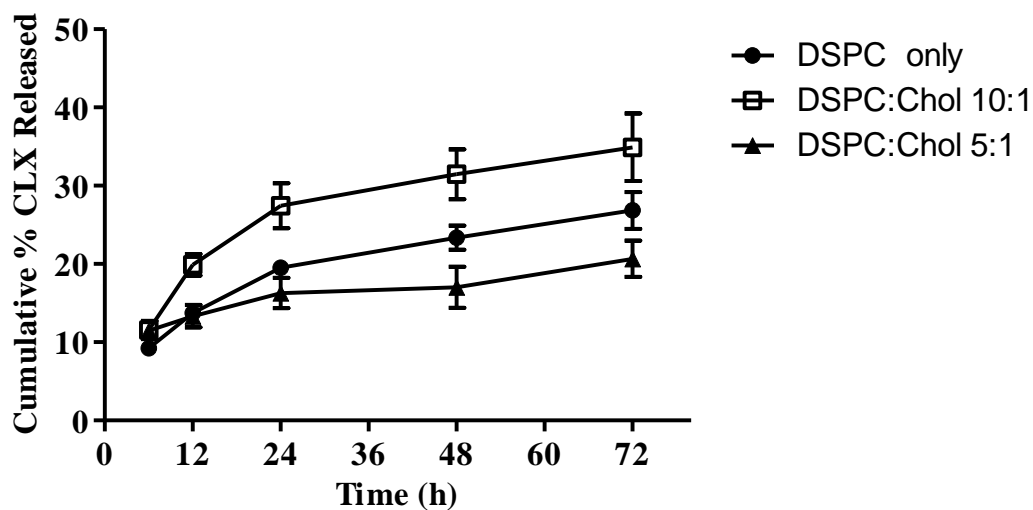


Figure 3- 5 *In vitro* CLX release from non-PEGylated LUVs in PBS at 37°C

Values denote Mean \pm S.E.M. of three independent experiments, $n \geq 6$

100% corresponds to the total amount of CLX entrapped in 1ml of LUVs at the beginning of the experiment

When PEG-DSPE was added to the liposome formulations; the highest amount of CLX release was observed in the first 6 to 12 hours of incubation in PBS. Cholesterol-free 0.5% PEGylated liposomes released significantly higher amounts of CLX than other formulations, whereas no significant difference was found between the other liposomal preparations (One-way ANOVA, Tukey's multiple comparison test). The cumulative amount of drug released to media was constant after the 48th hour in all the liposomal formulations (Figure 3-6)

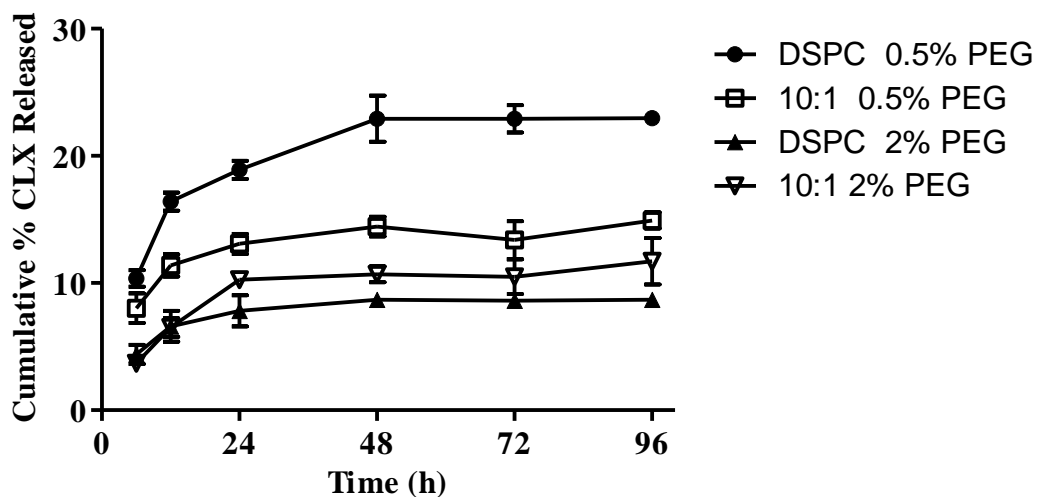


Figure 3- 6 *In vitro* CLX release from PEGylated LUVs in PBS at 37°C

Values denote Mean \pm S.E.M., $n \geq 6$

100% corresponds to the total amount of CLX entrapped in 1ml of LUVs at the beginning of the experiment

3.2.4 Cellular association of PEGylated liposomes

Cellular association of liposomes was determined by incubating a pre-optimized liposomal formulation containing 10:1 ratio of DSPC to cholesterol and 2% PEG-DSPE with the SW620 colon cancer cell line (ATCC no: CCL-227). This cell line was isolated from the lymph node of a male Caucasian patient with a highly aggressive metastatic tumor and is highly tumorigenic in nude mice. The cell line has a R273H mutation in p53 and expresses c-myc, K-ras, H-ras and N-ras oncoproteins as reported by ATCC.

3.2.4.1 Laser scanning confocal microscopy analysis

SW620 cells treated with two different doses of Rhodamine labeled CLX loaded LUV-PEGs exhibited increased cellular association with increasing treatment duration (Figure 3- 7). At 30 minutes, cell associated fluorescent signal was barely detectable; whereas mostly surface bound liposomes were observed at 2 hours. At 6 hours, markedly higher amounts of fluorescently labeled liposomes were localized to the perinuclear space, and the cell associated signal was more homogeneously distributed throughout the cell population. Low dose (200 μ M of lipid) treatment was as effective as the high dose (500 μ M of lipid) treatment in the longer times of treatment.

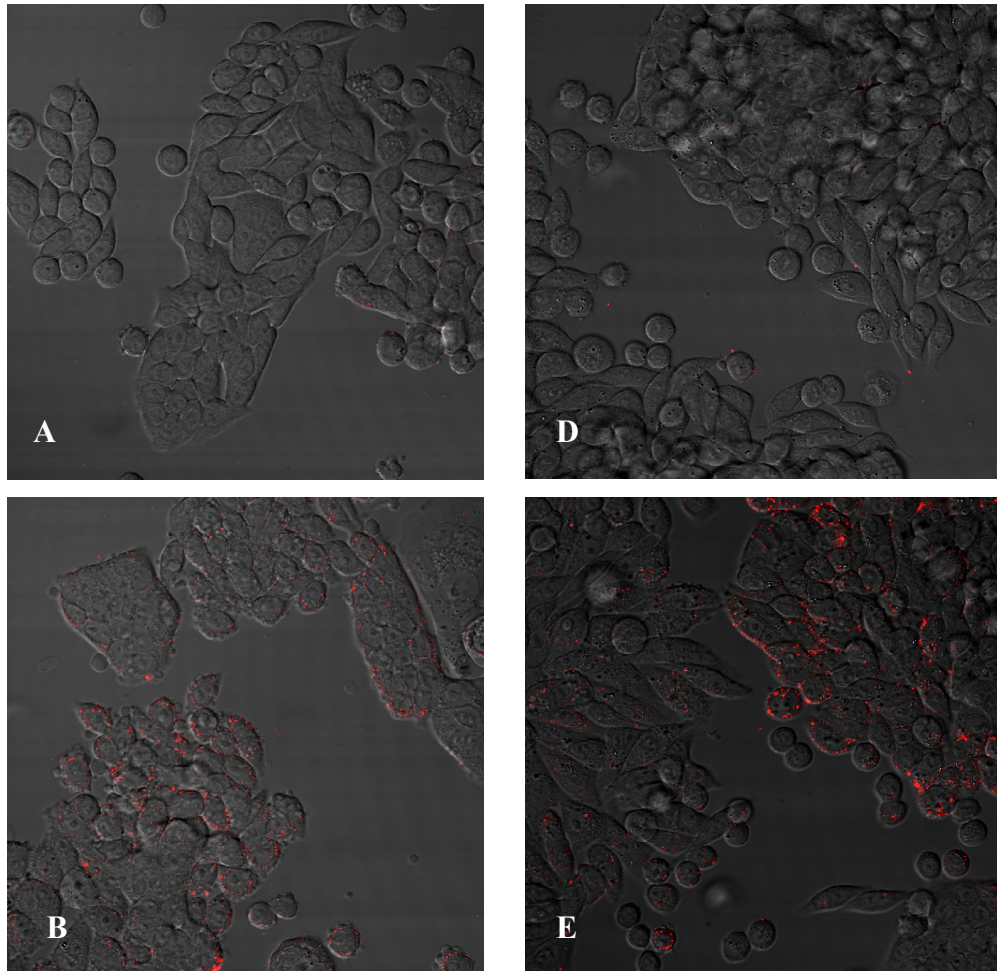


Figure 3- 7 LSCM analysis of cell associated Rhodamine labeled PEGylated liposomes.

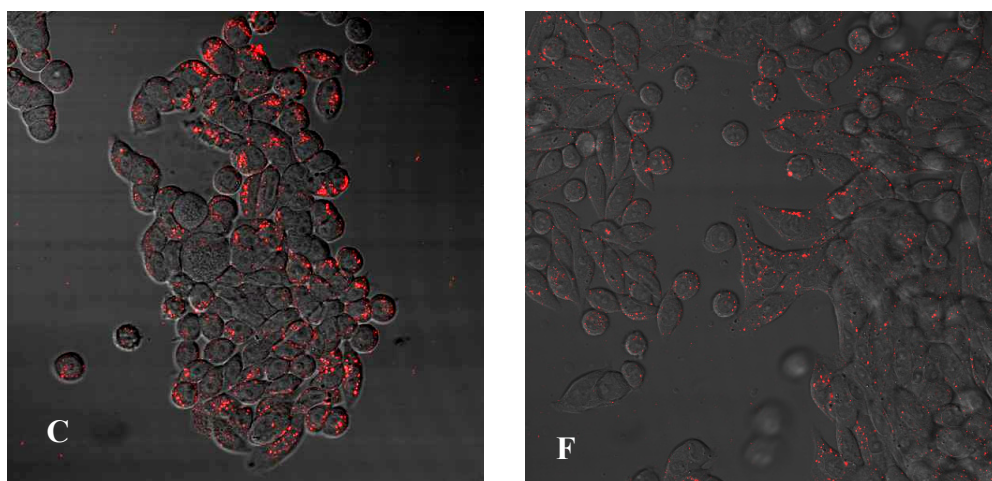


Figure 3-7 continued

SW620 cells treated with 500 μM lipid (A-C) and 200 μM lipid (D-F) for 30 minutes (A&D), 2 hours (B&E) and 6 hours (C&F). Fluorescent pseudo-colored images were merged with transmission images where Rhodamine signal was pseudo colored as red. Brightness and contrast of the images were adjusted for optimum visualization.

In order to assess the cellular localization of internalized liposomes, co-treatment study with fluorescently labeled transferrin (Transferrin-AlexaFluor680 conjugate) was performed via LSCM. Transferrin is an iron binding protein that enters the cell upon binding to its specific receptor and is internalized by receptor-mediated endocytosis. It is therefore a marker for early or recycling endosomes. SW620 cells were treated with Rhodamine labeled liposomes (1000 μM lipid) for 30 minutes, 2 hours and 6 hours and co-treated with Transferrin-AF680 conjugate for 1 hour. The signal from drug loaded PEGylated liposomes rarely co-localized with transferrin signal; implying that liposomes were not localized to the endosomes following surface binding at the observed time points (Figure 3- 8, A-B-C). Although

transferrin-AF680 signal was detected in every cell, liposome associated Rhodamine signal was detected in a sub-population of the cells even at 6 hours of treatments (Figure 3-8, C). A detailed image analysis revealed the location of Rhodamine signal obtained from different z-planes. The z-stack images were initially collected to include the total cell thickness by marking the first and last planes where AF680 signal was observed. The presence of Rhodamine signal collected from several z-planes supports the observation that liposomes were internalized. The distinct locations for Rhodamine and AF680 signals indicated that liposomes were rarely localized to recycling endosomes but mostly contained in non-recycling vesicles. (Figure 3-9, Figure 3-10 and Figure 3-11).

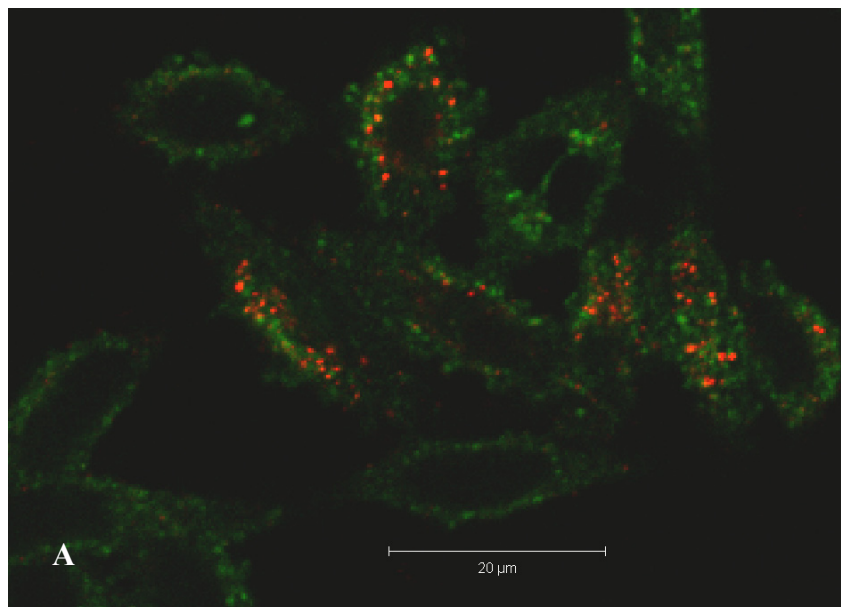


Figure 3- 8 LSCM analysis of localization of cell associated Rhodamine labeled liposomes and Transferrin-AlexaFluor680 conjugate

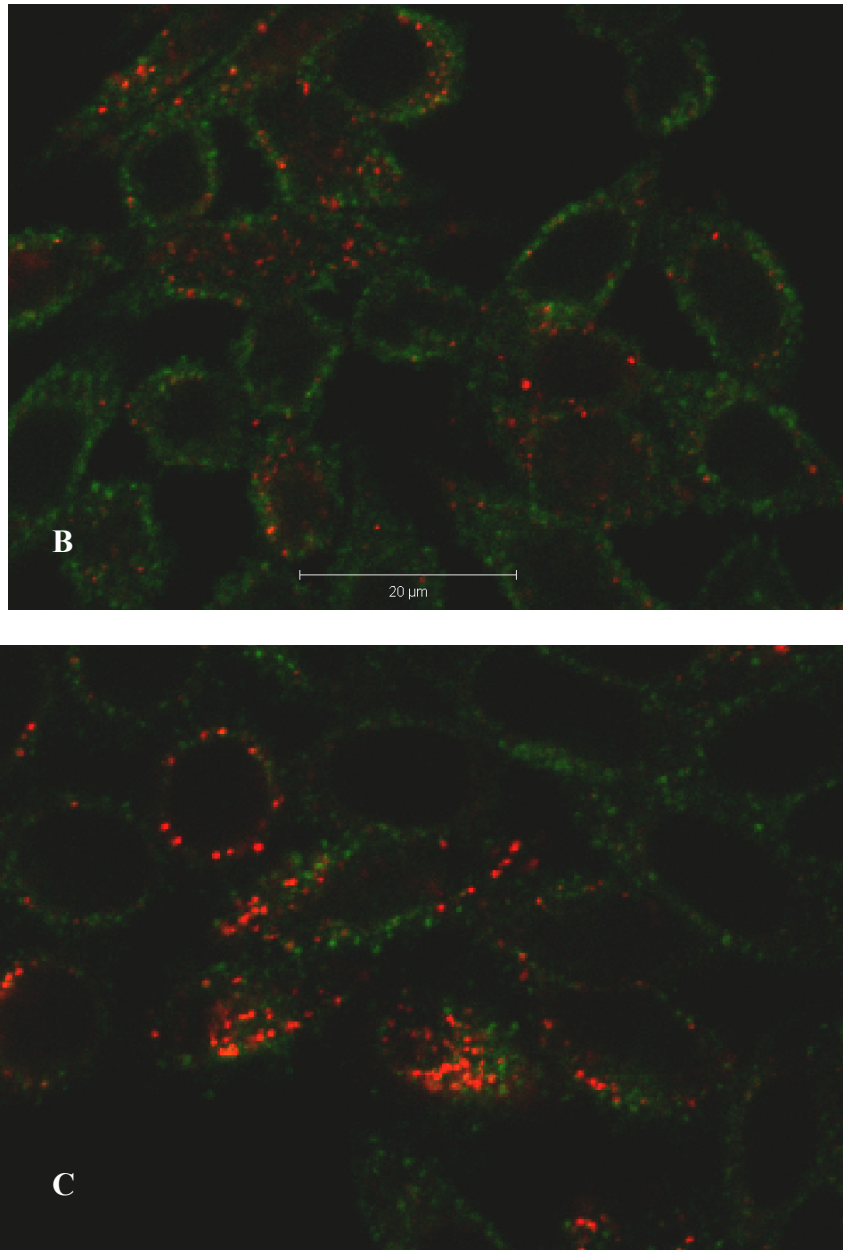


Figure 3-8 continued

Signal from Rhodamine label was pseudo colored as red and AF680 signal was pseudo colored as green. A: 30 minutes, B: 2 hours, C: 6 hours of Rhodamine labeled liposomes treatments

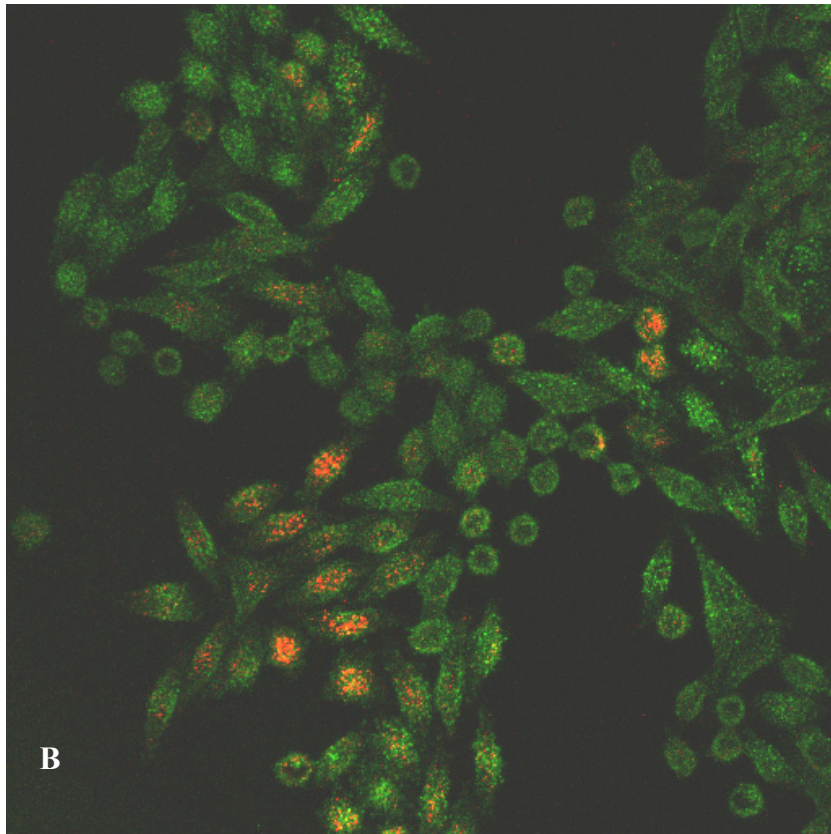


Figure 3-9 Cellular localization of Rhodamine labeled liposomes after 30 minutes of treatment

A: 2D projection of z-stack image

B: Reconstructed 3D image

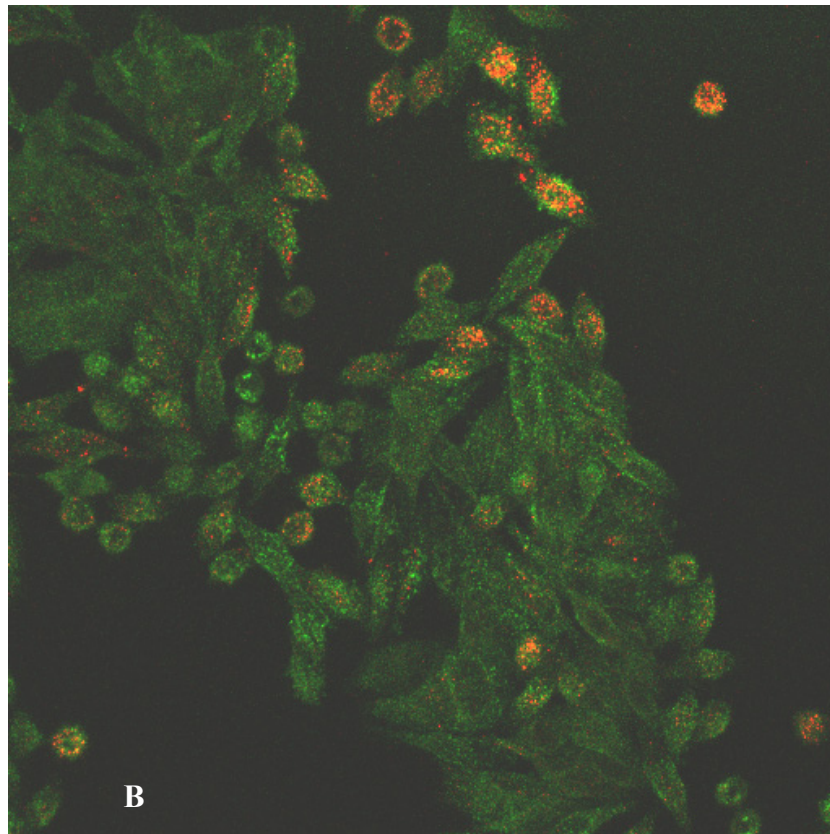
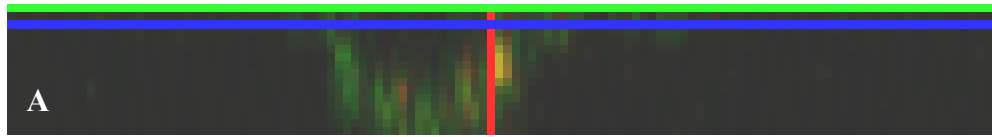


Figure 3-10 Cellular localization of Rhodamine labeled liposomes after 2 hours of treatment

A: 2D projection of z-stack image

B: Reconstructed 3D image

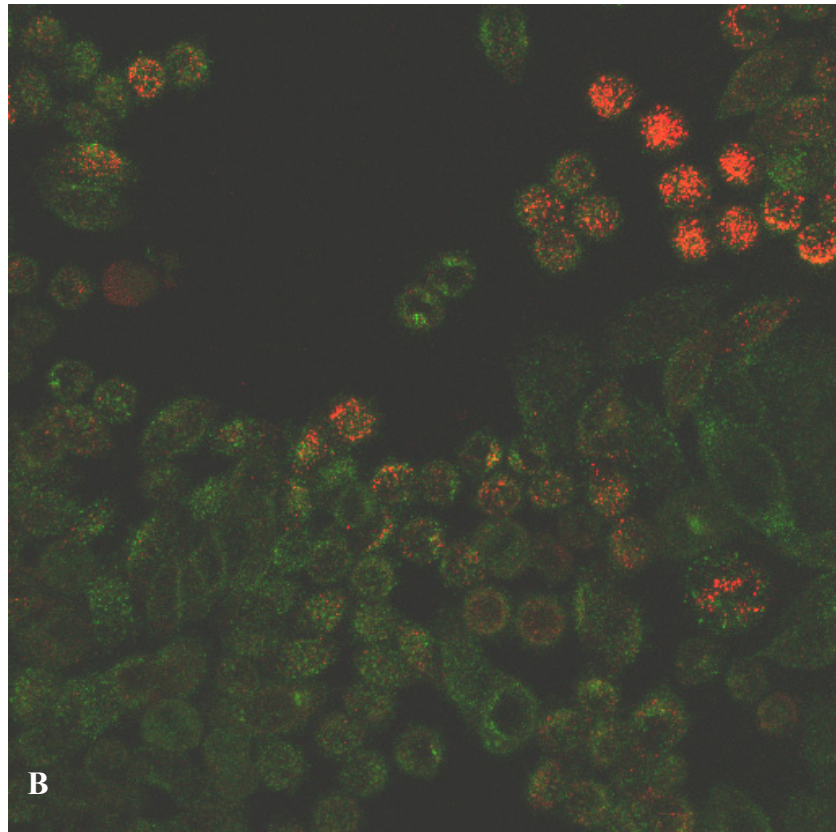
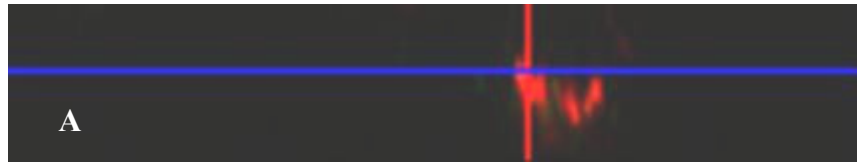


Figure 3-11 Cellular localization of Rhodamine labeled liposomes after 6 hours of treatment

A: 2D projection of z-stack image

B: Reconstructed 3D image

3.2.4.2 Fluorescence activated cell sorting analysis (FACS)

HCT-116 and SW620 colon cancer cell lines were used to determine the cellular association of liposomes by FACS. The HCT-116 cell line is a widely used colon cancer cell line that has a mutation on codon 13 of the *RAS* proto-oncogene and has a wild type TP53.

In HCT-116 cells, the Mean Relative Fluorescence Intensity (RFI of Mean FL-1) was significantly higher when the cells were incubated with the liposomes for 2h and 6h than in cells treated for 30 minutes ($p < 0.01$, One-way ANOVA Tukey's Multiple Comparison Test). A statistically significant difference was observed only in the 6h samples in SW620 cells ($p < 0.05$, One-way ANOVA Tukey's Multiple Comparison Test) (Figure 3-12). In addition to RFI, percent of the population with FL-1 signal intensity above the threshold level of negative control (untreated cells) was calculated and plotted as % Population versus time. In HCT-116 cells, population of cells with fluorescent signal increased from 2.8% at 30 minutes to 15.1% at 2 hours and up to 61.5% at 6 hours where the increase of 6h samples were statistically significant than other time points ($p < 0.001$, One-way ANOVA). In SW620 cells, similar calculations lead to 2.4% at 30 minutes, 27.5% at 2 hours and 80.9% at 6 hours where the significant increase at 2 hours ($p < 0.05$, One-way ANOVA) was found to be more pronounced at 6 hours ($p < 0.001$, One-way ANOVA) (Figure 3-16). The marked shift of the fluorescent signal intensities of cell populations are shown in histograms for both cell lines (Figure 3-13, Figure 3-14 and Figure 3-15).

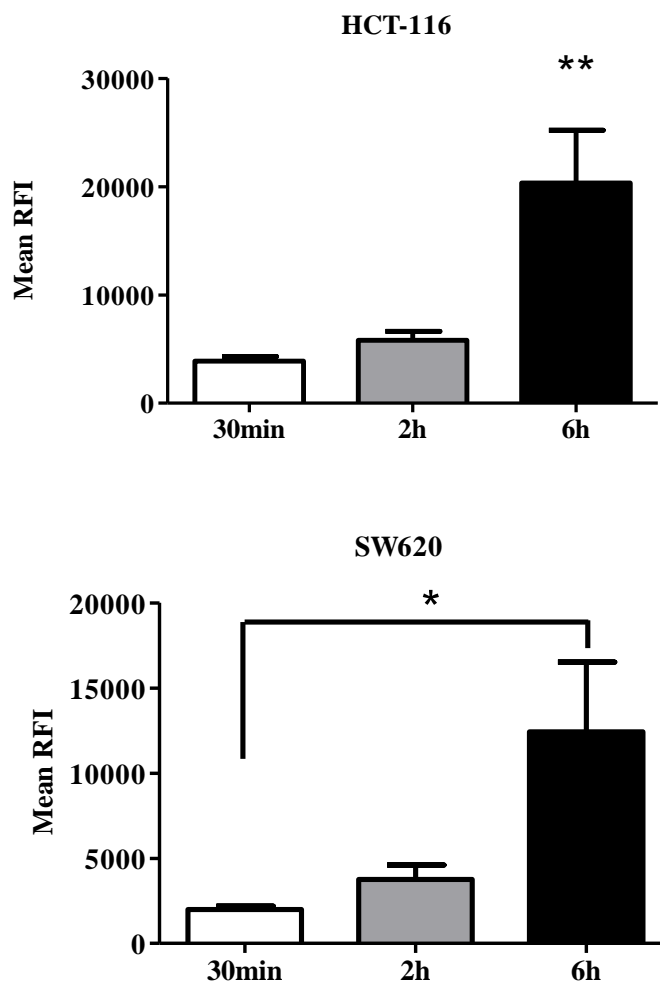


Figure 3-12 *In vitro* cellular association of fluorescently labeled liposomes by FACS

Columns, mean of three independent experiments with duplicates of each group; bars, S.E.M. Results analyzed by One-way ANOVA, Tukey's Multiple Comparison Test. * $p < 0.05$ compared to 30 min (SW620), ** $p < 0.01$ with respect to 30 min and 2 hours (HCT-116).

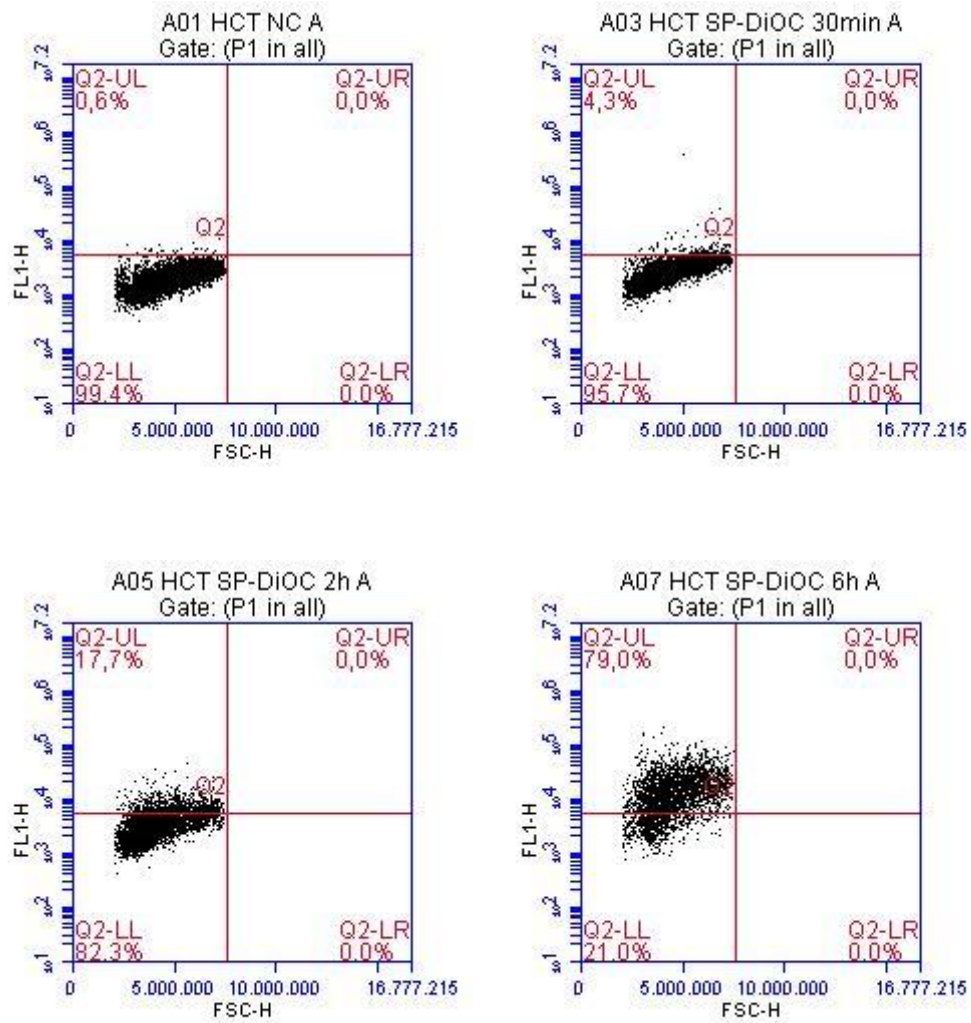


Figure 3-13 Dot plots for HCT-116 cell populations associated with fluorescently labeled liposomes

Representative images. x-axis: Forward Scatter Height, y-axis: FL1 signal Height

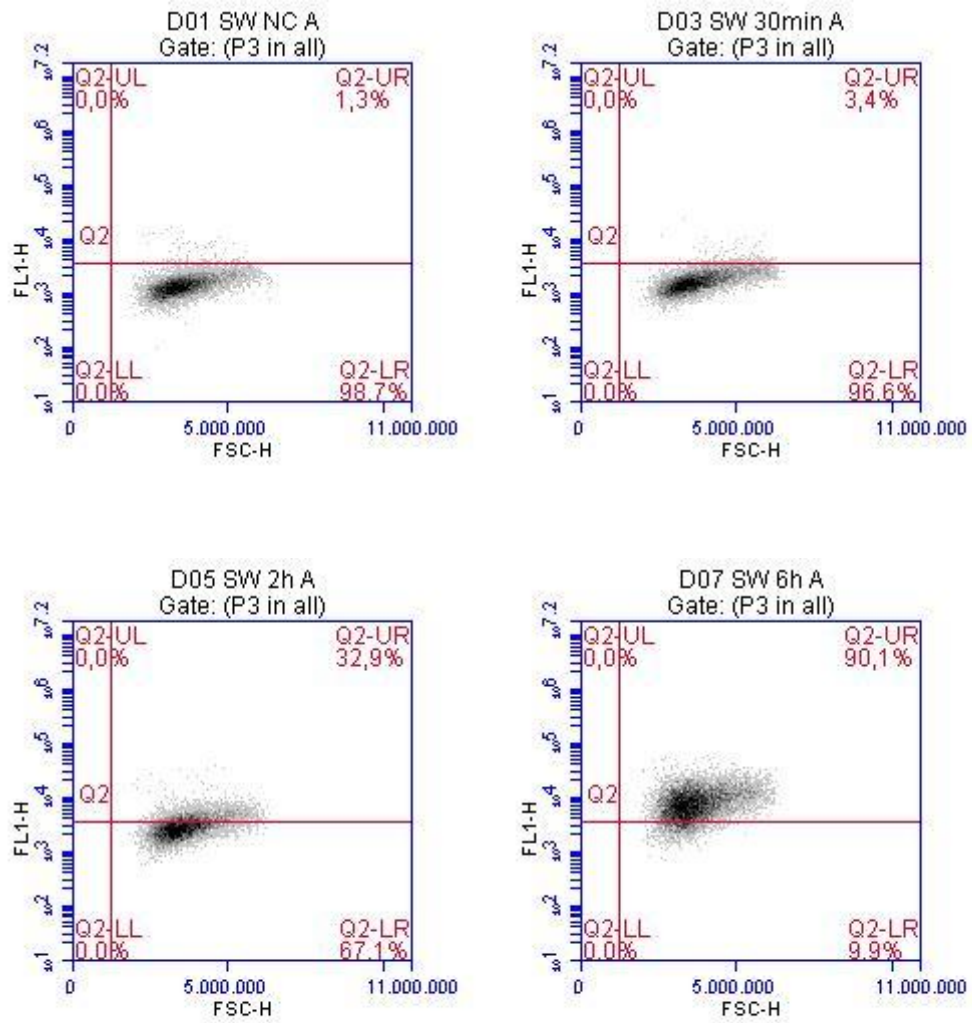


Figure 3-14 Dot plots for SW620 cell populations associated with fluorescently labeled liposomes

Representative images. x-axis: Forward Scatter Height, y-axis: FL1 signal Height

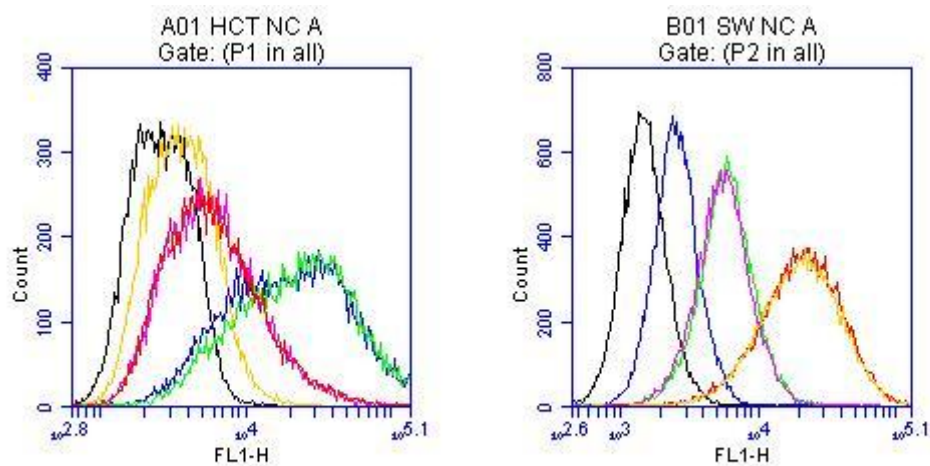


Figure 3-15 Single parameter histograms for cell populations associated with fluorescently labeled liposomes

For HCT-116 cells (left); black line represents Negative control, yellow line represents 30 minutes treatment, red line represents 2 hours treatment and green line represents 6 hours treatments.

For SW620 cells (right); black line represents Negative control, blue line represents 30 minutes treatment, purple line represents 2 hours treatment and orange line represents 6 hours treatments.

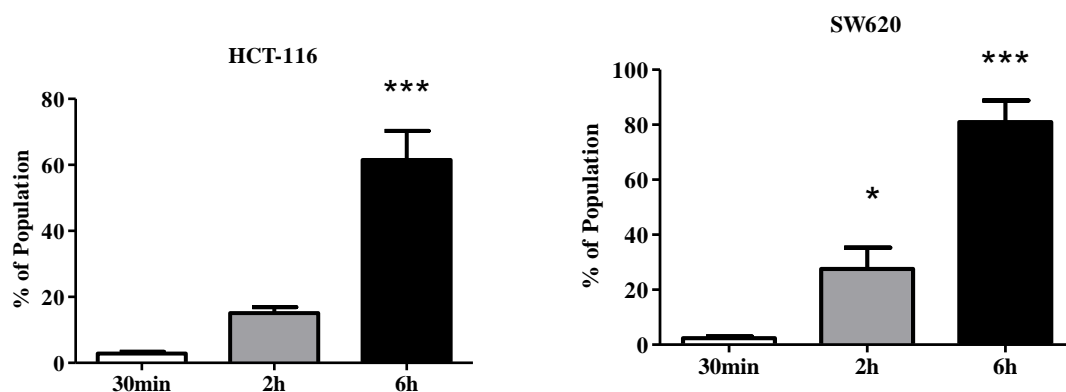


Figure 3-16 Percentage of liposome associated cells detected by FACS analysis
Columns are the mean of three independent experiments with duplicates of each group; bars, S.E.M. Results analyzed by One-way ANOVA, Tukey's Multiple Comparison Test. * $p < 0.05$ compared to 30 min (SW620), *** $p < 0.01$ with respect to 30 min and 2 hours (HCT-116 and SW620).

3.2.5 Cellular toxicity of pure CLX and CLX loaded liposomes

The cytotoxic effect of free CLX was tested on HT-29 (high COX-2 expressing) and SW620 (COX-2 non-expressing) cell lines by an MTT assay. Cells were treated with 20-100 μM of CLX for 24, 48 and 72 hours which corresponds to more than two population doubling times for both cell lines. The vehicle control was not toxic on cells since the final concentration of DMSO was reduced to 0.1%. In HT-29 cells, 30 μM CLX inhibited 50% of cellular proliferation and increasing CLX concentration to 50 μM resulted in 76% inhibition of proliferation in 72 hours of treatment. In SW620 cells, 30 μM CLX inhibited only 30% of cellular proliferation

at 72 hours, and increasing CLX concentration to 50 μ M resulted in 60% inhibition of proliferation. Both cell lines responded dramatically to 100 μ M CLX treatment at 48 and 72 hours. The cytotoxic effects of CLX were observed at lower concentrations and comparably earlier time points for HT-29 cells compared to SW620, which can be explained by COX-2 dependent anti-proliferative action of CLX on HT-29 cell line.

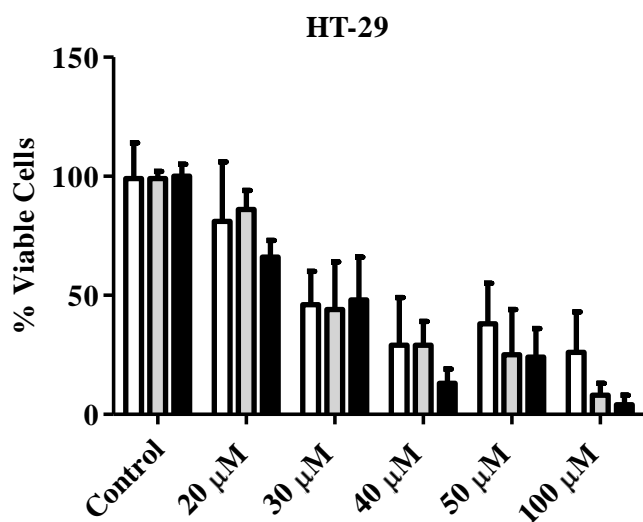


Figure 3- 17 Cellular toxicity of pure CLX on HT-29 and SW620 cells by MTT assay

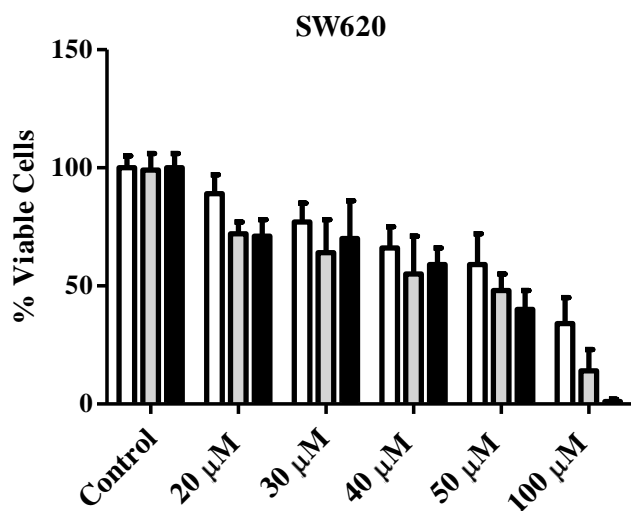


Figure 3-17 continued

24 h (white bars), 48 h (gray bars) and 72 h (black bars) treatments. Columns represent means; bars represent S.D. , $n \geq 5$. 20 μM – 100 μM values in x-axis represent final CLX concentrations in treatments. Control group was untreated cells.

Treatment with CLX loaded PEGylated liposomes showed an inhibition of cellular proliferation in HT-29 and SW620 cells as determined by MTT cell proliferation assay (**Figure 3-18** and **Figure 3-19**). As a general trend, increasing the treatment duration from 24 hours to 48 and 72 hours resulted in enhanced cytotoxic effect on both cell lines. At 24 hours of treatment, 50 and 100 μM of CLX loaded liposomes showed slight toxicity on cells that were not significantly different from empty liposomes.

In high COX-2 expressing HT-29 cell line, the cytotoxic effect of liposomal CLX was found to increase in a dose dependent manner, in which the most dramatic

response was found at 600 μM treatment leading to 95% cellular death at 72 hours. 400 μM liposomal CLX treatment caused 19%, 63% and 73% inhibition of cellular proliferation in 24, 48 and 72 hours, respectively. Empty liposomes were not toxic relatively at 24 and 48 hours, while showed 65% inhibition at 72 hours when compared to control group.

In the COX-2 non-expressing SW620 cell line, the dose dependent cytotoxic effect of liposomal CLX was evident above 100 μM . Cellular viability after 24 h and 72 h treatments with 200 μM dose was 49% and 43%, respectively. Percentage of viable cells at the corresponding time points with 400 μM treatment was 45% and 28%, respectively. The most concentrated treatment with 600 μM lead to 62% inhibition of cellular proliferation at 24 hours, and 78% inhibition at 72 hours. Interestingly, toxic effect of empty liposome treatment was observed to be highest as 25% at 24 hours which dropped down to 10% at 72 hours of treatment.

HT29

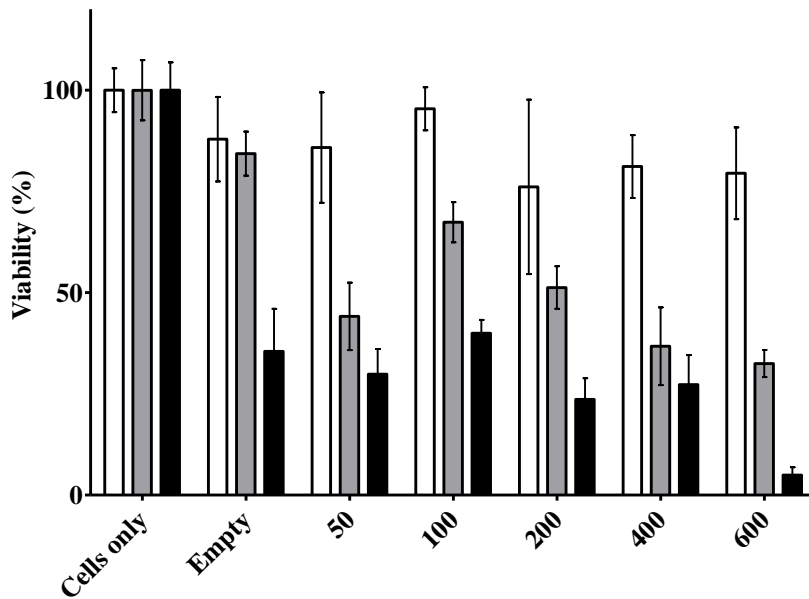


Figure 3-18 Cellular toxicity of CLX loaded PEGylated liposomes on HT-29 cells by MTT assay

24 h (white bars), 48 h (gray bars) and 72 h (black bars) treatments. Values 50-600 indicate final liposomal CLX concentration in treatments. Empty liposomes were used at equal dose of lipids corresponding to 600 μ M CLX loaded liposomes. Control group was untreated cells.

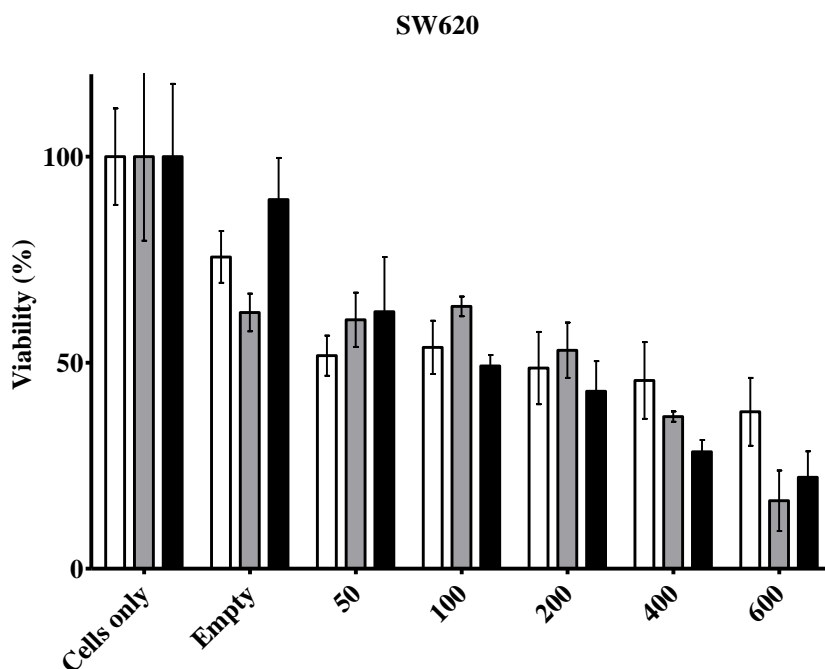


Figure 3- 19 Cellular toxicity of CLX loaded PEGylated liposomes on SW620 cells by MTT assay

24 h (white bars), 48 h (gray bars) and 72 h (black bars) treatments. Values 50-600 indicate final liposomal CLX concentration in treatments. Empty liposomes were used at equal dose of lipids corresponding to 600 μ M CLX loaded liposomes. Control group was untreated cells.

3.2.6 Inhibition of cellular motility by CLX loaded PEGylated liposomes

CLX loaded PEGylated liposomes were tested for effects on cellular motility in a 2D cell culture model. Since SW620 cell line is COX-2 negative, COX-2 independent effects of CLX in the liposomal formulation were evaluated in this assay. Representative 4X magnified images in Figure 3-20 display the exact same location on the cell culture plate on day zero up to day five. Empty liposomes served as a control group to test the effect of liposomal constituents on wound closure at the lipid dose corresponding to high dose of liposomal CLX. The inhibition of the wound closure by two different doses of CLX loaded liposomes was monitored up to 120. Results of three independent experiments showed that 120 hours of treatment with 400 μ M CLX-LUV-PEG resulted in significant reduction in wound closure when compared to control or Empty liposome treated cells (Figure 3- 21). One hundred μ M CLX-LUV-PEG treatment did show an inhibitory effect; however, it was not significantly different from the empty liposomes. Additionally, representative 10X magnified images belonging to another independent experiment are displayed in Figure 3-22 where free CLX at 30 μ M final concentration was included in order to compare the effective doses of free and liposomal form of the drug in this functional assay. Higher magnification clearly aided in observing the single cells moving towards the empty space in the plate, instead of a moving line due to a mass proliferation of the cells. Imaging was performed up to 60 hours, where no significant difference was observed between 100 μ M and 400 μ M liposomal CLX treatments.

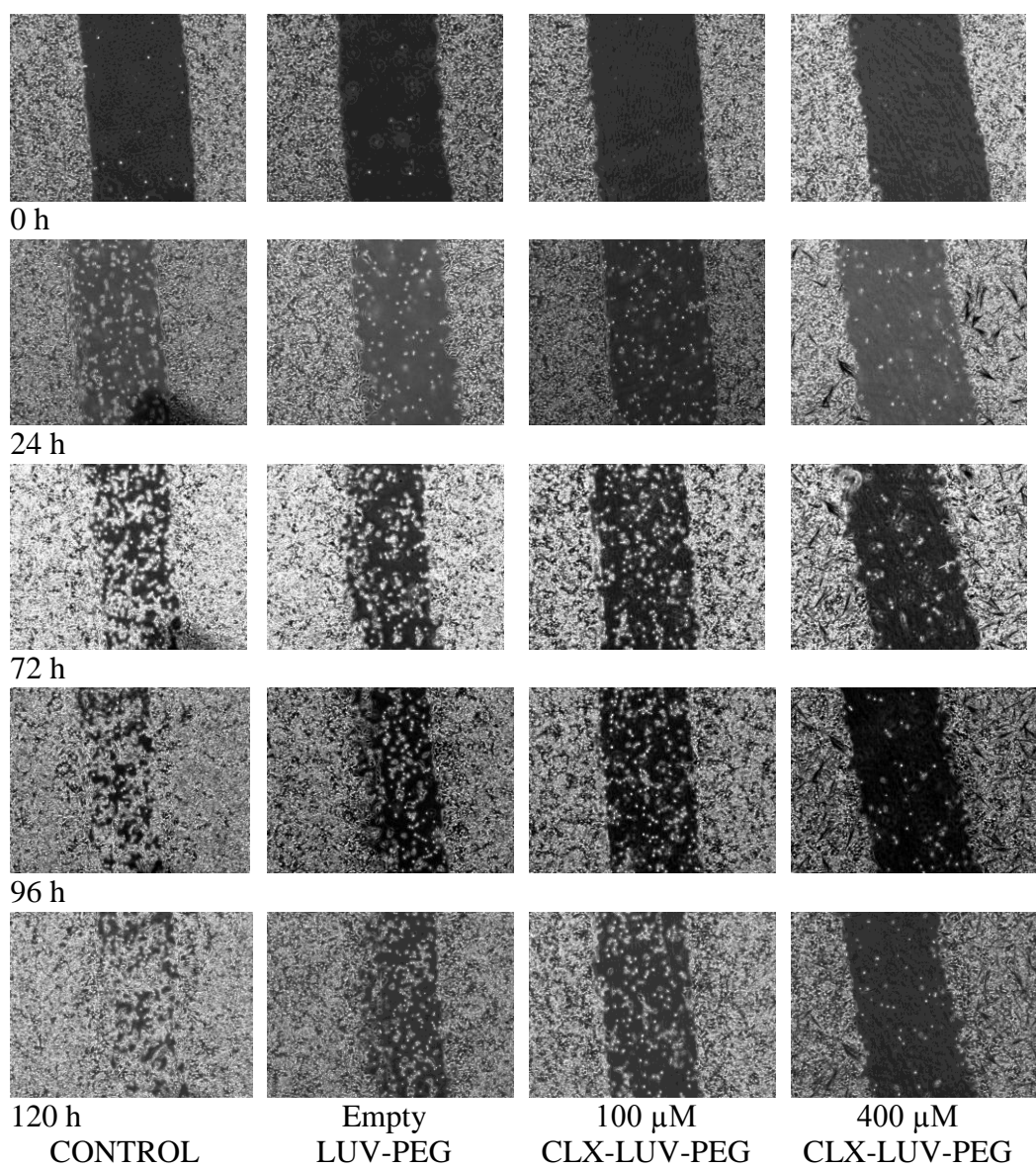


Figure 3-20 *In vitro* scratch wound healing assay with SW620 cells up to 120 h

Figure 3-20 continued

Representative images for indicated treatments with 4X magnification. 100 μ M CLX-LUV-PEG and 400 μ M CLX-LUV-PEG indicate final concentrations of liposomal CLX in the wells. Lipid dose in Empty LUV-PEG treatments was equal to highest dose (400 μ M) of CLX-LUV-PEG treatment. Control group was untreated cells.

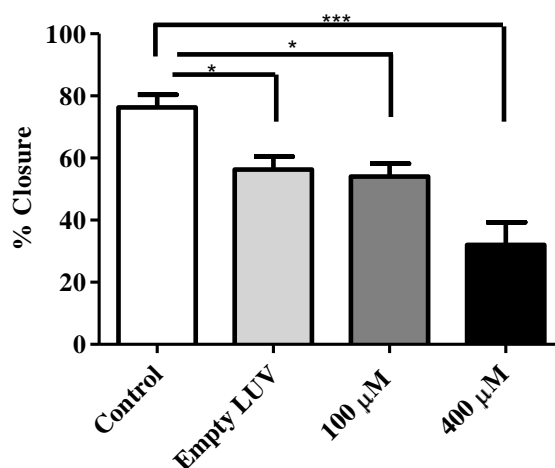


Figure 3- 21 Percent area closure in wound healing assay after 120 hours

Values denote Mean \pm S.E.M. of three independent experiments in duplicates (n=6). 100 μ M CLX-LUV-PEG and 400 μ M CLX-LUV-PEG indicate final concentrations of liposomal CLX in the wells. Lipid dose in Empty LUV-PEG treatments was equal to highest dose (400 μ M) of CLX-LUV-PEG treatment. Control group was untreated cells. * $p < 0.05$ and *** $p < 0.001$ with respect to Control group analyzed by One-way ANOVA, Dunnet's multiple comparison test.

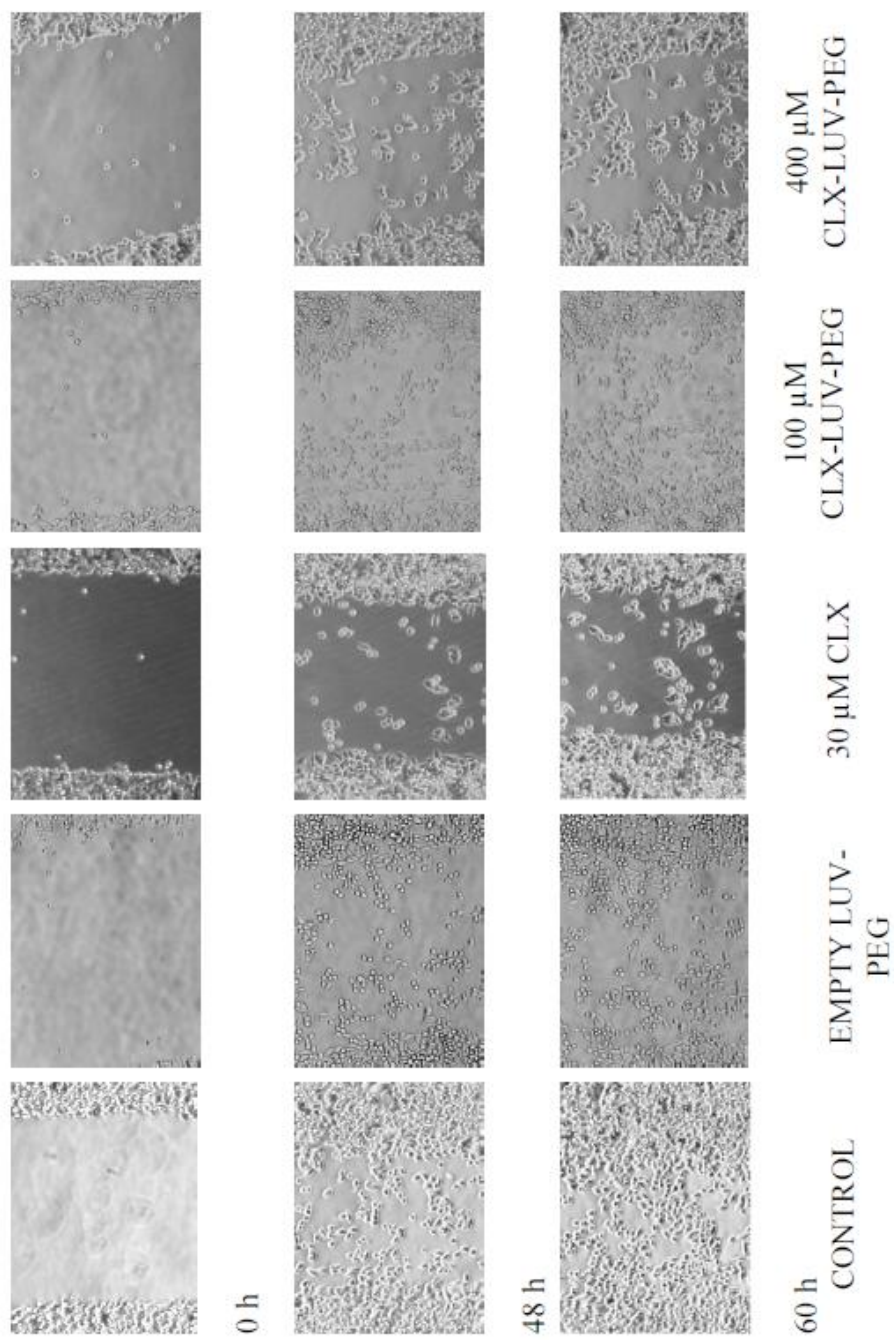


Figure 3- 22 *In vitro* scratch wound healing assay with SW620 cells up to 60 h

Figure 3-22 continued

Representative 10X magnified images with indicated treatments. 30 μM CLX indicates final concentration of pure CLX (in DMSO solution). 100 μM CLX-LUV-PEG and 400 μM CLX-LUV-PEG indicate final concentrations of liposomal CLX in the wells. Lipid dose in Empty LUV-PEG treatments was equal to highest dose (400 μM) of CLX-LUV-PEG treatment. Control group was untreated cells.

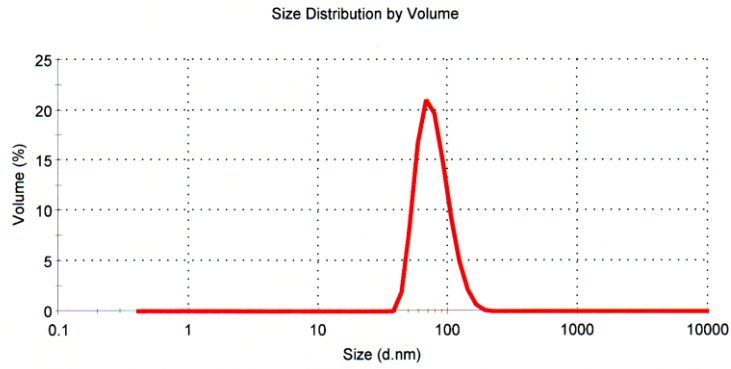
3.3 Characterization of CLX loaded ILs

3.3.1 ILs prepared by mouse IgG conjugation

3.3.1.1 Particle size distribution analysis

The average vesicle sizes were measured for ILs prepared by conjugation of mouse IgG isotype controls. When 100 μg of IgG was used as starting material for 20 μmol of lipids, Empty ILs were at 101.4 ± 3.7 nm diameter, and when 200 μg of IgG was used as starting material CLX loaded ILs were at 93.6 ± 4.1 nm. Average PDI values for Empty ILs and CLX-ILs were 0.047 ± 0.024 and 0.096 ± 0.045 , respectively; indicating nearly monodisperse populations or mid-range polydispersity. The representative results for particle size analysis are given in Figure 3-23.

	Diam. (nm)	% Volume	Width (nm)
Z-Average (d.nm): 88.99	Peak 1: 78.84	100.0	22.73
Pdl: 0.117	Peak 2: 0.000	0.0	0.000
Intercept: 0.961	Peak 3: 0.000	0.0	0.000
Result quality Good			



	Diam. (nm)	% Volume	Width (nm)
Z-Average (d.nm): 100.3	Peak 1: 93.35	100.0	22.47
Pdl: 0.023	Peak 2: 0.000	0.0	0.000
Intercept: 0.958	Peak 3: 0.000	0.0	0.000
Result quality Good			

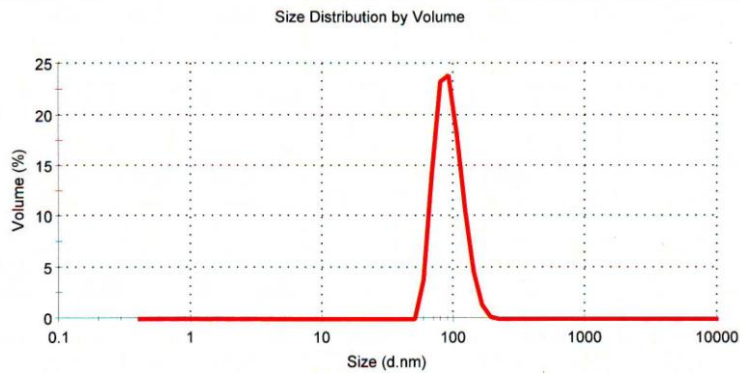


Figure 3- 23 Representative images for particle size distribution analysis of ILs CLX-IL (top) and Empty IL (bottom)

3.3.1.2 Drug encapsulation efficiency

In the IL formulations prepared by conjugation of 100 μg and 200 μg of IgG, no significant difference was found between the two groups in terms of percentage of CLX encapsulated. As shown by the dot plots below (Figure 3- 24), preparations with 200 μg starting material had a more scattered distribution of data within the group, but the mean values were not different at statistically significant levels (Mann Whitney test). Mean values were 61.4 ± 1.9 and 52.8 ± 5.4 for the 100 μg and 200 μg group, respectively.

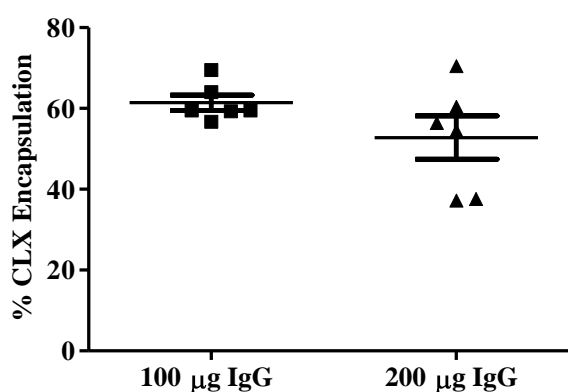


Figure 3- 24 CLX encapsulation efficiency in IL preparations

Values denote Mean \pm S.E.M. (n=6)

100 μg IgG and 200 μg IgG indicate ILs prepared with 100 μg and 200 μg IgG as starting material, respectively. Means of populations were not significantly different with P value=0.2290, according to Mann Whitney test (non-parametric t-test)

3.3.1.1 IgG conjugation efficiency

Products of IgG reduction reaction were visualized by SDS-PAGE analysis and Coomassie blue staining (Figure 3-25). The molecular weight of reaction product “half-IgG” molecules were 95-100 kDa, as expected. The reduction reaction was tested for 15, 30 and 90 minutes. 15 minutes of reaction lead to reduction of only a portion of the IgG molecules as deduced from the band around 150 kDa size. On the other hand, 30 minutes and 90 minutes of reaction were found to be sufficient to obtain the desired product of half-IgG molecules. The longer reaction time did not cause excessive reduction of the disulfide bonds, as heavy and light chain fragments were not observed as in the positive control (+C) in the 6th lane.

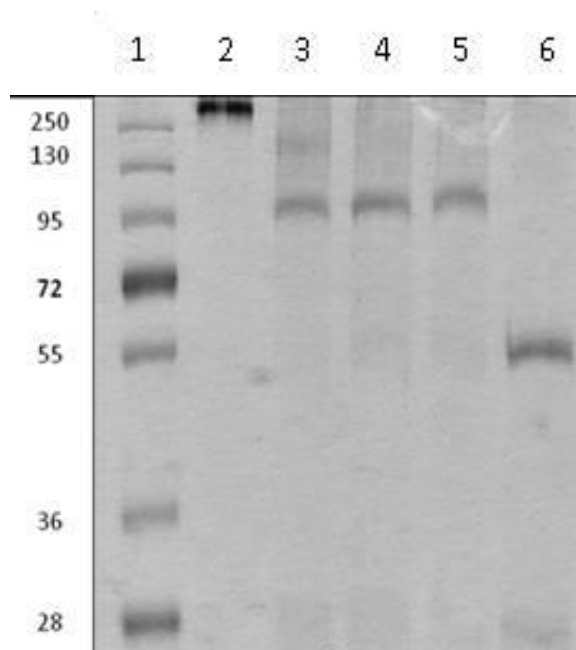


Figure 3- 25 SDS-PAGE analysis of reduced IgG molecules

IgG molecules (2 μg in each well) reduced with 100 mM 2-MEA were resolved in 12% non-reducing SDS-PA gel, visualized after Coomassie Staining for 1 hour.

Lanes: 1. Marker 2. Unreduced IgG, 3. 15 min reduced IgG 4. 30 min reduced IgG 5. 90 min reduced IgG 6. IgG reduced with β -ME and boiled (+C)

The efficiency of IgG conjugation to PEGylated liposomes with Maleimide functional groups was investigated in CLX loaded and empty liposomes with two different amounts of starting material. The results summarized in Figure 3- 26 were not significantly different from each other (One-way ANOVA with Tukey's multiple comparison test). The IgG conjugation efficiency ranged from $41.3 \pm 4.2\%$ in CLX-IL prepared with 100 μg IgG to $51.8 \pm 2.1\%$ in Empty-IL prepared with 100 μg IgG.

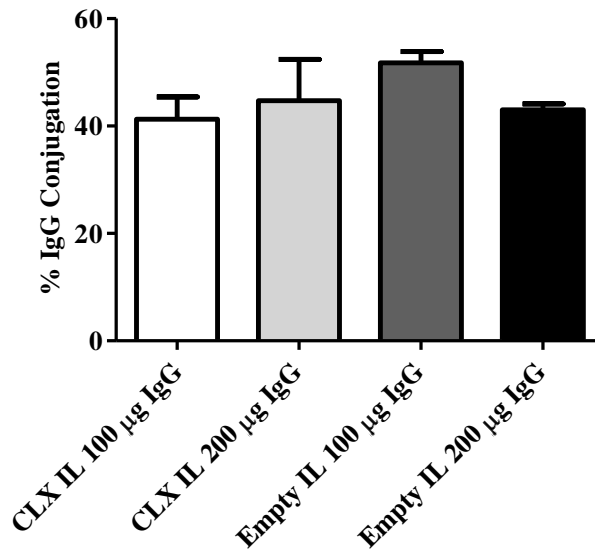


Figure 3- 26 IgG conjugation efficiency for CLX loaded and Empty ILs

Values denote Mean \pm S.E.M. ($n \geq 3$). 100% was the the starting amount of IgG.

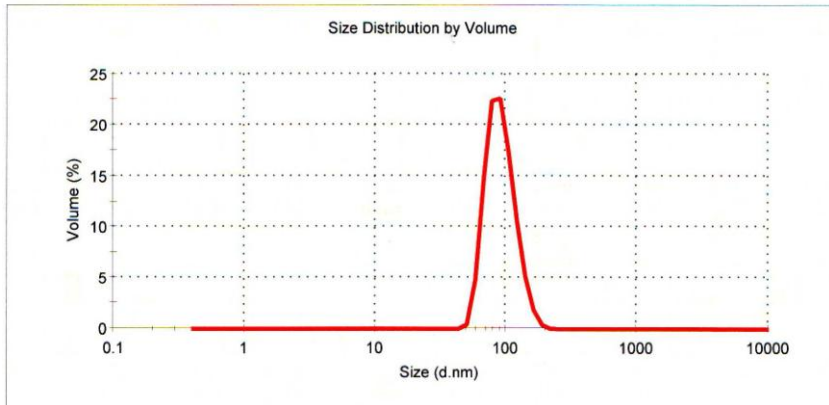
CLX IL and Empty IL refer to CLX loaded immunoliposomes and Empty immunoliposomes, respectively. 100 µg IgG and 200 µg IgG indicate ILs prepared with 100 µg and 200 µg IgG as starting material, respectively. Means of populations were not significantly different with P value=0.2290, according to One-way ANOVA with Tukey's multiple comparison test.

3.3.2 Anti-EGFR IgG conjugated ILs

Empty ILs were at 98.4 ± 1.8 nm diameter and CLX loaded ILs were at 99.4 ± 3.1 nm diameter. Average PDI values were 0.166 for Empty IL formulation and 0.091 for CLX-IL formulation, indicating nearly monodisperse populations in both of the liposome preparations. Two representative images for particle size analysis are given in Figure 3-27. After concentration of the samples by centrifugal ultra-filtration device, the final concentration of CLX was 4.4 to 7 mM and DSPC was approximately 95 mM. Anti-EGFR MAb conjugation efficiency to Empty-ILs and CLX loaded ILs was calculated as $88.0 \pm 2.8\%$ and $86.9 \pm 5.9\%$, respectively.

	Diam. (nm)	% Volume	Width (nm)
Z-Average (d.nm): 105.5	Peak 1: 93.61	100.0	24.05
Pdl: 0.157	Peak 2: 0.000	0.0	0.000
Intercept: 0.941	Peak 3: 0.000	0.0	0.000

Result quality Good



	Diam. (nm)	% Volume	Width (nm)
Z-Average (d.nm): 96.56	Peak 1: 86.65	100.0	21.43
Pdl: 0.166	Peak 2: 0.000	0.0	0.000
Intercept: 0.947	Peak 3: 0.000	0.0	0.000

Result quality Good

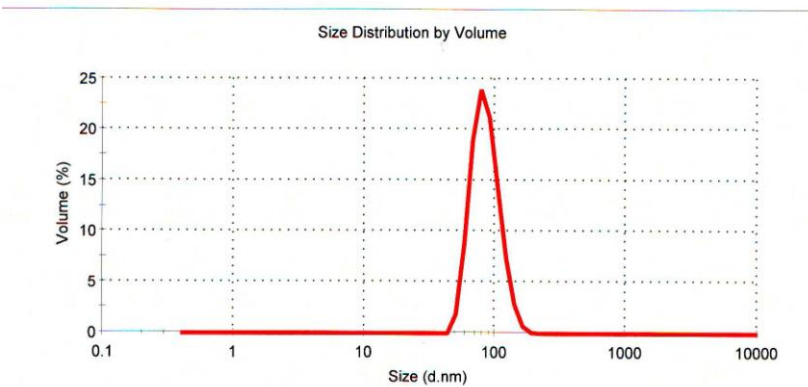


Figure 3- 27 Representative images of size distribution analysis of ILs CLX-IL (top) and Empty IL (bottom)

3.3.3 Cellular toxicity of EGFR targeted ILs

The two cell lines used to determine the cellular toxicity of EGFR targeted ILs are HCT-116 and SW620 cells. In addition to the characteristics of the cells described earlier, the EGFR expression of HCT-116 is between moderate to high, whereas SW620 cells do not overexpress EGFR (Table A. 2).

All liposomal formulations except Empty-LUV-PEGs exhibited amplified toxic effects as the treatment duration increased (**Figure 3-28**). In HCT-116 cells; in the 12 hours treatments, effect of Empty-IL formulation was not significantly different from Empty-LUV-PEG control, whereas CLX-LUV-PEG and CLX-IL showed significantly increased inhibition of proliferation as 52% and 93% when compared to Empty-LUV-PEG ($p < 0.05$ and $p < 0.001$ respectively; One-way ANOVA, Dunnett's Multiple Comparison Test). CLX-IL was even significantly more effective than CLX-LUV-PEG ($p < 0.001$, Unpaired two-tailed t-test). In the 24 hours of treatment, CLX-IL was the most effective formulation in inhibition of proliferation. Effect of CLX-IL was significantly higher than Empty-IL and CLX-LUV-PEG ($p < 0.001$ and $p < 0.01$ respectively; One-way ANOVA, Tukey's Multiple Comparison Test). In the 48 hours of treatment; the three formulations inhibited cellular proliferation significantly more than control Empty-LUV-PEGs (Table 3. 5). This long duration of time enabled non-targeted CLX loaded liposomes to show their toxic effect, which was not observed in 12 hours. The 48 hours of treatment duration covers two population doubling times for HCT-116 cells.

In SW620 cells; CLX-ILs showed increased inhibitory effect on proliferation although the response of SW620 cells was definitely not comparable to HCT-116 cells, most likely due to a lack of EGFR expression in these cells. Oddly, Empty-

ILs were the most toxic formulation in all time points for SW620 cells. We currently do not have an explanation for this discrepancy.

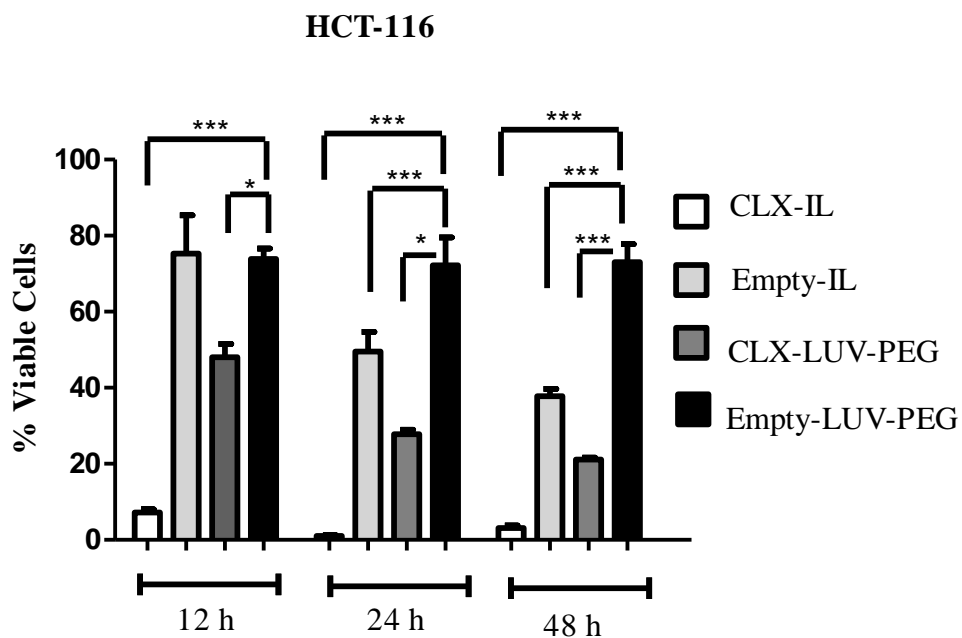


Figure 3-28 Cellular toxicity of CLX loaded EGFR targeted liposomes

SW620

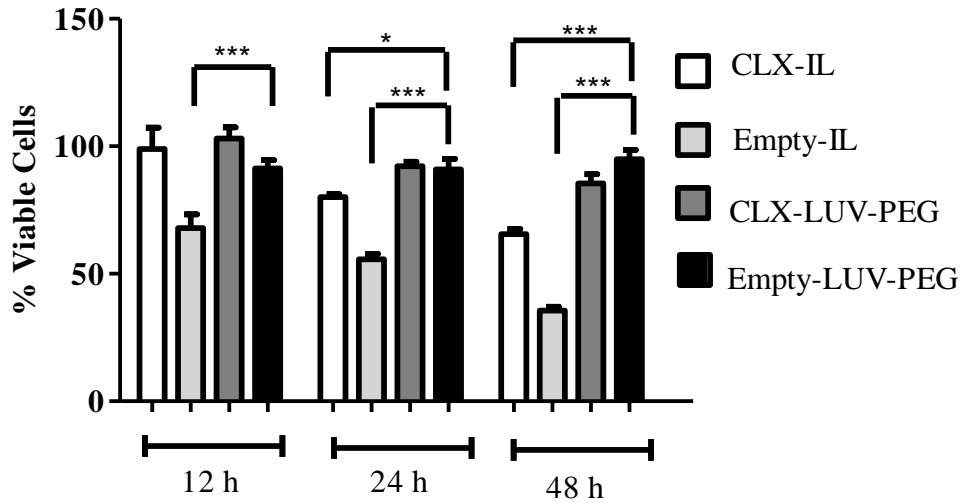


Figure 3-28 continued

Values denote Mean \pm S.E.M. ($n \geq 4$ replicate wells of 1 experiment) of percentage of viable cells with respect to untreated control cells

* $p < 0.05$, *** $p < 0.001$ One-way ANOVA, Dunnet's multiple comparison test, Empty-LUV-PEG as the control group.

Table 3. 5 Percentage of viable HCT-116 cells after liposome treatments

Liposome formulation	12 h	24h	48h
CLX-IL	7.25 ± 0.77	1.07 ± 0.22	3.15 ± 0.63
Empty-IL	75.26 ± 10.10	49.53 ± 5.20	37.78 ± 1.93
CLX-LUV-PEG	48.04 ± 3.51	27.76 ± 1.17	21.09 ± 0.55
Empty-LUV-PEG	73.91 ± 2.69	72.17 ± 7.37	73.05 ± 4.70

Values denote Mean ± S.E.M. ($n \geq 4$ replicate wells of 1 experiment) of percentage of viable cells with respect to untreated control cells

CHAPTER 4

DISCUSSION

4.1 Characteristics of CLX loaded MLVs

Celecoxib is a highly hydrophobic molecule, therefore liposomal formulations stand as good candidates for encapsulation and delivery of this molecule. In initial attempts to develop a liposomal delivery system for CLX; multilamellar vesicles were prepared and analyzed for particle size distribution and morphology as well as CLX encapsulation and release characteristics. Chemical reactions like hydrolysis or oxidation cause degradation of the constituents of the bilayer and in turn accelerate the destabilization of vesicles. The synthetic saturated phospholipid DSPC (18:0 PC) was selected as the major constituent of the liposomes due to the advantageous physicochemical characteristics; mainly high phase transition temperature (55°C) and resistance to lipid peroxidation (Drummond et al., 1999). Formation of vesicles requires an energy input in the form of mechanical processes (for example sonication, vortex mixing) or heat; therefore, lipid film hydration was performed at 70°C to maintain the lipids in the liquid phase and combined with vigorous vortex mixing for one hour.

The hydrodynamic diameters of vesicles were measured by the widely used light scattering method. It is a rapid and easy method that provides not only mean particle size data but also gives information about the heterogeneity of the distribution. Vesicles that are formed by energy input are not thermodynamically

stable structures and therefore susceptible to aggregation, fusion or precipitation. Vigorous vortexing and brief sonication steps are known to result in the formation of smaller vesicles with more uniform size distribution, although standardizing sonication power and duration is not easy (Szoka and Papahadjopoulos, 1980). Therefore, it is likely that the slight differences (statistically insignificant) in mean diameters might have resulted from the experimental procedures employed in this study. Since DSPC is a neutral phospholipid, liposomes composed of DSPC tend to aggregate in solution (Drummond et al., 1999). In some of the CLX loaded multi lamellar vesicle (MLV) samples, vesicles might have aggregated or fused as observed in large sized peaks in particle size distribution analysis (Figure 3-1, B). At the micron scale; compositional changes might not be reflected in vesicle size, consequently a correlation between cholesterol content and vesicle size was not observed.

The multilamellarity of the vesicles were observed using TEM by negative staining with uranyl acetate. The heavy metal salt forms an electron-dense layer around the lamellae and can be visualized as dark regions. In the CLX loaded MLV samples, multilamellar features were observed (Figure 3-2). Since TEM analysis involved dehydration after negative staining, vesicles lost their spherical morphology and had distorted shapes. A better experimental protocol to visualize multilamellar liposomes would be freeze-fracture cryo electron microscopy (Torchilin and Weissig, 2003). Deductions about vesicle size were not made from TEM images mainly because the sample size was not sufficient as number of samples should be above 500 for reaching conclusions about size distribution.

The method of CLX quantification was a direct spectrophotometric measurement of absorbance at 260 nm, which was previously determined by scanning of UV-visible

range with CLX solutions. Since CLX is insoluble in aqueous solvents, several different organic solvents were tested for suitability. Although CLX was soluble in DMSO, salt precipitations occurred and consequently prevented the quantification when liposome suspensions were mixed with DMSO. The spectrophotometric quantification method was developed to remove all the water content from liposome samples by drying under vacuum and dissolving the contents in chloroform. Since the organic solvent could dissolve all the liposome constituents (except salts), DSPC and cholesterol was tested for interference with the absorbance values at 260 nm. The CLX encapsulation efficiency results above 100% were considered as experimental error resulting from the rapid evaporation of chloroform during spectrophotometric measurement. In order to improve the accuracy of the quantification method, empty liposomes at the corresponding concentrations could be used as blank. A better approach would be developing a HPLC method for quantification of CLX in the liposomal formulations that would eliminate the limitations of the spectrophotometry.

Regarding the encapsulation of CLX in MLVs composed of DSPC, increasing the cholesterol content was found to cause a decrease in percentage of encapsulated CLX. The reduction of CLX encapsulation efficiency due to addition of cholesterol (Chol) was statistically significant in formulation with DSPC:Chol 2:1 ratio (Table 3.2). Similarly, in several other studies high cholesterol content was reported to result in lower encapsulation percentages of hydrophobic molecules. MLVs prepared with egg PC could encapsulate 29.5% of Ibuprofen while the encapsulation efficiency dropped to 23.2% with 30% Chol and even to 17.1% with 50% Chol addition (Mohammed et al., 2004). However, in some of the reported cases, increasing cholesterol amount in MLVs showed an opposite effect in terms of drug loading. Bhatia et al. (2004) reported that 30% cholesterol in the formulation

increased the entrapment efficiency of tamoxifen in PC liposomes from 45.2% to 57.5% (Bhatia et al., 2004). These differential effects of cholesterol on encapsulation efficiency of hydrophobic molecules can be attributed to individual molecular interactions between phospholipids, cholesterol and drug molecules. The fact that cholesterol increases the hydrophobicity in the central region of the membrane bilayer may favor the inclusion of hydrophobic molecules (Subczynski et al., 1994). On the other hand, considering the fact that both cholesterol and the drug prefer to align themselves in the hydrophobic region of the membrane and there is limited space available for both, cholesterol and hydrophobic drug molecules might compete for this space between the acyl chains of phospholipids, resulting in lower encapsulation with increasing cholesterol content. It is claimed that incorporation of cholesterol in liposomal drug delivery systems increases the vesicle stability, however, utilizing polyethylene glycol (PEG) chains is also proposed as a means of stabilization, both *in vitro* and *in vivo*, especially when the encapsulation of hydrophobic drugs is affected negatively by the presence of cholesterol (Dos Santos et al., 2002). The effect of cholesterol on CLX encapsulation and release characteristics together with detailed physicochemical characterization of CLX loaded MLVs was reported in the previously published manuscript by our group (Deniz et al., 2010).

It is important to note that, a capsule formulation of CLX was used during the experiments for both the published manuscript on CLX encapsulated in MLVs and part of the presented thesis where *in vitro* characterizations of the liposomes (encapsulation and release) were conducted. The capsule formulations often contain small amounts of excipients which are substances other than the active substance. These substances might have interfered with the experimental results, especially in the interaction of CLX with liposomal membrane components

including cholesterol. Using the pure active substance can circumvent these possibilities and provide a more reliable characterization. Therefore, all other studies' including cell culture studies and preparation and preliminary characterizations of immunoliposomes were conducted with a 99% pure CLX with a certificate of analysis.

In vitro CLX release from four different MLV compositions was investigated and a sustained release profile was observed for more than 72 hours. The amount of drug released in terms of mol drug/mol lipid was calculated in order to take into account the variations in the amount of liposomes aliquoted during sampling and possible losses during preparation steps. In other words, the amount of drug molecules released from the liposome structure per lipid molecule was calculated. This was an indication of the type of drug release behavior; either diffusion from the liposomes or loss of drug due to disintegration of MLV structures. The profiles of percentage of cumulative drug released (Figure 3-3) and above mentioned mol drug/mol lipid were similar, implying total moles of drug released and moles of drug released per moles of lipid were comparable. Therefore the mechanism of drug release in this system was thought to be via diffusion as similar to other hydrophobic drugs, nonetheless *in vivo* drug release mechanism might reveal different mechanisms (Drummond et al., 2008). Drug loss due to liposome burst was not anticipated because there were no sudden changes in the amount of drug released through the 72 hours of release period. A comparable slow release profile of CLX could not be achieved in other studies reporting drug delivery formulations for CLX. For instance; a burst effect was observed for chitosan microspheres, releasing almost 50% of CLX in the first hour (Thakkar et al., 2004). Similarly, solid lipid nanoparticles were shown to release approximately 70% of CLX after 72 hours (Thakkar et al., 2007) and cholesterol-free liposomal formulations of

dexamethasone released higher amounts of the drug in 24 and 48 hours (Tsotas et al., 2007). CLX released from MLVs with different amounts of cholesterol, however were not significantly different from each other at the 72h time point. It was shown here that the cumulative release profile of CLX was similar for MLVs with low cholesterol content as well. Considering the significant reduction in encapsulation at high cholesterol concentrations, a lipid:Chol ratio of 10:1 was considered to be suitable for liposomal formulations of CLX.

MLVs capable of considerable amount of CLX retention after 72 hours are encouraging motives for designing long circulating LUVs for *in vivo* CLX delivery.

4.2 Characteristics of CLX loaded LUVs and PEGylated LUVs

LUVs were prepared by extrusion of MLV suspensions through PC membranes via a mini-extruder apparatus and necessary pressure for extrusion was provided manually. Extrusion process is known to have a better performance in terms of homogeneity of size distribution compared to the other commonly used sonication techniques (Torchilin and Weissig, 2003). As a result extrusion through 800 nm, 400 nm and finally 100 nm PC membranes, LUVs with diameters below 150 nm were obtained (Table 3.3). The Zeta Sizer Nano instrument used to determine the particle size employs laser diffraction principle. It measures the rate of the intensity fluctuation to calculate the intensity distribution and then these data can be converted to volume distribution data employing Mie theory by the software of the instrument. The reported values “Zavg” are the hydrodynamic diameters which correspond to the diameters of spherical particles having the same diffusion speed in solution. Any modification on the particle surface including addition of PEG

chains and even conformations of the polymers can affect the hydrodynamic diameter measurements by altering the diffusion speed of the particles. Therefore, although data obtained by laser diffraction method does not yield the actual particle size, the hydrodynamic diameter of the colloidal DDS is still an important parameter of the behavior *in vitro* and *in vivo*.

The Z_{avg} values of LUV-PEGs with different cholesterol and PEG contents were determined. Presence of Chol or incorporation of PEG-DSPE molecules did not cause significant differences in hydrodynamic diameters of vesicles (Table 3.3) except for DSPC:Chol 10:1 formulation with 0.5% PEG. As an indication of stability during release, size distribution analysis was repeated two weeks later and demonstrated a minor reduction in vesicle diameters (results not shown). It is worth noting that the reduction was not statistically significant for the formulations containing 2% PEG. The hydrophilic shell formed by PEG chains on liposome surfaces contributes essentially to colloidal stability, reduces nonspecific interactions and self-aggregation mainly due to the steric barrier (Drummond et al., 1999). Another observation on the effect of PEGylation was that the PDI values were considerably lower for 2% PEGylated liposomes when compared to non-PEGylated liposomes (Table 3.3). Apparently, PEGylation at 2% of total lipids resulted in a nearly monodisperse population of liposomes which was a desirable feature. In contrast, non-PEGylated liposomes displayed a mid-range polydispersity and this might have resulted from partial fusions or aggregations of the vesicles. TEM analysis revealed the spherical and unilamellar morphology of PEGylated LUVs, supporting the size distribution analysis results (Figure 3- 4).

The percentage of CLX incorporation to cholesterol containing LUVs was not altered at statistically significant levels by addition of PEG molecules (Table 3. 4).

Changes in cholesterol or PEG content did not correlate with CLX encapsulation efficiency. Likewise, percentage CLX loading, indicating the number of CLX molecules for 100 molecules of DSPC and Chol, was comparable and close to the theoretical percentage loading values in all the tested formulations. A recent study reported cholesterol free CLX loaded liposomes (DSPC only) prepared by sonication instead of extrusion and 46% of entrapment efficiency (Perumal et al., 2011). Another immunoliposome containing CLX targeted to vascular cell adhesion molecule-1 (VCAM-1) was prepared with 1,2-dimyristoyl-sn-glycero-3-phosphocholine (DMPC), Chol and 1,2-dipalmitoyl-sn-glycero-3-phosphoethanolamine-N-(glutaryl) (glutaryl-N-PE) in 65:25:10 or 70:25:5 mol% by sonicated in a bath type sonicator for 2 h at 37°C. This preparation was reported to result in 208 to 308 µg/ml CLX which in fact corresponds to only 2.7 to 3% loading (Kang et al., 2011). The reason for low percentage of CLX might be the 14 carbon phospholipid DMPC that is in fluid phase at 37°C and method of preparation that includes sonication at relatively low temperature.

Evaluation of *in vitro* CLX release profiles from LUVs involved comparison of three different amounts of Chol. All three formulations exhibited sustained release profile up to 72 hours, maintaining more than 65% of the incorporated CLX in the liposome structure. Interestingly; LUVs with cholesterol ratio of 10:1 resulted in increased amount of CLX release in addition to increased loading (Figure 3- 5). Since there is a single bilayer in LUV structure, this observation might be explained in a manner to include effects of both cholesterol and CLX. Walter et al. have already shown by small angle X-ray diffraction that CLX is located close to the phospholipids headgroup region in the upper hydrocarbon core, 5–20°A from the center of the membrane (Walter et al., 2004). This region is also where cholesterol is located, its polar beta hydroxyl group close to glycerol backbone carbon of PC

and steroid rings aligned parallel to hydrocarbon chains. Differential scanning calorimetry (DSC) analyses of CLX loaded DSPC:Chol membranes performed by our group indicated that, at 10:1 and 5:1 molar ratios, the main transition peak split into two signals, which might indicate phase separation and presence of more than one domain in the membrane system (Deniz et al., 2010). The release behavior of these domains would differ from a homogeneously loaded membrane, therefore formation of CLX rich and poor domains with different cholesterol contents might be the reason for variations in the release profiles.

In vitro CLX release profiles from PEGylated LUVs involved cholesterol-free and DSPC:Chol 10:1 formulation with two different levels of PEGylation as 0.5% and 2% of lipid content. Presence of hydrophilic PEG molecules in cholesterol-free liposomes provided a superior barrier for the release of hydrophobic CLX as observed by the significantly lower amount of drug release from 2% PEGylated liposomes. However; in cholesterol containing liposomes, the increase in PEG content did not result in significant difference in terms of total amount of drug released (Figure 3- 6). The potential of high CLX retention in LUVs can enable delivery of this bioactive agent to target site at effective concentrations with less liposomal carrier requirement, also with minimum exposure of healthy tissues to CLX during circulation time of liposomes.

The extent of cellular association of PEGylated liposomes was qualitatively analyzed via fluorescent LSCM. Fluorescent probe selection played an important role in the study of cellular association and more importantly cellular localization of labeled liposomes. Lipophilic long-chain carbocyanines such as DiI, DiO and their analogs are often used for labeling liposomal and cellular membranes. These fluorophores are highly photostable when incorporated into membranes. On the

other hand, lipophilic fluorescent probes were reported to diffuse laterally through the entire membrane and they can even transfer between intact membranes (Lassailly et al., 2010). Preliminary studies with DiIC₁₈(3) were abandoned due to this diffusion behavior, since the fluorophore stained the cellular membranes rapidly after cellular association and the localization of liposomes was not traced under these circumstances. The ideal probe for labeling and tracing the cellular localization of liposomes was a phospholipid analogue that has a covalently bound fluorescent molecule in the phospholipid headgroup region. Rhodamine labeled DHPE was considered as a proper candidate for this purpose. Rh-PE is maintained in the liposomal membrane structure and is not subject to lateral diffusion to cellular membranes (Nichols and Pagano, 1982). Due to the combined action of CLX, Chol and PEG-DSPE in LUVs composed of DSPC; determination of dose of treatment and effective duration was essential.

Cellular association of Rhodamine labeled PEGylated LUVs was evaluated after 30 minutes, 2 hours and 6 hours of incubation using 200 μ M and 500 μ M of final lipid dose (Figure 3- 7) in SW620 colon cancer cells. Fluorescent signal was barely detectable at 30 minutes of treatment regardless of the dose (Figure 3- 7, A&D). At 2 hours, higher cellular association was observed at 500 μ M dose than 200 μ M (Figure 3- 7, B&E). Although a nuclear stain was not used in this study, merged images of fluorescent Rhodamine channel and transmission channel enabled visualization of the cellular and nuclear borders and localization of liposomes was traced in that respect. Surface bound and occasionally internalized liposomes were observed and the extent of cellular association increased from 2 hours to 6 hours. Six hours of treatment resulted in a homogeneous population of cells with fluorescent signal and more importantly, signal localized to perinuclear space (Figure 3- 7, C&F).

CLX loaded liposomes were internalized by the cells after surface binding and localized to intracellular vesicles. The punctuate pattern and not a diffused pattern of Rhodamine signal suggests that, liposomes were contained in vesicles rather than being distributed in the cytoplasmic space. In order to trace the intracellular fate of the liposomes, fluorescently labeled transferrin was used as a marker probe. Transferrin is a marker for early endosomes and also perinuclear recycling endosomes. The signal from drug loaded Rhodamine labeled PEGylated liposomes did not co-localize with Tr-AF680 signal indicating that liposomes were not localized to early endosomes or recycling endosomes at the time of observation. Instead, the absence of co-localization might indicate that liposomes were most probably localized to lysosomes. Although transferrin-AF signal was detected in every cell, liposome associated Rhodamine signal was detected in a sub-population of the cells even at 6 hours of treatment. (Figure 3-8, C). During the LSCM imaging, z-stack images were collected and used for analyzing the presence of rhodamine signal from several foci. Additionally, 3D images were reconstructed by forming projections of z-stack images on either x or y plane (Figure 3-9, Figure 3-10 and Figure 3-11). When the projection images were examined on both x-y and x-z planes, representing a cross-sectional view of the cellular volume, the Rhodamine signal was detected in locations corresponding to intracellular volume rather than boundaries of cell surface. CLX loaded PEGylated liposomes were internalized by the cells and localized to perinuclear vesicles, most probably to lysosomes, similar to reported results by several other studies (Huth et al., 2006; Straubinger et al., 1990).

For quantitative evaluation of the extent of cellular association of PEGylated liposomes, FACS analyses were conducted on HCT-116 and SW620 colon cancer

cell lines. For fluorescent post-labeling of PEGylated LUVs, a DiO analogue SP-DiOC₁₈(3) was used. This lipophilic molecule is reported to persist the fixation procedure using formaldehyde. In both cell lines, 6 hours of treatment with labeled liposomes lead to significantly higher mean fluorescence intensity values (Figure 3-12). The labeled cell populations were observed to shift above the threshold value as the treatment duration was extended from 30 minutes to 2 hours and up to 6 hours in both cell lines (Figure 3-13 and 3-14). When histograms were plotted for three different time points, the clear trend was observed as treatment duration increased, the population shifted right (Figure 3-15). These data were informative in relation to non-specific cellular binding and internalization of PEGylated liposomes loaded with high amount of CLX. Targeting strategies are expected to improve the extent of cellular association in the target cell populations (for example EGFR overexpressing cells) and accelerate the uptake kinetics due to specific ligand-receptor binding characteristics.

Cytotoxic effects of free CLX and CLX loaded PEGylated liposomes were tested on COX-2 positive HT-29 cells and COX-2 negative SW620 cells using MTT assay, enabled evaluation of effects from a viewpoint of COX-2 dependency. The cytotoxic effects of free CLX were observed at comparably earlier time points and at lower concentrations for HT-29 cells compared to SW620. For example, at 24 hours of treatment with 50 μ M CLX, only 38% of HT-29 cells were viable while 59% of SW620 cells were viable, with respect to untreated control cells. In a similar manner, after 72 hours of treatment of HT-29 cells, 30 μ M CLX inhibited 50% and 50 μ M CLX inhibited 76% of proliferation. On the other hand, in SW620 cells, 30 μ M CLX inhibited only 30% of cellular proliferation, and increasing CLX concentration to 50 μ M resulted in 60% inhibition of proliferation at 72 hours. Both cell lines responded dramatically to 100 μ M free CLX after 48 and 72 hours of

treatment. These differences in the two cell lines in response to CLX treatment are in accordance with available information in the literature; however, the reported cellular viability values by Buecher et al. were slightly different (Table A. 2, last row). The dissimilar results are most probably due to different methodology used; namely treatment for 6 days and quantification of cellular viability by crystal violet staining of the DNA (Buecher et al., 2005). On the overall, using high COX-2 expressing and COX-2 negative cell lines served as a means to observe that cytotoxic effects were more apparent in COX-2 expressing cell line most likely due to inhibition of pathways downstream of prostaglandin synthesis. Nevertheless, the COX-2 negative cell line SW620 was also affected due to the well documented COX-2 independent effects of CLX (Grosch et al., 2006; Grosch et al., 2001; Maier et al., 2004). In addition, the functional *in vitro* assays including anchorage independent growth, migration and invasion through Matrigel performed with free CLX in the same cell lines were reported to be irrespective of COX-2 expression status by our group (Sade et al., 2012).

The cytotoxic effect of liposome entrapped CLX was also tested in HT-29 and SW620 cells. As a general trend, increasing the treatment duration from 24 hours to 48 and 72 hours resulted in enhanced cytotoxic effect on both cell lines. At 24 hours of treatment, 50 and 100 μM of CLX loaded liposomes showed slight toxicity on cells that were not significantly different from empty liposomes (**Figure 3-18** and **Figure 3-19**).

In high COX-2 expressing HT-29 cell line, the cytotoxic effect of liposomal CLX was found to increase in a dose dependent manner, in which the most dramatic response was found at 600 μM treatment leading to 95% cellular death at 72 hours (**Figure 3-18**).

A rough comparison of doses of free and liposomal CLX to inhibit approximately 50% of cellular proliferation for HT-29 cell line at 48 hours revealed that, 200 μ M liposomal CLX treatment corresponded to 30 μ M free CLX (**Figure 3- 17** and **Figure 3-18**).

In the COX-2 non-expressing SW620 cell line, the dose dependent cytotoxic effect of liposomal CLX was evident above 100 μ M. The most concentrated treatment with 600 μ M lead to 62% inhibition of cellular proliferation at 24 hours, and 78% inhibition at 72 hours. Comparing of doses of free and liposomal CLX required to inhibit approximately 50% of cellular proliferation for SW620 cell line at 48 hours revealed that, 200 μ M liposomal treatment corresponded to CLX 50 μ M free CLX (**Figure 3- 17** and **Figure 3- 19**). The relevant concentration was 30 μ M for HT-29 cells, hence underlining that liposomal CLX dose to obtain cytotoxicity was higher for COX-2 negative cell line that is in parallel with free CLX treatment. In an independent experiment, different doses of Empty LUV-PEGs were tested and were found to show mild cytotoxic effects regardless of the treatment dose (results not shown). Although DSPC, cholesterol and PEG-DSPC are generally regarded as non-toxic; the observed partial toxicity of empty liposomes indicates that the duration of liposome treatment has certain effect on cells and should be kept at minimum when possible.

The obvious difference regarding the inhibitory concentrations of free and liposomal CLX most probably lies in the cellular uptake mechanism of the two formulations. Free CLX was added directly to cell culture media as a solution of DMSO. This enabled rapid diffusion of CLX upon contact with the cell membrane. On the contrary, liposomal CLX is a colloidal DDS that can remain in suspension in

the aqueous cell culture media, and CLX can have indirect contact with cells due to fusion or internalization of liposomes or by release in the free form followed by uptake. Since the proposed liposomal CLX formulation was aimed for *in vivo* stability in blood circulation, the rigid structure of DSPC-Chol membranes did not favor the membrane fusions and resulted in high CLX retention instead of a fast release profile.

For the assessment of the effects of liposomal CLX formulation on cellular motility of cancer cells, an *in vitro* scratch wound healing assay was employed. During cancer progression, tumor tissue undergoes reorganization and invading cells need to alter their cell-cell adhesion properties, rearrange the extracellular matrix environment and reorganize their cytoskeletons to facilitate cellular motility (Yilmaz and Christofori, 2010). PGE₂, the enzymatic product of COX-2, was implicated in breaking cell-cell junctions maintained by cadherins such as E-cadherin, therefore inhibition of COX-2 activity by coxibs can be used to interfere with cellular motility processes. In addition, CLX was previously reported to be involved in inhibition of motility and invasion properties of breast cancer cell lines (Basu et al., 2005), primary oral carcinoma cells (Kwak et al., 2007) and head and neck carcinoma cells (Kim et al., 2010). Concerning the proposed liposomal CLX formulation; before progressing to functional assays including *in vitro* invasion and migration assays in 3D cell culture models, the duration and dose of CLX-LUV-PEG treatment was determined in a simpler experimental design. The *in vitro* scratch wound healing assay is an easy, low-cost and frequently used method to measure cell migration *in vitro* in 2D cell culture plates (Liang et al., 2007). It should be noted that the assay takes into account the combined action of proliferation and cellular migration.

SW620 cells are known for their high migratory potential, therefore a convenient model to test the effectiveness of the duration and dose of liposomal CLX treatments in terms of cellular motility. 10X magnified images of wound closure up to 60 hours displayed the ability of single cells to migrate towards the wound area created and enabled the evaluation of motility rather than proliferation of cells in the entire wound area. Similar to cytotoxicity results, empty liposomes exhibited a partial inhibition of wound closure, nevertheless after 120 hours of treatment, 400 μ M liposomal CLX treatment provided a significantly higher inhibition of cellular motility compared to both untreated control wells and empty liposome treatments (Figure 3- 21). Due to the fact that the experimental conditions in MTT assays and scratch wound healing assays were entirely different in terms of cellular confluency; the response of cells to treatments might have been dissimilar. For instance; while 400 μ M liposomal CLX treatment caused more than 50% inhibition of proliferation in exponentially growing cells, this inhibitory effect might not be identically observed in confluent cultures used in wound healing assay (Figure 3- 23).

4.3 Characteristics of CLX loaded ILs

IL formulations were prepared via conjugation of half-IgG fragments to the distal ends of Maleimide functionalized PEG chains grafted on CLX loaded liposomes.

The conventional method for liposome or IL preparation involves addition of all constituents during the formation of the vesicles, while an alternative method was suggested (Ishida et al., 1999) that is widely known as “post-insertion” of PEG conjugated ligands or PEG-DSPE molecules to pre-formed liposomes. The post-insertion method requires formation of PEG-DSPE micelles first and then

incubation of the micelles with liposomes at temperatures higher than the T_m of the lipids. This method was used for preparation of PEGylated LUVs. The incorporation of PEG to the liposome structure was reported to be time and dose dependent (Ishida et al., 1999). Since T_m of DSPC is 55 °C, the incubation needs to be above that temperature which increases the risk of denaturing the MAb and abolishing the binding ability to the receptor. Additionally; maleimide groups are susceptible to hydrolysis in aqueous environments, therefore the duration for processes that Maleimide terminated PEG-DSPE is in solution has to be minimized. To sum up, a direct coupling technique was applied for covalent conjugation of IgG to maleimide functionalized PEG groups.

Optimization studies with non-specific mouse IgG isotype controls enabled testing the effectiveness of the IgG reduction and conjugation reactions in addition to the evaluation of liposome diameters and CLX encapsulation efficiency after the IgG conjugation and purification steps. A mild reduction reaction was carried out with β -mercaptoethylamine in order to obtain half-IgG molecules and preventing excessive reduction of disulfide bonds, which would lead to dissociation of heavy and light chains of IgG. Formation of stable thioether bonds between maleimide groups and sulfhydryl groups is specific at pH 6.5 to 7.5 with 1000 fold higher reaction rate for thiols than amine groups (Hermanson, 2008). This advantage of high selectivity was utilized for site specific conjugation of reduced IgG molecules to maleimide functionalized PEG-DSPE molecules without cross reactivity with amino groups in the protein structure. The IgG conjugation efficiency was indirectly calculated by quantification of the unconjugated MAb, because IL samples displayed indeterminate results in SDS-PAGE analyses for a direct quantification of IgG molecules since the high lipid content in ILs interfered with the migration pattern of the samples.

Characterization studies carried out on the ILs indicated that using isotypic mouse IgG or anti-EGFR IgG resulted in highly similar vesicle diameters and IgG conjugation efficiencies. IL sizes were at 93.6 to 101.4 nm with mouse IgG and 98.4 to 99.4 nm with anti-EGFR IgG. IgG conjugation efficiencies ranged from 41.3% to 51.8% with mouse IgG while improved conjugation efficiency of 88% was measured with anti-EGFR IgG. This difference in percentage of conjugated IgGs might have resulted from differences in the starting materials. Mouse IgG product was supplied in lyophilized powder form and was originally isolated from mouse serum while anti-EGFR MAb was supplied as a solution free of carrier proteins and was maintained at -20°C. The manufacturers recommend optimization of conditions for reduction and conjugations reactions in order to take into account the variations of each product.

The overall efficiency of liposome preparation in terms of percentage of lipid and percentage of CLX encapsulation were remarkably lower when anti-EGFR MAb was used. CLX loaded LUVs occasionally had aggregations after the overnight incubation with the reduced IgGs. During IL purification by centrifugal ultra-filtration process, these aggregates resulted in clogging, therefore ILs were neither filtered nor recovered. The low concentration of CLX in the final product brought about the necessity to use high amounts of liposomes during the treatments to achieve required dose of 400 μ M of CLX, in turn made the results difficult to interpret in terms of the contribution of anti-EGFR MAb and CLX to the combined effect.

Cytotoxicity of CLX loaded and EGFR targeted ILs were analyzed via MTT assay in HCT-116 cell line with high EGFR expression and SW620 cell line with no

EGFR expression. CLX loaded non-targeted, Empty EGFR-targeted and Empty non-targeted liposomes were prepared and used in treatments simultaneously. Treatment durations of 12, 24 and 48 hours allowed for evaluation of both short and long term effects.

In HCT-116 cells; CLX-IL treatment inhibited cellular proliferation starting from 12 hours at significantly higher levels than the other formulations (**Figure 3-28**). This drastic effect was more than the additive effect of Empty-IL and CLX-LUV-PEG treatments at 12th hour, when neither Empty IL nor CLX effect has reached considerable levels yet. Although HCT-116 cell line was reported as non-responsive to anti-EGFR MAb therapy (Jhaver et al., 2009); high level of EGFR expression on the cell surface might have accelerated the cellular uptake of liposomes and enhance the cytotoxic effect of CLX. As the treatment duration was extended, the effects of Empty-IL and CLX-LUV-PEG formulations also became significantly different from the control group.

In SW620 cells, the cytotoxic effect of CLX-IL formulation was remarkably lower than the HCT-116 cells (**Figure 3-28**). Although the effect was observed to increase with longer incubations, the data shown is not conclusive due the toxic effect of Empty-IL formulation. CLX-LUV-PEG formulation inhibited SW620 cellular proliferation at very minor levels and the effect was not significantly different from Empty-LUV-PEG formulation.

Cellular response to the anti-EGFR MAb treatment was not the primary determinant of the efficacy of the targeted drug delivery system studied in the context of this thesis. The cytotoxic effect of anti-EGFR MAb (Cetuximab) was not correlated with EGFR protein level or EGFR mutation status (Wheeler et al., 2010). Several

studies argue a link between K-RAS mutation status and Cetuximab response, as tumors with wild type K-Ras showing improved response to this agent, yet there is no established correlation. Cytotoxic effect Cetuximab on various cancer cell lines was investigated and reported previously (Jhaver et al., 2009); a summary of results are given in Figure A- 8.

Targeting ligands are required not only to enable binding to surface proteins with high affinity, but also to induce internalization of the drug delivery systems. In HER2-overexpressing tumors, Doxorubicin-loaded HER2 targeted immunoliposomes resulted in notable increase in therapeutic efficacy when compared to free doxorubicin, free anti-HER2 MAb (trastuzumab), nontargeted liposomal doxorubicin and combinations of these agents (Park et al., 2002). Although the accumulation of non-targeted liposomes in solid tumor site due to EPR effect did not show anti-tumor efficacy, HER2 targeted IL were effective in binding and internalization by HER2 overexpressing cells (Kirpotin et al., 2006). Another example was immunoliposomes containing anti-CD19 ligand that can be internalized exhibiting a more significant therapeutic outcome, while immunoliposomes prepared with non-internalizing anti-CD20 ligand did not lead to comparable efficacy (Sapra and Allen, 2002). In contrast to these examples, delivery by DDSs that are not internalized might be argued to offer other advantages such as exposure of more number of cells in the solid tumor area after the contents are released and in addition death of neighboring cells even if they lack the target surface proteins (Allen, 1994).

The results obtained from cytotoxic effect of CLX-IL formulation require validation by testing the formulation on a larger panel of cells with different EGFR, COX-2 and K-Ras mutation status. Overexpression of EGFR via plasmid transfection in

SW620 cells will provide an isogenic background to test the contribution of EGFR targeting, while another similar approach could be silencing of EGFR in HCT-116 cell line. Also other colorectal cell lines with different expression levels of EGFR and COX-2 will be valuable tools for further analysis of CLX-IL formulation at the functional level before moving to in vivo studies.

CHAPTER 5

CONCLUSION

Liposomal drug delivery systems have been alluded as the “magic bullet” in the war against cancer since their tumor selective accumulation can overcome the widely known adverse systemic effects of conventional chemotherapy (Maeda and Matsumura, 1989). Nano sized liposomes designed to target cancer specific cellular features offer the advantage of optimizing personalized medicine for patients, as well as diminishing the ineffective treatment modalities, hence the financial burden of healthcare on the governments.

In the presented thesis, the highly hydrophobic COX-2 inhibitor drug CLX was successfully incorporated into liposomes composed of DSPC and cholesterol for the first time in literature. The potential for developing liposomal CLX formulations was first investigated by studying the molecular interactions of CLX and cholesterol in DSPC model membranes (Deniz et al., 2010).

For the intravenous delivery route, CLX loaded LUVs were prepared at the nano level to serve as a framework for constructing EGFR targeted immunoliposomes. The effects of cholesterol and lipid anchored PEG polymers on vesicle size, CLX encapsulation and *in vitro* CLX release profile were examined. Optimum liposome formulation was determined as 10:1 DSPC:Cholesterol molar ratio and PEG grafting at 2% of phospholipids. The extent of cellular association of these

PEGylated liposomes was evaluated both quantitatively and qualitatively, revealing efficient internalization by the cells and localization to perinuclear vesicles.

CLX loaded PEGylated liposomes were shown to have cytotoxic effects significantly higher than empty liposomes at 24 and 72 hours of treatments, and were capable of inhibiting cellular motility of cancer cells in a 2D cell culture model system. These functional assays, together with data available in the literature suggest that the CLX in the liposomal formulation can provide COX-2 dependent and independent anti-proliferative and anti-tumorigenic effects.

Long circulating liposomes are known to accumulate at solid tumor sites due to enhanced permeability and retention (EPR) effect; however, improved antitumor efficacy can be achieved by targeting of liposomes to specific cells and internalization through receptor mediated endocytosis. EGFR is a frequently overexpressed cell surface protein that appears as a viable candidate for immunoliposome targeting for chemoprevention and treatment of colorectal and several other epithelial tumors. The initial studies conducted with EGFR targeted CLX loaded ILs showed that the formulation was extremely cytotoxic in HCT-116 cells (high EGFR expression) at early time points while this effect was not observed in SW620 cells (no EGFR expression).

The results presented in the current thesis are preliminary and they simply show the necessity for investigating cellular association and localization and exploring the cytotoxic effects of CLX-IL formulation on other cell lines with different levels of COX-2 and EGFR expression and eventually proof of principle studies of anti-tumor efficacy in *in vivo* xenograft models.

At the clinical level, liposomal CLX formulation developed in this study has the potential to exert its effects by:

- i. COX-2 dependent action of CLX; inhibition of PGE2 production
- ii. COX-2 independent actions of CLX; induction of apoptosis, regulation of cell cycle, and inhibition of angiogenesis or metastasis
- iii. In case of CLX loaded EGFR targeted ILs; delivery of CLX to EGFR overexpressing cells to provide selective treatment of cancer

Several recent studies have espoused a shift towards personalized medicine. Further research into the utilization of smart drug delivery systems, better targeting strategies and careful patient selection may enhance the efficacy of these tailored therapies even further and indeed bring us closer to the reality of a ‘magic bullet’ for cancer therapy.

REFERENCES

- Aaltonen, L. A., P. Peltomaki, J. P. Mecklin, H. Jarvinen, J. R. Jass, J. S. Green, H. T. Lynch, P. Watson, G. Tallqvist, M. Juhola, and et al., 1994, Replication errors in benign and malignant tumors from hereditary nonpolyposis colorectal cancer patients: *Cancer Res*, v. 54, p. 1645-8.
- Aaronson, S. A., 1991, Growth-factors and cancer: *Science*, v. 254, p. 1146-1153.
- Abuchowski, A., T. van Es, N. C. Palczuk, and F. F. Davis, 1977, Alteration of immunological properties of bovine serum albumin by covalent attachment of polyethylene glycol: *J Biol Chem*, v. 252, p. 3578-81.
- Akimoto, T., N. R. Hunter, L. Buchmiller, K. Mason, K. K. Ang, and L. Milas, 1999, Inverse relationship between epidermal growth factor receptor expression and radiocurability of murine carcinomas: *Clinical Cancer Research*, v. 5, p. 2884-2890.
- Allen, T. M., 1994, Long-circulating (sterically stabilized) liposomes for targeted drug-delivery: *Trends in Pharmacological Sciences*, v. 15, p. 215-220.
- Allen, T. M., C. B. Hansen, and D. E. L. de Menezes, 1995, Pharmacokinetics of long-circulating liposomes: *Advanced Drug Delivery Reviews*, v. 16, p. 267-284.
- Ansell, S. M., T. O. Harasym, P. G. Tardi, S. S. Buchkowsky, M. B. Bally, and P. R. Cullis, 2000, Antibody conjugation methods for active targeting of liposomes: *Methods Mol Med*, v. 25, p. 51-68.
- Banerjee, S., and H. Flores-Rozas, 2010, Monoclonal antibodies for targeted therapy in colorectal cancer: *Cancer Biol Ther*, v. 9, p. 563-71.

- Bangham, A. D., M. M. Standish, and J. C. Watkins, 1965, Diffusion of univalent ions across lamellae of swollen phospholipids: *Journal of Molecular Biology*, v. 13, p. 238-&.
- Baron, J. A., B. F. Cole, R. S. Sandler, R. W. Haile, D. Ahnen, R. Bresalier, G. McKeown-Eyssen, R. W. Summers, R. Rothstein, C. A. Burke, D. C. Snover, T. R. Church, J. I. Allen, M. Beach, G. J. Beck, J. H. Bond, T. Byers, E. R. Greenberg, J. S. Mandel, N. Marcon, L. A. Mott, L. Pearson, F. Saibil, and R. U. van Stolk, 2003, A randomized trial of aspirin to prevent colorectal adenomas: *N Engl J Med*, v. 348, p. 891-9.
- Baselga, J., and J. Mendelsohn, 1994, Receptor blockade with monoclonal-antibodies as anticancer therapy: *Pharmacology & Therapeutics*, v. 64, p. 127-154.
- Basu, G. D., L. B. Pathangey, T. L. Tinder, S. J. Gendler, and P. Mukherjee, 2005, Mechanisms underlying the growth inhibitory effects of the cyclooxygenase-2 inhibitor celecoxib in human breast cancer cells: *Breast Cancer Research*, v. 7, p. R422-R435.
- Beduneau, A., P. Saulnier, F. Hindre, A. Clavreul, J. C. Leroux, and J. P. Benoit, 2007, Design of targeted lipid nanocapsules by conjugation of whole antibodies and antibody Fab' fragments: *Biomaterials*, v. 28, p. 4978-4990.
- Bertrand, N., and J. C. Leroux, 2011, The journey of a drug-carrier in the body: An anatomo-physiological perspective: *J Control Release*.
- Bhatia, A., R. Kumar, and O. P. Katare, 2004, Tamoxifen in topical liposomes: development, characterization and in-vitro evaluation: *Journal of Pharmacy and Pharmaceutical Sciences*, v. 7, p. 252-259.
- Brigger, I., C. Dubernet, and P. Couvreur, 2002, Nanoparticles in cancer therapy and diagnosis: *Advanced Drug Delivery Reviews*, v. 54, p. 631-651.
- Buchanan, F. G., V. Holla, S. Katkuri, P. Matta, and R. N. DuBois, 2007, Targeting cyclooxygenase-2 and the epidermal growth factor receptor for the prevention and treatment of intestinal cancer, *Cancer Res*, v. 67, p. 9380-8.
- Buecher, B., D. Bouancheau, A. Broquet, S. Bezieau, M. G. Denis, C. Bonnet, M. F. Heymann, A. Jarry, J. P. Galmiche, and H. M. Blottiere, 2005, Growth

- inhibitory effect of celecoxib and rofecoxib on human colorectal carcinoma cell lines: *Anticancer Research*, v. 25, p. 225-233.
- Chen, Z., L. D. Ke, X. H. Yuan, and K. Adler-Storthz, 2000, Correlation of cisplatin sensitivity with differential alteration of EGFR expression in head and neck cancer cells: *Anticancer Research*, v. 20, p. 899-902.
- Choe, M. S., X. Zhang, H. J. Shin, D. M. Shin, and Z. G. Chen, 2005, Interaction between epidermal growth factor receptor- and cyclooxygenase 2-mediated pathways and its implications for the chemoprevention of head and neck cancer, *Mol Cancer Ther*, v. 4, p. 1448-55.
- Chonn, A., S. C. Semple, and P. R. Cullis, 1992, Association of blood proteins with large unilamellar liposomes *in vivo* - relation to circulation lifetimes: *Journal of Biological Chemistry*, v. 267, p. 18759-18765.
- Ciardiello, F., R. Caputo, T. Troiani, G. Borriello, E. R. Kandimalla, S. Agrawal, J. Mendelsohn, A. R. Bianco, and G. Tortora, 2001, Antisense oligonucleotides targeting the epidermal growth factor receptor inhibit proliferation, induce apoptosis, and cooperate with cytotoxic drugs in human cancer cell lines, *Int J Cancer*, v. 93, 2001 Wiley-Liss, Inc., p. 172-8.
- Ciardiello, F., and G. Tortora, 2001, A novel approach in the treatment of cancer: Targeting the epidermal growth factor receptor: *Clinical Cancer Research*, v. 7, p. 2958-2970.
- Damen, J., J. Regts, and G. Scherphof, 1981, Transfer and exchange of phospholipid between small unilamellar liposomes and rat plasma high-density lipoproteins - dependence on cholesterol content and phospholipid-composition: *Biochimica Et Biophysica Acta*, v. 665, p. 538-545.
- Dannenbergh, A. J., S. M. Lippman, J. R. Mann, K. Subbaramaiah, and R. N. DuBois, 2005, Cyclooxygenase-2 and epidermal growth factor receptor: pharmacologic targets for chemoprevention: *J Clin Oncol*, v. 23, p. 254-66.
- de Heer, P., M. H. Sandel, G. Guertens, G. de Boeck, M. M. Koudijs, J. F. Nagelkerke, J. M. C. Junggeburst, E. A. de Bruijn, C. J. H. van de Velde, and P. J. K. Kuppen, 2008, Celecoxib inhibits growth of tumors in a syngeneic rat liver metastases model for colorectal cancer: *Cancer Chemotherapy and Pharmacology*, v. 62, p. 811-819.

- Deniz, A., A. Sade, F. Severcan, D. Keskin, A. Tezcaner, and S. Banerjee, 2010, Celecoxib-loaded liposomes: effect of cholesterol on encapsulation and in vitro release characteristics: *Bioscience Reports*, v. 30, p. 365-373.
- Dhabu, P. M., and K. G. Akamanchi, 2002, A stability-indicating HPLC method to determine celecoxib in capsule formulations: *Drug Development and Industrial Pharmacy*, v. 28, p. 815-821.
- Dos Santos, N., L. D. Mayer, S. A. Abraham, R. C. Gallagher, R. A. K. Cox, P. G. Tardi, and M. B. Bally, 2002, Improved retention of idarubicin after intravenous injection obtained for cholesterol-free liposomes: *Biochimica Et Biophysica Acta-Biomembranes*, v. 1561, p. 188-201.
- Drummond, D. C., O. Meyer, K. L. Hong, D. B. Kirpotin, and D. Papahadjopoulos, 1999, Optimizing liposomes for delivery of chemotherapeutic agents to solid tumors: *Pharmacological Reviews*, v. 51, p. 691-743.
- Drummond, D. C., C. O. Noble, M. E. Hayes, J. W. Park, and D. B. Kirpotin, 2008, Pharmacokinetics and In Vivo Drug Release Rates in Liposomal Nanocarrier Development: *Journal of Pharmaceutical Sciences*, v. 97, p. 4696-4740.
- Dubois, R. N., S. B. Abramson, L. Crofford, R. A. Gupta, L. S. Simon, L. B. Van De Putte, and P. E. Lipsky, 1998, Cyclooxygenase in biology and disease: *FASEB J*, v. 12, p. 1063-73.
- Eberhart, C. E., R. J. Coffey, A. Radhika, F. M. Giardiello, S. Ferrenbach, and R. N. Dubois, 1994, Up-regulation of cyclooxygenase-2 gene-expression in human colorectal adenomas and adenocarcinomas: *Gastroenterology*, v. 107, p. 1183-1188.
- Fan, Z., Y. Lu, X. Wu, and J. Mendelsohn, 1994, Antibody-induced epidermal growth factor receptor dimerization mediates inhibition of autocrine proliferation of A431 squamous carcinoma cells: *J Biol Chem*, v. 269, p. 27595-602.
- FitzGerald, G., 2003, COX-2 and beyond: Approaches to prostaglandin inhibition in human disease: *Nature Reviews Drug Discovery*, v. 2, p. 879-890.
- FitzGerald, G. A., and C. Patrono, 2001, The coxibs, selective inhibitors of cyclooxygenase-2: *N Engl J Med*, v. 345, p. 433-42.

- Funk, C. D., 2001, Prostaglandins and leukotrienes: advances in eicosanoid biology: *Science*, v. 294, p. 1871-5.
- Gabizon, A. A., H. Shmeeda, and S. Zalipsky, 2006, Pros and cons of the liposome platform in cancer drug targeting, *J Liposome Res*, v. 16, p. 175-83.
- Giardiello, F. M., S. R. Hamilton, A. J. Krush, S. Piantadosi, L. M. Hyland, P. Celano, S. V. Booker, C. R. Robinson, and G. J. A. Offerhaus, 1993, Treatment of colonic and rectal adenomas with sulindac in familial adenomatous polyposis: *New England Journal of Medicine*, v. 328, p. 1313-1316.
- Greish, K., J. Fang, T. Inutsuka, A. Nagamitsu, and H. Maeda, 2003, Macromolecular therapeutics - Advantages and prospects with special emphasis on solid tumour targeting: *Clinical Pharmacokinetics*, v. 42, p. 1089-1105.
- Grosch, S., T. J. Maier, S. Schiffmann, and G. Geisslinger, 2006, Cyclooxygenase-2 (COX-2)-independent anticarcinogenic effects of selective COX-2 inhibitors: *Journal of the National Cancer Institute*, v. 98, p. 736-747.
- Grosch, S., I. Tegeder, E. Niederberger, L. Brautigam, and G. Geisslinger, 2001, COX-2 independent induction of cell cycle arrest and apoptosis in colon cancer cells by the selective COX-2 inhibitor celecoxib: *Faseb Journal*, v. 15, p. 2742-+.
- Gryfe, R., C. Swallow, B. Bapat, M. Redston, S. Gallinger, and J. Couture, 1997, Molecular biology of colorectal cancer: *Curr Probl Cancer*, v. 21, p. 233-300.
- Gupta, R. A., and R. N. DuBois, 2000a, Combinations for cancer prevention: *Nat Med*, v. 6, p. 974-5.
- Gupta, R. A., and R. N. DuBois, 2000b, Translational studies on COX-2 inhibitors in the prevention and treatment of colon cancer: *Colorectal Cancer: New Aspects of Molecular Biology and Immunology and Their Clinical Applications*, v. 910, p. 196-206.
- Gupta, R. A., and R. N. Dubois, 2001, Colorectal cancer prevention and treatment by inhibition of cyclooxygenase-2: *Nat Rev Cancer*, v. 1, p. 11-21.

- Hamilton, S. R., 1992, The adenoma-adenocarcinoma sequence in the large bowel: variations on a theme: *J Cell Biochem Suppl*, v. 16G, p. 41-6.
- Harashima, H., K. Sakata, K. Funato, and H. Kiwada, 1994, Enhanced hepatic uptake of liposomes through complement activation depending on the size of liposomes: *Pharm Res*, v. 11, p. 402-6.
- Hermanson, G. T., 2008, *Bioconjugate techniques*, Academic Press.
- Higuchi, T., T. Iwama, K. Yoshinaga, M. Toyooka, M. M. Taketo, and K. Sugihara, 2003, A randomized, double-blind, placebo-controlled trial of the effects of rofecoxib, a selective cyclooxygenase-2 inhibitor, on rectal polyps in familial adenomatous polyposis patients: *Clinical Cancer Research*, v. 9, p. 4756-4760.
- Hobbs, S. K., W. L. Monsky, F. Yuan, W. G. Roberts, L. Griffith, V. P. Torchilin, and R. K. Jain, 1998, Regulation of transport pathways in tumor vessels: role of tumor type and microenvironment: *Proc Natl Acad Sci U S A*, v. 95, p. 4607-12.
- Huth, U. S., R. Schubert, and R. Peschka-Suss, 2006, Investigating the uptake and intracellular fate of pH-sensitive liposomes by flow cytometry and spectral bio-imaging: *Journal of Controlled Release*, v. 110, p. 490-504.
- Immordino, M. L., F. Dosio, and L. Cattel, 2006, Stealth liposomes: review of the basic science, rationale, and clinical applications, existing and potential: *International Journal of Nanomedicine*, v. 1, p. 297-315.
- Ishida, T., D. L. Iden, and T. M. Allen, 1999, A combinatorial approach to producing sterically stabilized (Stealth) immunoliposomal drugs: *FEBS Lett*, v. 460, p. 129-33.
- Itzkowitz, S. H., and X. Y. Yio, 2004, Inflammation and cancer - IV. Colorectal cancer in inflammatory bowel disease: the role of inflammation: *American Journal of Physiology-Gastrointestinal and Liver Physiology*, v. 287, p. G7-G17.
- Jain, S. K., Y. Gupta, A. Jain, and M. Bhole, 2007, Multivesicular liposomes bearing celecoxib-beta-cyclodextrin complex for transdermal delivery: *Drug Delivery*, v. 15, p. 327-335.

- Jannot, C. B., R. R. Beerli, S. Mason, W. J. Gullick, and N. E. Hynes, 1996, Intracellular expression of a single-chain antibody directed to the EGFR leads to growth inhibition of tumor cells: *Oncogene*, v. 13, p. 275-82.
- Jhawer, M., S. Goel, A. J. Wilson, C. Montagna, Y. H. Ling, D. S. Byun, S. Nasser, D. Arango, J. Shin, L. Klampfer, L. H. Augenlicht, R. Perez-Soler, and J. M. Mariadason, 2009, PIK3CA Mutation/PTEN Expression Status Predicts Response of Colon Cancer Cells to the Epidermal Growth Factor Receptor Inhibitor Cetuximab (vol 68, pg 1953, 2008): *Cancer Research*, v. 69, p. 9156-9156.
- Jones, A., and A. L. Harris, 1998, New developments in angiogenesis: A major mechanism for tumor growth and target for therapy: *Cancer Journal from Scientific American*, v. 4, p. 209-217.
- Kang, D. I., S. Lee, J. T. Lee, B. J. Sung, J. Y. Yoon, J. K. Kim, J. Chung, and S. J. Lim, 2011, Preparation and in vitro evaluation of anti-VCAM-1-Fab"-conjugated liposomes for the targeted delivery of the poorly water-soluble drug celecoxib: *Journal of Microencapsulation*, v. 28, p. 220-227.
- Kim, Y. Y., E. J. Lee, Y. K. Kim, S. M. Kim, J. Y. Park, H. Myoung, and M. J. Kim, 2010, Anti-cancer effects of celecoxib in head and neck carcinoma: *Molecules and Cells*, v. 29, p. 185-194.
- Kirpotin, D. B., D. C. Drummond, Y. Shao, M. R. Shalaby, K. Hong, U. B. Nielsen, J. D. Marks, C. C. Benz, and J. W. Park, 2006, Antibody targeting of long-circulating lipidic nanoparticles does not increase tumor localization but does increase internalization in animal models, *Cancer Res*, v. 66, p. 6732-40.
- Klein, R. D., C. S. Van Pelt, A. L. Sabichi, J. Dela Cerda, S. M. Fischer, G. Furstenberger, and K. Muller-Decker, 2005, Transitional cell hyperplasia and carcinomas in urinary bladders of transgenic mice with keratin 5 promoter-driven cyclooxygenase-2 overexpression: *Cancer Res*, v. 65, p. 1808-13.
- Konishi, M., R. Kikuchi-Yanoshita, K. Tanaka, M. Muraoka, A. Onda, Y. Okumura, N. Kishi, T. Iwama, T. Mori, M. Koike, K. Ushio, M. Chiba, S. Nomizu, F. Konishi, J. Utsunomiya, and M. Miyaki, 1996, Molecular nature of colon tumors in hereditary nonpolyposis colon cancer, familial polyposis, and sporadic colon cancer: *Gastroenterology*, v. 111, p. 307-17.

- Kwak, Y. E., N. K. Jeon, J. Kim, and E. J. Lee, 2007, The cyclooxygenase-2 selective inhibitor celecoxib suppresses proliferation and invasiveness in the human oral squamous carcinoma: Signal Transduction Pathways, Pt C: Cell Signaling in Health and Disease, v. 1095, p. 99-112.
- Lassailly, F., E. Griessinger, and D. Bonnet, 2010, "Microenvironmental contaminations" induced by fluorescent lipophilic dyes used for noninvasive in vitro and in vivo cell tracking: Blood, v. 115, p. 5347-5354.
- Lehmann, J. M., J. M. Lenhard, B. B. Oliver, G. M. Ringold, and S. A. Kliewer, 1997, Peroxisome proliferator-activated receptors alpha and gamma are activated by indomethacin and other non-steroidal anti-inflammatory drugs: Journal of Biological Chemistry, v. 272, p. 3406-3410.
- Leslie, A., F. A. Carey, N. R. Pratt, and R. J. Steele, 2002, The colorectal adenoma-carcinoma sequence: Br J Surg, v. 89, p. 845-60.
- Liang, C. C., A. Y. Park, and J. L. Guan, 2007, In vitro scratch assay: a convenient and inexpensive method for analysis of cell migration in vitro: Nature Protocols, v. 2, p. 329-333.
- Liu, J. B., H. Lee, M. Huesca, A. P. Young, and C. Allen, 2006, Liposome formulation of a novel hydrophobic aryl-imidazole compound for anti-cancer therapy: Cancer Chemotherapy and Pharmacology, v. 58, p. 306-318.
- Lorusso, D., A. Di Stefano, V. Carone, A. Fagotti, S. Pisconti, and G. Scambia, 2007, Pegylated liposomal doxorubicin-related palmar-plantar erythrodysesthesia ('hand-foot' syndrome): Annals of Oncology, v. 18, p. 1159-1164.
- Maeda, H., and Y. Matsumura, 1989, Tumorotropic and lymphotropic principles of macromolecular drugs: Crit Rev Ther Drug Carrier Syst, v. 6, p. 193-210.
- Maier, T. J., K. Schilling, R. Schmidt, G. Geisslinger, and S. Grosch, 2004, Cyclooxygenase-2 (COX-2)-dependent and -independent anticarcinogenic effects of celecoxib in human colon carcinoma cells: Biochemical Pharmacology, v. 67, p. 1469-1478.
- Mann, J. R., and R. N. DuBois, 2004, Cyclooxygenase-2 and gastrointestinal cancer: Cancer Journal, v. 10, p. 145-152.

- Matsumura, Y., M. Gotoh, K. Muro, Y. Yamada, K. Shirao, Y. Shimada, M. Okuwa, S. Matsumoto, Y. Miyata, H. Ohkura, K. Chin, S. Baba, T. Yama, A. Kannami, Y. Takamatsu, K. Ito, and K. Takahashi, 2004, Phase I and pharmacokinetic study of MCC-465, a doxorubicin (DXR) encapsulated in PEG immunoliposome, in patients with metastatic stomach cancer: *Annals of Oncology*, v. 15, p. 517-525.
- McCormick, D., P. J. Kibbe, and S. W. Morgan, 2002, Colon cancer: prevention, diagnosis, treatment: *Gastroenterol Nurs*, v. 25, p. 204-11; quiz, 211-2.
- Mendelsohn, J., and J. Baselga, 2003, Status of epidermal growth factor receptor antagonists in the biology and treatment of cancer: *Journal of Clinical Oncology*, v. 21, p. 2787-2799.
- Mohammed, A. R., N. Weston, A. G. A. Coombes, M. Fitzgerald, and Y. Perrie, 2004, Liposome formulation of poorly water soluble drugs: optimisation of drug loading and ESEM analysis of stability: *International Journal of Pharmaceutics*, v. 285, p. 23-34.
- Moscatoello, D. K., M. Holgado-Madruga, D. R. Emlet, R. B. Montgomery, and A. J. Wong, 1998, Constitutive activation of phosphatidylinositol 3-kinase by a naturally occurring mutant epidermal growth factor receptor: *Journal of Biological Chemistry*, v. 273, p. 200-206.
- Neufang, G., G. Furstenberger, M. Heidt, F. Marks, and K. Muller-Decker, 2001, Abnormal differentiation of epidermis in transgenic mice constitutively expressing cyclooxygenase-2 in skin: *Proceedings of the National Academy of Sciences of the United States of America*, v. 98, p. 7629-7634.
- Nichols, J. W., and R. E. Pagano, 1982, Use of resonance energy-transfer to study the kinetics of amphiphile transfer between vesicles: *Biochemistry*, v. 21, p. 1720-1726.
- Noonberg, S. B., and C. C. Benz, 2000, Tyrosine kinase inhibitors targeted to the epidermal growth factor receptor subfamily - Role as anticancer agents: *Drugs*, v. 59, p. 753-767.
- Oshima, M., J. E. Dinchuk, S. L. Kargman, H. Oshima, B. Hancock, E. Kwong, J. M. Trzaskos, J. F. Evans, and M. M. Taketo, 1996, Suppression of intestinal polyposis in Apc(Delta 716) knockout mice by inhibition of cyclooxygenase 2 (COX-2): *Cell*, v. 87, p. 803-809.

- Park, J. W., K. L. Hong, D. B. Kirpotin, G. Colbern, R. Shalaby, J. Baselga, Y. Shao, U. B. Nielsen, J. D. Marks, D. Moore, D. Papahadjopoulos, and C. C. Benz, 2002, Anti-HER2 immunoliposomes: Enhanced efficacy attributable to targeted delivery: *Clinical Cancer Research*, v. 8, p. 1172-1181.
- Peer, D., J. M. Karp, S. Hong, O. C. FaroKhzad, R. Margalit, and R. Langer, 2007, Nanocarriers as an emerging platform for cancer therapy: *Nature Nanotechnology*, v. 2, p. 751-760.
- Perrault, S. D., C. Walkey, T. Jennings, H. C. Fischer, and W. C. W. Chan, 2009, Mediating Tumor Targeting Efficiency of Nanoparticles Through Design: *Nano Letters*, v. 9, p. 1909-1915.
- Perry, J. E., M. E. Grossmann, and D. J. Tindall, 1998, Epidermal growth factor induces cyclin D-1 in a human prostate cancer cell line: *Prostate*, v. 35, p. 117-124.
- Perumal, V., S. Banerjee, S. Das, R. Sen, and M. Mandal, 2011, Effect of liposomal celecoxib on proliferation of colon cancer cell and inhibition of DMBA-induced tumor in rat model, p. 67-79.
- Phillips, R. K. S., M. H. Wallace, P. M. Lynch, E. Hawk, G. B. Gordon, B. P. Saunders, N. Wakabayashi, Y. Shen, S. Zimmerman, L. Godio, M. Rodrigues-Bigas, L. K. Su, J. Sherman, G. Kelloff, B. Levin, G. Steinbach, and F. A. P. S. Grp, 2002, A randomised, double blind, placebo controlled study of celecoxib, a selective cyclooxygenase 2 inhibitor, on duodenal polyposis in familial adenomatous polyposis: *Gut*, v. 50, p. 857-860.
- Prescott, S. M., and F. A. Fitzpatrick, 2000, Cyclooxygenase-2 and carcinogenesis, *Biochim Biophys Acta*, v. 1470: Netherlands, p. M69-78.
- Rochlitz, C., R. Ritschard, B. Vogel, T. Dieterle, L. Bubendorf, C. Hilker, S. Deuster, R. Herrmann, and C. Mamot, 2011, A phase I study of doxorubicin-loaded anti-EGFR immunoliposomes in patients with advanced solid tumors: *Onkologie*, v. 34, p. 109-109.
- Sade, A., S. Tuncay, I. Cimen, F. Severcan, and S. Banerjee, 2012, Celecoxib reduces fluidity and decreases metastatic potential of colon cancer cell lines irrespective of COX-2 expression: *Biosci Rep*, v. 32, p. 35-44.

- Salomon, D. S., R. Brandt, F. Ciardiello, and N. Normanno, 1995, Epidermal growth factor-related peptides and their receptors in human malignancies: *Critical Reviews in Oncology/Hematology*, v. 19, p. 183-232.
- Sano, H., Y. Kawahito, R. L. Wilder, A. Hashiramoto, S. Mukai, K. Asai, S. Kimura, H. Kato, M. Kondo, and T. Hla, 1995, Expression of cyclooxygenase-1 and cyclooxygenase-2 in human colorectal-cancer: *Cancer Research*, v. 55, p. 3785-3789.
- Sapra, P., and T. M. Allen, 2002, Internalizing antibodies are necessary for improved therapeutic efficacy of antibody-targeted liposomal drugs: *Cancer Research*, v. 62, p. 7190-7194.
- Schiffmann, S., T. J. Maier, I. Wobst, A. Janssen, H. Corban-Wilhelm, C. Angioni, G. Geisslinger, and S. Grosch, 2008, The anti-proliferative potency of celecoxib is not a class effect of coxibs: *Biochemical Pharmacology*, v. 76, p. 179-187.
- Senger, D. R., S. J. Galli, A. M. Dvorak, C. A. Perruzzi, V. S. Harvey, and H. F. Dvorak, 1983, Tumor-cells secrete a vascular-permeability factor that promotes accumulation of ascites-fluid: *Science*, v. 219, p. 983-985.
- Senior, J., and G. Gregoriadis, 1982, Is half-life of circulating liposomes determined by changes in their permeability: *Febs Letters*, v. 145, p. 109-114.
- Smalley, W., W. A. Ray, J. Daugherty, and M. R. Griffin, 1999, Use of nonsteroidal anti-inflammatory drugs and incidence of colorectal cancer: a population-based study: *Arch Intern Med*, v. 159, p. 161-6.
- Smalley, W. E., and R. N. DuBois, 1997, Colorectal cancer and nonsteroidal anti-inflammatory drugs: *Adv Pharmacol*, v. 39, p. 1-20.
- Steinbach, G., P. M. Lynch, R. K. S. Phillips, M. H. Wallace, E. Hawk, G. B. Gordon, N. Wakabayashi, B. Saunders, Y. Shen, T. Fujimura, L. K. Su, B. Levin, L. Godio, S. Patterson, M. A. Rodriguez-Bigas, S. L. Jester, K. L. King, M. Schumacher, J. Abbruzzese, R. N. DuBois, W. N. Hittelman, S. Zimmerman, J. W. Sherman, and G. Kelloff, 2000, The effect of celecoxib, a cyclooxygenase-2 inhibitor, in familial adenomatous polyposis: *New England Journal of Medicine*, v. 342, p. 1946-1952.

- Stewart, J. C. M., 1980, Colorimetric determination of phospholipids with ammonium ferrothiocyanate: *Analytical Biochemistry*, v. 104, p. 10-14.
- Storm, G., S. O. Belliot, T. Daemen, and D. D. Lasic, 1995, Surface modification of nanoparticles to oppose uptake by the mononuclear phagocyte system: *Advanced Drug Delivery Reviews*, v. 17, p. 31-48.
- Straubinger, R. M., D. Papahadjopoulos, and K. Hong, 1990, Endocytosis and intracellular fate of liposomes using pyranine as a probe: *Biochemistry*, v. 29, p. 4929-4939.
- Subbaramaiah, K., N. Telang, J. T. Ramonetti, R. Araki, B. DeVito, B. B. Weksler, and A. J. Dannenberg, 1996, Transcription of cyclooxygenase-2 is enhanced in transformed mammary epithelial cells: *Cancer Res*, v. 56, p. 4424-9.
- Subczynski, W. K., A. Wisniewska, J. J. Yin, J. S. Hyde, and A. Kusumi, 1994, Hydrophobic barriers of lipid bilayer-membranes formed by reduction of water penetration by alkyl chain unsaturation and cholesterol: *Biochemistry*, v. 33, p. 7670-7681.
- Swartz, M. A., 2001, The physiology of the lymphatic system: *Advanced Drug Delivery Reviews*, v. 50, p. 3-20.
- Szoka, F., and D. Papahadjopoulos, 1980, Comparative properties and methods of preparation of lipid vesicles (liposomes): *Annual Review of Biophysics and Bioengineering*, v. 9, p. 467-508.
- Thakkar, H., R. Kumar Sharma, and R. S. Murthy, 2007, Enhanced retention of celecoxib-loaded solid lipid nanoparticles after intra-articular administration: *Drugs R D*, v. 8, p. 275-85.
- Thakkar, H., R. K. Sharma, A. K. Mishra, K. Chuttani, and R. S. R. Murthy, 2004, Celecoxib incorporated chitosan microspheres: In vitro and in vivo evaluation: *Journal of Drug Targeting*, v. 12, p. 549-557.
- Thun, M. J., M. M. Namboodiri, and C. W. Heath, 1991, Aspirin use and reduced risk of fatal colon cancer: *New England Journal of Medicine*, v. 325, p. 1593-1596.
- Torchilin, V., and V. Weissig, 2003, *Liposomes - A Practical Approach*, Oxford University Press, USA.

- Torchilin, V. P., 2005, Recent advances with liposomes as pharmaceutical carriers: *Nat Rev Drug Discov*, v. 4, p. 145-60.
- Torchilin, V. P., 2007, Targeted pharmaceutical nanocarriers for cancer therapy and imaging: *AAPS J*, v. 9, p. E128-47.
- Tsotas, V. A., S. Mourtas, and S. G. Antimisiaris, 2007, Dexamethasone incorporating liposomes: Effect of lipid composition on drug trapping efficiency and vesicle stability: *Drug Delivery*, v. 14, p. 441-445.
- US Library of Medicine, ClinicalTrials.gov A service of the US National Institutes of Health., <http://clinicaltrials.gov/>. last visited on February 2012
- Voldborg, B. R., L. Damstrup, M. Spang-Thomsen, and H. S. Poulsen, 1997, Epidermal growth factor receptor (EGFR) and EGFR mutations, function and possible role in clinical trials: *Annals of Oncology*, v. 8, p. 1197-1206.
- Vonarbourg, A., C. Passirani, P. Saulnier, P. Simard, J. C. Leroux, and J. P. Benoit, 2006, Evaluation of pegylated lipid nanocapsules versus complement system activation and macrophage uptake: *J Biomed Mater Res A*, v. 78, p. 620-8.
- Walter, M. F., R. F. Jacob, C. A. Day, R. Dahlborg, Y. J. Weng, and R. P. Mason, 2004, Sulfone COX-2 inhibitors increase susceptibility of human LDL and plasma to oxidative modification: comparison to sulfonamide COX-2 inhibitors and NSAIDs: *Atherosclerosis*, v. 177, p. 235-243.
- Wells, A., 1999, EGF receptor: *International Journal of Biochemistry & Cell Biology*, v. 31, p. 637-643.
- Wheeler, D. L., E. F. Dunn, and P. M. Harari, 2010, Understanding resistance to EGFR inhibitors-impact on future treatment strategies: *Nature Reviews Clinical Oncology*, v. 7, p. 493-507.
- Williams, C. S., A. J. M. Watson, H. M. Sheng, R. Helou, J. Y. Shao, and R. N. DuBois, 2000, Celecoxib prevents tumor growth in vivo without toxicity to normal gut: Lack of correlation between in vitro and in vivo models: *Cancer Research*, v. 60, p. 6045-+.
- Wolfe, M. M., D. R. Lichtenstein, and G. Singh, 1999, Gastrointestinal toxicity of nonsteroidal antiinflammatory drugs: *New England Journal of Medicine*, v. 340, p. 1888-1899.

- Woodburn, J. R., 1999, The epidermal growth factor receptor and its inhibition in cancer therapy: *Pharmacology & Therapeutics*, v. 82, p. 241-250.
- Yamamoto, Y., M. J. Yin, K. M. Lin, and R. B. Gaynor, 1999, Sulindac inhibits activation of the NF-kappa B pathway: *Journal of Biological Chemistry*, v. 274, p. 27307-27314.
- Yamazaki, H., H. Kijima, Y. Ohnishi, Y. Abe, Y. Oshika, T. Tsuchida, T. Tokunaga, A. Tsugu, Y. Ueyama, N. Tamaoki, and M. Nakamura, 1998, Inhibition of tumor growth by ribozyme-mediated suppression of aberrant epidermal growth factor receptor gene expression: *J Natl Cancer Inst*, v. 90, p. 581-7.
- Yamazaki, N., S. Kojima, N. V. Bovin, S. Andre, S. Gabius, and H. J. Gabius, 2000, Endogenous lectins as targets for drug delivery: *Advanced Drug Delivery Reviews*, v. 43, p. 225-244.
- Yilmaz, M., and G. Christofori, 2010, Mechanisms of Motility in Metastasizing Cells: *Molecular Cancer Research*, v. 8, p. 629-642.
- Yin, M. J., Y. Yamamoto, and R. B. Gaynor, 1998, The anti-inflammatory agents aspirin and salicylate inhibit the activity of I kappa B kinase-beta: *Nature*, v. 396, p. 77-80.
- Yuan, F., M. Dellian, D. Fukumura, M. Leunig, D. A. Berk, V. P. Torchilin, and R. K. Jain, 1995, Vascular-permeability in a human tumor xenograft - molecular-size dependence and cutoff size: *Cancer Research*, v. 55, p. 3752-3756.
- Zhang, L., J. Yu, B. H. Park, K. W. Kinzler, and B. Vogelstein, 2000, Role of BAX in the apoptotic response to anticancer agents: *Science*, v. 290, p. 989-+.
- Zhang, X., Z. G. Chen, M. S. Choe, Y. Lin, S. Y. Sun, H. S. Wieand, H. J. Shin, A. Chen, F. R. Khuri, and D. M. Shin, 2005, Tumor growth inhibition by simultaneously blocking epidermal growth factor receptor and cyclooxygenase-2 in a xenograft model, *Clin Cancer Res*, v. 11, p. 6261-9.
- Zhang, X. P., S. G. Morham, R. Langenbach, and D. A. Young, 1999, Malignant transformation and antineoplastic actions of nonsteroidal antiinflammatory drugs (NSAIDs) on cyclooxygenase-null embryo fibroblasts: *Journal of Experimental Medicine*, v. 190, p. 451-459.

APPENDICES

APPENDIX A CALIBRATION CURVES AND CHROMATOGRAMS

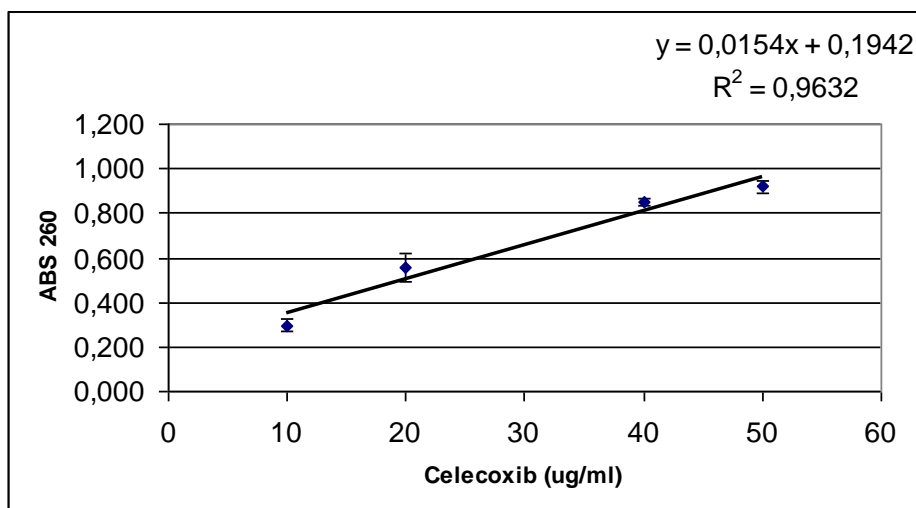


Figure A- 1 CLX calibration curve for spectrophotometric quantification

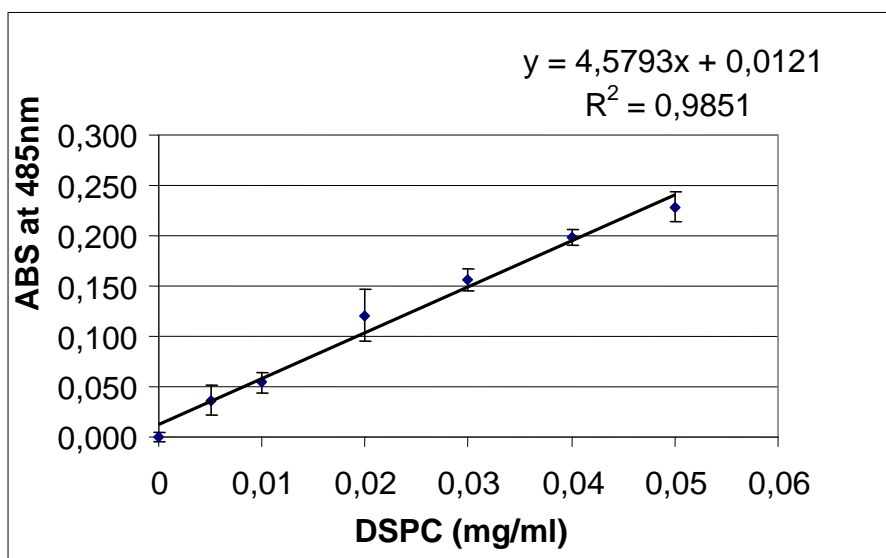


Figure A- 2 DSPC calibration curve for spectrophotometric quantification

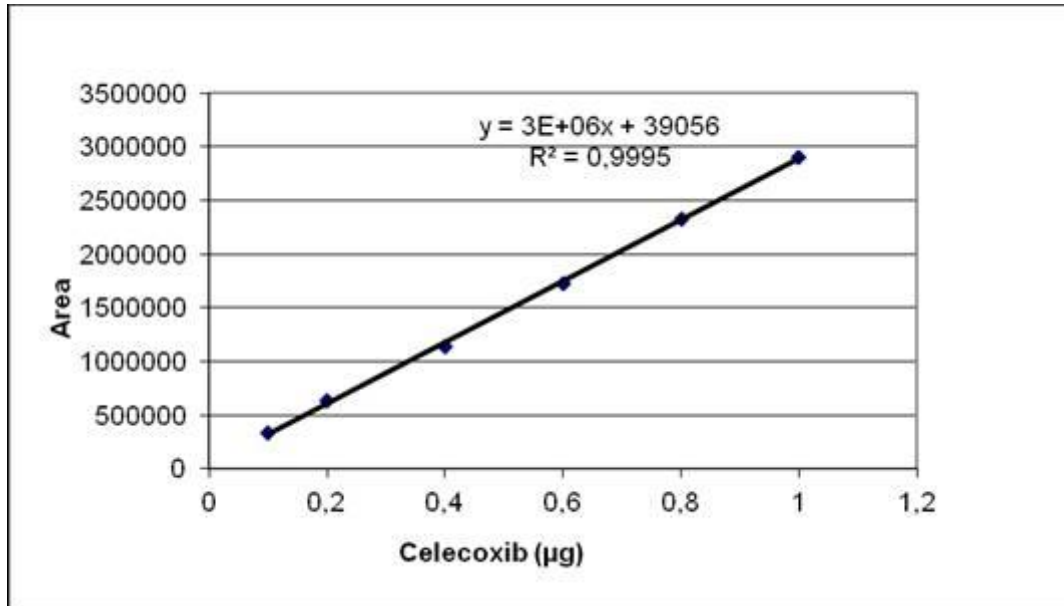


Figure A- 3 CLX calibration curve for quantification by HPLC

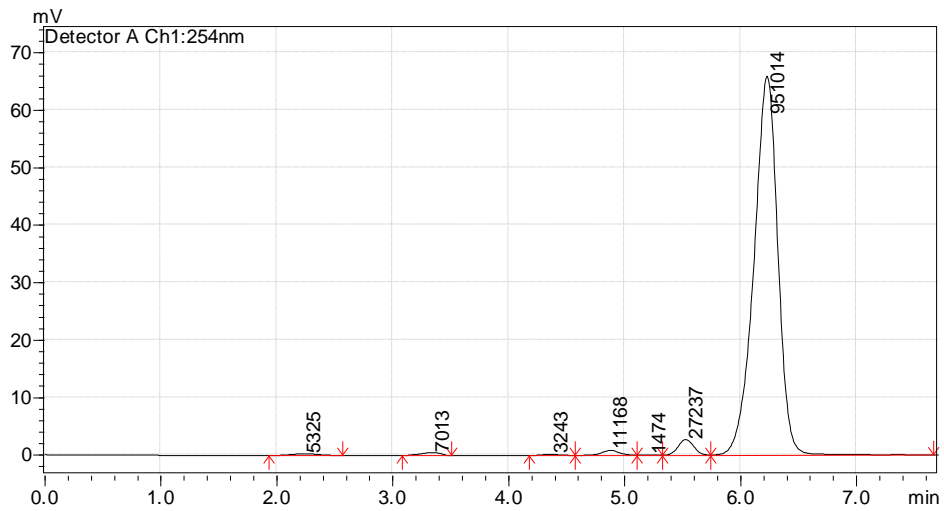


Figure A- 4 A representative HPLC chromatogram of CLX standard (19 µg/ml) dissolved in methanol

APPENDIX B FLUORESCENCE EXCITATION AND EMISSION SPECTRA OF FLUOROPHORES

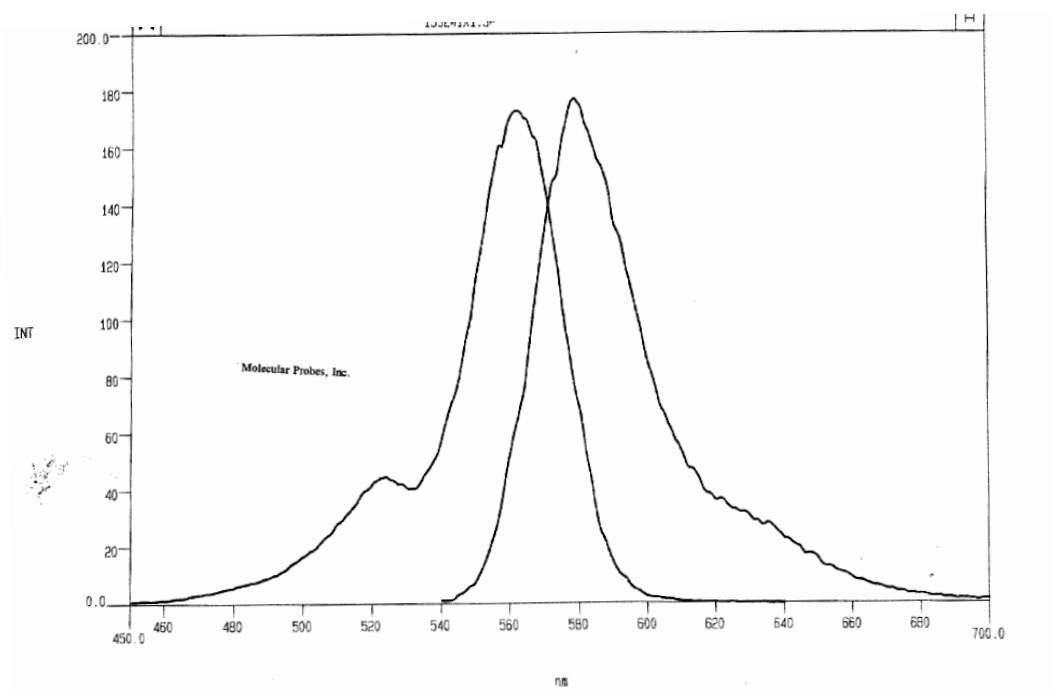


Figure A- 5 Fluorescence excitation and emission spectra of Rhodamine-DHPE
Left curve: excitation, right curve: emission spectrum

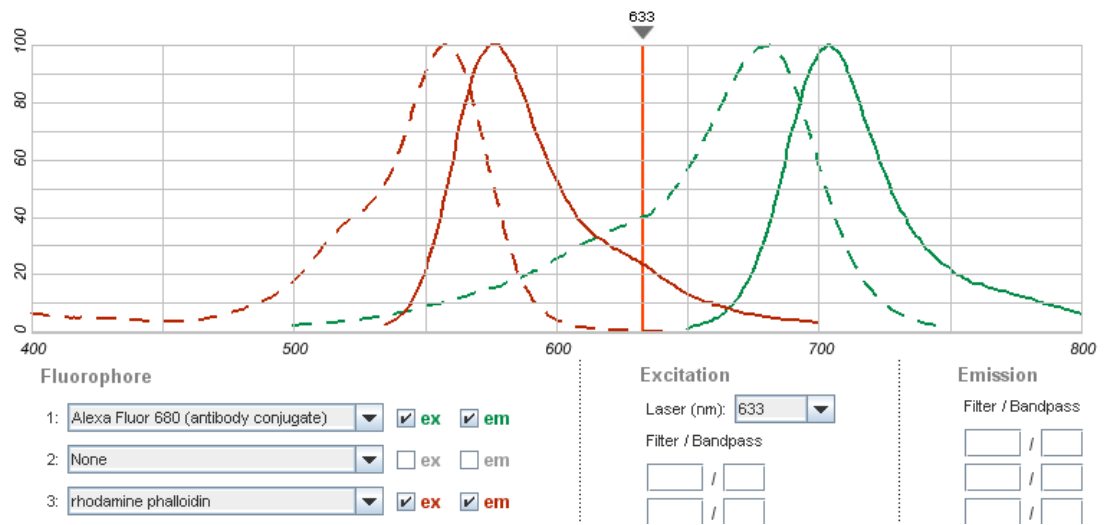


Figure A- 6 Fluorescence excitation and emission spectra of AlexaFluor680 and Rhodamine-DHPE

Left: Rhodamine right: AF680. Dotted lines: excitation, solid lines: emission spectra (Image captured from Invitrogen SpectraViewer).

**APPENDIX C CLX CONCENTRATIONS USED IN *IN VITRO*
EXPERIMENTS**

Table A. 1 Celecoxib concentrations used in *in vitro* experiments to achieve anticarcinogenic effects

Effect	Drug concentration
<i>Mechanisms involved in inhibition of cell cycle progression</i>	
Proteins decreasing expression of cell cycle promoting proteins and increasing expression of cell cycle inhibiting proteins	10 – 40 μ M Celecoxib 100 μ M Celecoxib 40 – 100 μ M Celecoxib 10 – 30 μ M Celecoxib
Inhibition of PKB	10 – 60 μ M Celecoxib 10 – 50 μ M Celecoxib
Inhibition of PDK-1	25 – 100 μ M Celecoxib 10 – 100 μ M Celecoxib 50 μ M Celecoxib
Increase in ceramide	25 – 50 μ M Celecoxib
Inhibition of ODC	2.5 – 50 μ M Celecoxib
<i>Mechanisms involved in induction of apoptosis</i>	
Decreased expression of antiapoptotic proteins	10 μ M Celecoxib 25 – 100 μ M Celecoxib
Increased expression of proapoptotic proteins	10 μ M Celecoxib
Activation of intrinsic apoptotic pathway	10 – 40 μ M Celecoxib 75 – 100 μ M Celecoxib 50 μ M Celecoxib 50 – 100 μ M Celecoxib
Activation of extrinsic apoptotic pathway	3 – 100 μ M Celecoxib 25 – 75 μ M Celecoxib
Inhibition of endoplasmic reticulum Ca ²⁺ ATPase	10 – 100 μ M Celecoxib
Inhibition of CA	Nanomolar concentrations of celecoxib
Increased expression of 15-LOX-1	12.5 μ M Celecoxib
Effects on NF- κ B	3 – 100 μ M Celecoxib 10 – 40 μ M Celecoxib 75 – 100 μ M Celecoxib 1 – 50 μ M Celecoxib

Table A.1 Continued

<i>Inhibition of angiogenesis and metastasis</i>	
Inhibition of Egr-1	2.5 – 50 μ M Celecoxib
Suppression of VEGF	10 – 30 μ M Celecoxib
Antiproliferative effects on HUVECs or HMVECs	50 – 100 μ M Celecoxib 1 – 50 μ M Celecoxib
Inhibition of MMPs	10 – 25 μ M Celecoxib 3 – 30 μ M Celecoxib
Effects on the APC – β –catenin pathway	10 – 100 μ M Celecoxib

PKB = protein kinase B; PDK-1 = phosphoinositide-dependent kinase 1; ODC = ornithine decarboxylase; CA = carbonic anhydrase; LOX = lipoxygenase; NF- κ B = nuclear factor κ B; Egr-1 = early growth response protein 1; VEGF = vascular endothelial growth factor; HUVEC = human umbilical vein endothelial cell; HMVEC = human dermal microvascular endothelial cell; MMP = matrix metalloprotease; APC = adenomatous polyposis coli. (Grosch et al., 2006)

**APPENDIX D CHARACTERISTICS OF HUMAN COLORECTAL
ADENOCARCINOMA CELL LINES**

**Table A. 2 Characteristics of human colorectal adenocarcinoma cell lines
HCT-116, HT-29 and SW620**

Cell line	HCT-116 (DSMZ no. ACC 581)	HT-29 (ATCC Number HTB-38)	SW620 (ATCC Number: CCL-227)
Cell type	colon carcinoma	colorectal adenocarcinoma	colorectal adenocarcinoma
Origin	established from primary colon carcinoma	established from primary colon adenocarcinoma	Derived from metastatic site lymph node
Population Doubling Time	25-48 hours	19 hours	23-24 hours
Mutations	RAS mutation in codon 13 PIK3CA mutation	myc +; ras +; myb +; fos +; sis +; p53 +; abl -; ros -; src -	myc +; myb +; ras +; fos +; sis +; p53 +; abl -; ros -; src -
EGFR status	EGFR moderate expression (Jhawer et al., 2009)	low EGFR expression (Jhawer et al., 2009)	no EGFR expression (Jhawer et al., 2009)
Cetuximab response	resistant (100% viability at 100 µg/ml) (Jhawer et al., 2009)	moderately resistant (65% viability at 100 µg/ml) (Jhawer et al., 2009)	moderately resistant (85% viability at 100 µg/ml) (Jhawer et al., 2009)
COX-2 status	COX-2 negative	high COX-2	COX-2 negative
Celecoxib response	72.7% viability at 10 µM 6.7% viability at 50 µM (Buecher et al., 2005)	60.6% viability at 10 µM 6 % viability at 50 µM (Buecher et al., 2005)	79.2% viability at 10 µM 16 % viability at 50 µM (Buecher et al., 2005)

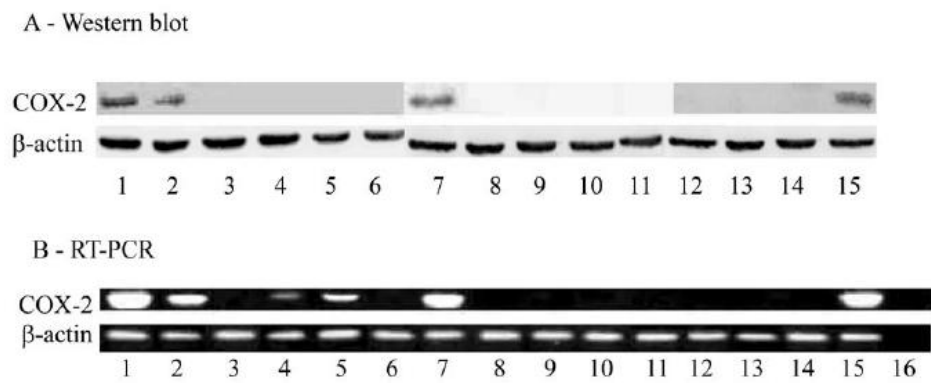


Figure A- 7 COX-2 expression in colorectal adenocarcinoma cell lines

Lane 2: HT-29, Lane 6: HCT-116, Lane 9: SW620 (Buecher et al., 2005)

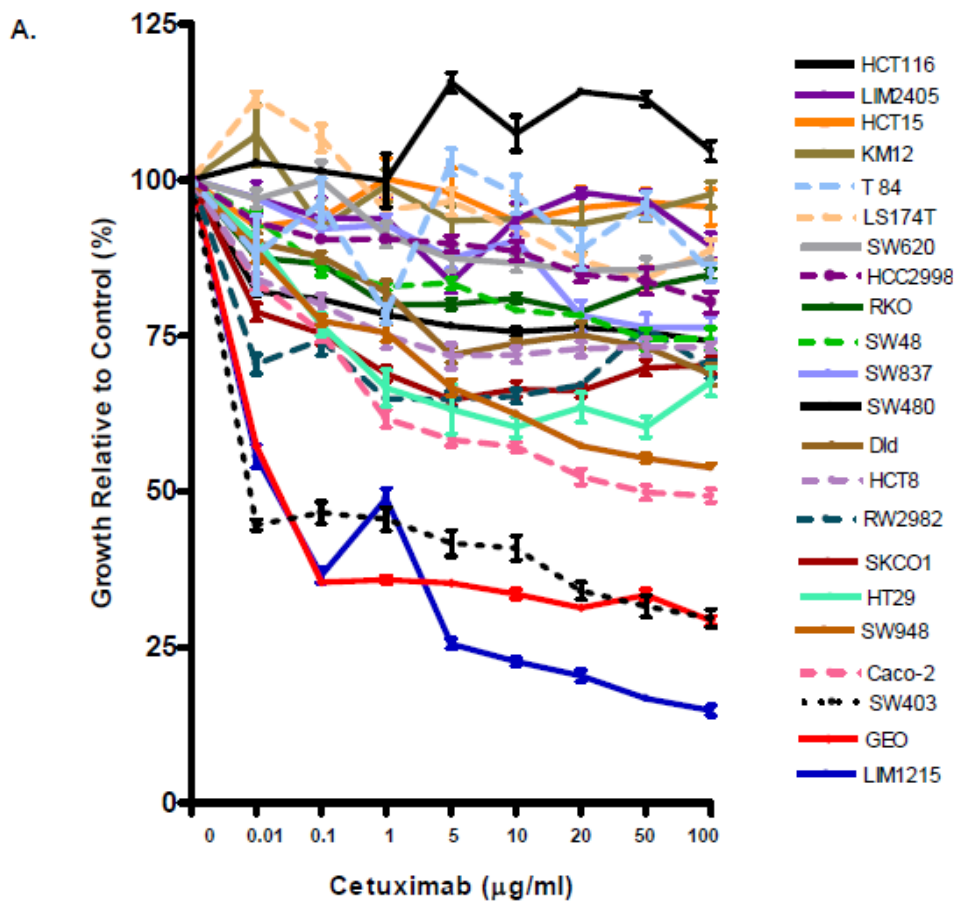


Figure A- 8 Growth inhibition effect of therapeutic anti-EGFR MAb Cetuximab on human colorectal adenocarcinoma cell lines
(Jhawer et al., 2009)

**APPENDIX E STATISTICAL ANALYSES OF RELEASE AND
ENCAPSULATION CHARACTERISTICS OF LIPOSOMES**

Table A. 3 Statistical analyses of released amount of CLX from MLVs

MLV composition	6h	12h	24h	48h	72h
DSPC vs DSPC:chol 10:1	ns	ns	*	***	***
DSPC vs DSPC:chol 5:1	ns	***	***	***	***
DSPC vs DSPC:chol 2:1	*	***	***	***	***
DSPC:chol 10:1 vs DSPC:chol 5:1	ns	***	ns	*	ns
DSPC:chol 10:1 vs DSPC:chol 2:1	ns	***	*	*	ns
DSPC:chol 5:1 vs DSPC:chol 2:1	ns	ns	ns	ns	ns

One-way ANOVA, ns stands for not significant, * p<0.05, **p<0.01, ***p<0.001

Table A. 4 Statistical analyses of CLX EE and percentage loading

Liposome formulation	t-test for EE	t-test for % Loading
DSPC only LUV vs DSPC 0.5%PEG	ns	ns
DSPC only LUV vs DSPC 2%PEG	**	ns
DSPC 0.5%PEG vs DSPC 2%PEG	***	ns
10:1 LUV vs 10:1 0.5%PEG	ns	ns
10:1 LUV vs 10:1 2%PEG	ns	ns
10:1 0.5%PEG vs 10:1 2%PEG	ns	ns
DSPC only LUV vs 10:1 LUV	ns	ns
DSPC only LUV vs 10:1 0.5%PEG	ns	*
DSPC only LUV vs 10:1 2%PEG	ns	ns
10:1 LUV vs DSPC 0.5%PEG	*	ns
10:1 LUV vs DSPC 2%PEG	ns	ns
DSPC 0.5%PEG vs 10:1 0.5%PEG	ns	*
DSPC 0.5%PEG vs 10:1 2%PEG	ns	ns
10:1 0.5%PEG vs DSPC 2%PEG	**	***
DSPC 2%PEG vs 10:1 2%PEG	ns	*

Results were analyzed by unpaired two-tailed t test.

ns: not significant, * p<0.05, ** p< 0.01, ***p<0.001

CURRICULUM VITAE

Ash Erdoğ

+90 535 356 40 09

aslierdog@gmail.com

Date of Birth: 31.07.1982

EDUCATION

- 09.2005- 02.2012 PhD on B.S in Biotechnology Graduate, Institute of Natural and Applied Sciences, Middle East Technical University (METU), CGPA:3.79/4.00
Funded by The Scientific and Technological Research Council of Turkey (TUBITAK) bursary
- 09.2000 - 06.2005 B.S. in Food Engineering, Faculty of Engineering, METU
High honor degree, CGPA : 3.61/4.00

PUBLICATION LIST

SCI papers:

1. **Deniz A**, Sade A, Severcan F, TezcanerA, Keskin D, Banerjee S . Celecoxib Loaded Liposomes: Effect of Cholesterol on Encapsulation and *in vitro* Release Characteristics. Biosci Rep. 2010 Jun 3;30(5):365-73.

ISI Current Web Contents papers:

Banerjee S, **Erdoğ A**. ALOX12 (Arachidonate 12-Lipoxygenase) Homo sapiens. Atlas Genet Cytogenet Oncol Haematol 2007; 11 (3): 465-473.

Meetings and Seminars:

1. **Deniz A**, Banerjee S, Tezcaner A and Keskin D. Celecoxib Loaded Liposomes: Effect of Cholesterol on Encapsulation and *in vitro* Release Characteristics. International Symposium on Biotechnology: Developments and Trends. Sep 27-30, 2009, METU, Ankara, Turkey.
2. Sade A, **Erdoğ A**, Severcan F ve Banerjee S. Selekoksisib ile DSPC lipozomların etkileşiminin FTIR spektroskopisi ile incelenmesi. BİYOMUT 08 29-31 May 2008, METU, Ankara, Turkey.
3. **Erdoğ A**, Tezcaner A, Keskin D and Banerjee, S. Liposomes as nanocarriers to deliver celecoxib in cancer. International workshop on nanobiotechnology and genome technologies NANOMAT 2007. Oct 31-Nov 03, 2007, Antalya, Turkey.

SKILLS

Language skills:

English: Excellent in reading, writing and speaking

Russian: Beginner in reading, writing and speaking

Technical skills:

Molecular biology techniques

Mammalian cell culture techniques

Laser Scanning Confocal Microscopy analysis

MEMBERSHIPS

Turkish Biotechnology Association (2007-)

METU Scouts (2001-2005)